UNIVERSITÀ
DEGLI STUDI
DI PADOVA

Sede Amministrativa: Università degli Studi di Padova
Dipartimento di Matematica "Tullio Levi-Civita"
CORSO DI DOTTORATO DI RICERCA IN SCIENZE MATEMATICHE
CURRICULO MATEMATICA
CICLO XXXIV

Asymptotic dynamics and synchronization of dissipative systems of coupled pendula

Coordinatore: Ch.mo Prof. Giovanni Colombo

Supervisore: Ch.mo Prof. Francesco Fassò

Dottoranda: Sara Galasso

Abstract

In this thesis we investigate the dynamics of systems of coupled pendula and, in particular, we discuss the emergence of synchronization patterns in the asymptotic dynamics of these systems when suitable dissipative contributions are included in the model.

The core of the thesis is the spectral study of the linearisation of a system formed by a viscoelastic string, fixed at its ends, with n pendula hanging equally spaced from it. This is a 'hybrid' mechanical system with dissipation, and a motivation for it comes from the famous Huygens synchronization phenomenon. The novelty of our approach is that the coupling between the pendula is realised via a continuous string, and hence an infinite-dimensional mechanical system. Moreover, the string is supposed to be viscoelastic, and therefore inherently introduces dissipation.

We describe the coupled system starting from a Lagrangian formulation and we adopt the classical Kelvin-Voigt damping model for the viscoelasticity of the string. The equations of motion that we obtain for our system are a set of coupled ODEs and PDEs. Even though the Kelvin-Voigt viscoelastic string is a linear system, the pendula are not and the coupled system is nonlinear. The equilibrium state in which the string is at rest and the pendula hang downward is an attracting equilibrium, and we study the spectrum of the linearisation of the system at that equilibrium.

The linearised system decouples into a "vertical" system, which describes the vertical motion of the string with the pendula replaced by point masses, and a "horizontal" system, which describes the horizontal motion of the string and the linearised pendula. We determine a closed form for the eigenvalue equation for both the vertical and horizontal systems for any number of pendula. These expressions involve Chebyshev polynomials of the second kind. We also provide closed expressions for the eigenfunctions. We hence detail the study of the spectrum, without and with dissipation. This is done to a large extent analytically, but partly also resorting to a numerical investigation.

Next, we study the long-term dynamics of the system. Due to the frequency-dependent damping of the Kelvin-Voigt model, in the case of weak dissipation, the long-term dynamics is dominated by the damped normal modes that dissipate less. Hence, after a transient, motions of the system will tend to motions that are either periodic or quasi-periodic, even though with slowly decreasing amplitudes; particularly when n is small, these motions may appear as 'synchronised'. On these bases, a careful numerical study enables us to determine the regions in the parameter space in which, when $n = 2$, either the pendula synchronise in phase or in opposition of phase or where beats are present.

In the concluding part of the work, we advance a first attempt to extend the analysis beyond the linear level. We restrict the study to a finite-dimensional setting, and we investigate invariant structures in the phase space of holonomically constrained mechanical systems with dissipation and no forcing. In particular, we consider the case of velocity-proportional friction forces and we assume that the dissipation vanishes not only at zero velocity but also on a certain larger subset of the phase space. We initiate the analysis of such a situation, in the nonlinear setting, via the LaSalle invariance principle.

Sommario

In questa tesi studiamo la dinamica di sistemi di pendoli accoppiati e, in particolare, la comparsa di comportamenti di sincronizzazione nella dinamica asintotica di tali sistemi qualora si includano nel modello termini dissipativi.

La parte principale della tesi riguarda lo studio spettrale della linearizzazione di un sistema meccanico composto da una corda viscoelastica, fissata alle estremità, e da n pendoli identici, appesi ad essa a distanza regolare. Tale sistema è dissipativo e "ibrido", avendo una componente continua ed una discreta, e il suo studio trae ispirazione dal classico problema di sincronizzazione dei pendoli di Huygens. Una novità dell'approccio che proponiamo sta nel modellizzare l'accoppiamento tra i pendoli con una struttura continua, che è pertanto infinito-dimensionale. Questa caratteristica, inoltre, permette di includere la dissipazione in modo naturale, adottando un modello di corda viscoelastica.

Il sistema verrà descritto partendo da una formulazione Lagrangiana e adotteremo il modello di Kelvin-Voigt per la viscoelasticità della corda, ottenendo così un sistema di equazioni differenziali ordinarie e alle derivate parziali. La presenza di termini di pendolo rende tali equazioni non-lineari. Procederemo quindi col linearizzarle attorno alla configurazione di equilibrio stabile, nella quale la corda è a riposo e i pendoli sono appesi verso il basso, e ne studieremo lo spettro.

Nel linearizzarlo, il sistema si disaccoppia in una componente "verticale", che descrive il moto di una corda con delle masse puntiformi in luogo dei pendoli, e una "orizzontale", che descrive il moto della corda in un piano orizzontale con i pendoli linearizzati. Otterremo delle espressioni esplicite per le equazioni caratteristiche dei due sistemi e per le corrispondenti autofunzioni, in termini di polinomi di Chebyshev del secondo tipo, per un numero arbitrario di pendoli. Analizzeremo quindi gli spettri dei due sistemi, per la gran parte analiticamente, nel caso conservativo e in quello dissipativo.

Infine studieremo la dinamica asintotica del sistema. Questa è fortemente influenzata dall'aver adottato un modello di attrito che porta ad un tasso di smorzamento dipendente dalla frequenza, e pertanto essa è dominata nei tempi lunghi da un piccolo numero di modi normali smorzati poco dissipativi. Dopo un transiente iniziale, cioè, i moti del sistema tenderanno a dei moti che sono periodici o quasi-periodici, con delle ampiezze di oscillazione lentamente decrescenti. Uno studio numerico nel caso di $n = 2$ ci permetterà di determinare le regioni nello spazio dei parametri nelle quali i pendoli si sincronizzano asintoticamente in fase, in quali in contro fase, e dove invece si osservano battimenti.

Nella parte conclusiva del lavoro ci interessiamo al regime non-lineare. Considereremo sistemi finito-dimensionali e inizieremo uno studio delle strutture invarianti nello spazio delle fasi di sistemi dissipativi senza forzante. Specificamente, approfondiremo la trattazione del caso di sistemi meccanici olonomi in presenza di forze dissipative proporzionali alla velocità del sistema. Presenteremo un tentativo preliminare per la descrizione di tali sistemi nel caso in cui la dissipazione si annulli in un insieme più grande dei soli equilibri, applicando il classico principio di invarianza di LaSalle.

Il problema insomma non è quello, ma
forse sollevarlo non è stato inutile
perché serve a farci capire che le cose
non sono semplici come sembra e così
ci si avvicina lentamente al punto in
cui capiremo quanto sono complicate.

Italo Calvino, Ti con zero.

Acknowledgements

First and foremost, I wish to acknowledge my supervisor, Professor Francesco Fassò, as this thesis is really the outcome of his guidance. It is to him that I owe my interest in mathematical physics, as he has been an inspiring teacher first and advisor later. Throughout these many years, he devoted a great amount of his time and patience to mentoring me, being present at every step of my research, and encouraging me to experience many aspects of the academic world. For this, I am sincerely grateful. It has been an enriching experience to learn from him, and I am thankful for his lessons – for instance, the value of rigour and the need to call things by the right name: processes which I understood take long-term commitment and perseverance.

Secondly, I would like to express my gratitude to the two evaluators for taking the time to carefully read this work and for the useful comments and corrections.

Thanks to my PhD colleagues, who shared with me the everyday doctoral experience during these three years, chatting, drinking coffee, and staring at the mountains in the distance from the 7th floor.

Thanks to those who I met along this journey and stuck with me, the seniors Michaël and Stefano, who are full of motivating and wise words, the synchronization-mate Iván, who warmly supplies stimulating humanistic (and human) discussions, and Roberto, for the things that we have in common, and all the others.

Those who I love should know already that I will never be able to express myself properly enough. Thanks to my dearest friends Elena, Cristiano, Alberto, and Artur, for always being there, no matter the distance, no matter the mood. Wholeheartedly, thanks to my family, which gives me everything, for the lifelong support and for having built the certainty that every hardship can be overcome if it is the four of us together: grazie ai cielli per coccolarmi a casa e a mia sorella per portarmi in montagna.

Contents

Introduction

Motivation and background

The research material collected within this thesis was inspired by the observation of a physical experiment (like the one studied in [42], although from a completely different perspective and scope) consisting of a certain number of identical pendula hanging from a cable, and the remark that, in the dynamics of such a system, various dynamical patterns spontaneously do emerge, and evolve at different time scales. A similar context led to the first description of what is now called "synchronization". Originally, the mathematician C. Huygens (1629-1695) referred to it as "sympathy", denoting the behaviour that he first observed in a pair of pendulum clocks which would come to oscillate in opposition of phase when interacting ([17]). Motivated by these examples of eye-catching dynamics, we propose a study that aims to investigate some of the mechanisms underlying such phenomena.

Commonly understood as the spontaneous tendency of a system toward an organised collective state, synchronization phenomena have been observed, ever since, in the time-evolution of an increasing number of systems, ranging from biological populations (e.g. fireflies, cardiac pacemaker cells, neuronal networks), to electronics (e.g., Josephson junctions), from classical (e.g., pendula, metronomes, organ-pipes), celestial (e.g., tidal locking), and quantum (e.g., optomechanical arrays) mechanics, to social interactions (e.g., clapping). The oft-quoted books [37] and [9] collect many such examples and portray the richness of these phenomena. Accordingly, a comprehensive and rigorous definition of synchronization itself may only be satisfactory for the specific problem under investigation, as its manifestations – and related phenomena – are very numerous (in- or anti-phase, phase-locking, complete synchronization, chimera states, oscillation death, chaotic synchronization,...). An example of an attempted definition can be found, e.g., in [8]. As a consequence, the scientific communities interested in this topic are extremely variegated, together with the mathematical formulations employed for its description. The works cited above, for example, give unified models of several systems in terms of self-sustained phase oscillators, the former using the Kuramoto model and the latter using complex network dynamics.

As mentioned, coupled pendulum clocks are an example of a mechanical system where synchronicity patterns could emerge. Even in this field, research has been developing in different directions, both theoretical and applied, and there has been renewed enthusiasm

in the last decades. In particular, Huygens's problem is remarkably still up-to-date and several studies have been devoted to modelling coupled pendula systems and understanding the underlying core mechanisms that lead to their synchronization (see, e.g., [14] and references therein). Specifically, two essential factors, among possibly many others, greatly influence the dynamics of these systems and require a deeper investigation.

The first is the coupling. Huygens himself identified, for his set-up, the small movements of the common supporting beam as the source of the interaction between the two pendulum clocks. Therefore, an adequate modelling of the coupling structure is cardinal. But this is not an easy task, and a satisfactory description is still lacking, though necessary (as remarked, e.g., in [36]). As a matter of fact, to our knowledge, all the models of the coupling between the pendula are to date finite-dimensional.

The second factor is the dissipation. In [22], where the first mathematical attempt to explain Huygens observations is addressed, D.J. Korteweg argues that synchronization is the outcome of the action of dissipative sources, which make some motions "unsustainable". It is worth mentioning that another piece of evidence of the impact of dissipation on synchronization phenomena in mechanical systems is the so-called "tidal locking". It is indeed well-acknowledged that the $1:1$ resonance between the Moon's orbital period and the Earth's rotation period is the outcome of the dissipation of energy due to internal friction induced by deformation (see, e.g., [4] for a discussion on the asymptotic stability of this synchronous state). Therefore, as these examples indicate, the evaluation of the dissipative contributions is important for an accurate model.

The two pointed aspects are closely related, as the coupling often introduces a source of dissipation (as discussed, e.g., in [16]), and they lead our investigation in this work.

Problem statement and objectives

The overarching theme of this thesis is the asymptotic dynamics of dissipative mechanical systems without forcing, specifically having systems of coupled pendula in mind. In this context, being inclined in particular toward asymptotic synchronous behaviours and Huygens-like systems mentioned at the beginning, we are motivated to raise the following questions:

1. What kind of dynamics does a system of interacting pendula manifest when the continuous nature of the coupling is taken into account? And, in particular, how does the dissipation in the coupling structure affect the (asymptotic) motion of the pendula?

2. What information on the long-term nonlinear dynamics of an unforced mechanical system can we infer by studying the damping contributions? Can we expect the solutions to tend to invariant submanifolds of the phase space, if existent, on which the dissipation — at least at first approximation — does not act, and how their knowledge can be used to comprehend synchronization?

In this thesis, we exhaustively deal with question 1, and we advance an attempt to confront question 2, with the objective of better understanding the emergence of

synchronization phenomena in the absence of forcing. The approaches that we follow are complementary: on the one hand, we study in great detail a novel model, which presents a rich dynamics in its constitutive complexity; on the other, we refer to simple models to test grounding intuitions which may be useful to explore through a systematic approach dissipative mechanical systems. Specifically, our study progresses as follows.

1. We construct an infinite-dimensional model for a system consisting of an arbitrary number n of identical pendula coupled through a continuous structure, which we choose to be a viscoelastic string fixed at its ends. We derive the equations of motion of the system through a Lagrangian formulation of the problem and we then add dissipative forces. Specifically, we adopt the Kelvin-Voigt damping model for the viscoelasticity of the string, while we neglect other sources of dissipation. The study of such a system is highly nontrivial and offers several stimulating lines of investigation. We work in the hypothesis of small oscillations and we linearise the equations of motion about the stable equilibrium configuration. These equations are a system of coupled ODEs and PDEs, which, after being linearised, split into a "vertical" and a "horizontal" system. The vertical system describes a viscoelastic string carrying equally spaced point masses; the non-dissipative version of such "loaded string" is a classical system, introduced and studied by Lord Rayleigh for $n = 1$ ([40]) and later generalised to any n (see, e.g., [15]); its viscoelastic version is novel. The horizontal system describes the linearised pendula coupled to the horizontal motion of the string, and is an entirely new system.

   For the two systems, we investigate the damped normal modes. We first derive the eigenvalue equations and we then present an exhaustive description of the vertical and the horizontal spectra, in both the conservative and the dissipative cases. Finally, we focus our study on the asymptotic dynamics of the system with two pendula. We resort to a numerical analysis and we investigate feasible regimes of synchronization and their dependence on the parameters of the system.

   The interest in the comprehension of the full nonlinear dynamics of this complex system motivates the study of related finite-dimensional systems, as explained in the item below.

2. We consider a generic conservative mechanical system subject to holonomic constraints in a finite-dimensional phase space, described by a Lagrangian $L(q, \dot{q}) = T(q, \dot{q}) - V(q)$, with T and V being the kinetic energy and potential energy, respectively. We include dissipative contributions by choosing the classical model of forces of viscous friction (see, e.g., [3]), namely we add to the Lagrange equations a velocity-proportional damping term of the form $-\Gamma(q)\dot{q}$, where Γ is a symmetric and positive semi-definite tensor. Specifically, we assume that Γ has nontrivial kernel and constant rank. Indeed, we are motivated by some studies on unforced synchronization, such as [4] and [38], to consider the case of partially damped systems. In this context, we make an attempt to investigate, in this nonlinear framework, attracting invariant sets on which dissipation does not act, by exploiting

the classical LaSalle Invariance Principle ([26]). Some simple models accompany the discussion.

Structure of the thesis

The work is organised into three parts: an introductory part, which provides the background for our research; a main part, where we present a self-contained study for the problem of our interest; a closing part, where we lay the foundation for future investigations. The subdivision into chapters has the following structure.

Part I.

Chapter 1 is devoted to a brief review of the most relevant studies on coupled pendula, related to the Huygens synchronization problem. We schematically organise the main features of (some of) the models present in the literature to highlight the key strategies for the investigation of systems of coupled pendula and to critically assess some of the shortcomings in their modelling. In this context, we will find an opportunity to advance our meaning of synchronization and better explain our research approach.

Part II.

We consider a system of pendula, in the absence of driving forces, hanging from a viscoelastic string, and we detail its dynamics in the regime of small oscillations.

Chapter 2 presents the model for the coupled system. We provide a Lagrangian description of the undamped problem and then include dissipative forces in the Euler-Lagrange equations, accounting for internal friction acting within the string. Before introducing our model, we recall some tools from the Lagrangian formulation of mechanics, both in the finite- and infinite-dimensional settings, and compare damping models for the string.

Chapter 3 defines the class of solutions in which we are interested, namely, the damped normal modes for the linearised equations of motion. We derive explicit expressions for the eigenvalue equation and for the corresponding eigenfunctions for any number of pendula.

Chapter 4 presents a detailed spectral analysis for the eigenvalues, in the conservative limit first, and for the dissipative system afterwards. While in the former case the investigation is fully analytical, in the presence of dissipation the formulas are more involved, and the characterisation of the spectrum relies partly on a numerical study. In both cases, we provide a comprehensive description of the spectra.

Chapter 5 discusses the asymptotic dynamics of the pendula. The analysis proceeds in greater detail for the case of two pendula and weak damping, studying numerically the dependence of the decay rates of the eigenvalues on the physical parameters entering the model. A discussion of different synchronization regimes which are attainable in the asymptotic dynamics of the pendula closes the chapter and this part.

Part III.

Chapter 6 is a very preliminary attempt to deal with dissipation in a nonlinear framework. We recall some classical tools useful in the study of the asymptotic behaviour

of dissipative dynamical systems, and we describe two simple illustrative models, which exhibit a spontaneous tendency toward a synchronised state and motivate our setting. In particular, we discuss attractive invariant subsets of the phase space, and lay the foundation for studying the asymptotic nonlinear dynamics of finite-dimensional mechanical systems subject to viscous friction forces.

Contributions

The contents presented in Part II are, to our knowledge, original. Indeed, the model is completely new and our analysis led us to an exhaustive description of the linearised system, disclosing some interesting and unexpected features.

The modal analysis of our model can be decomposed into three subproblems: the viscoelastic string loaded with equally spaced point masses, the vibrating string with equally spaced hanging pendula, and, eventually, the pendula hanging from the viscoelastic string. Each can be investigated independently and represents a rich problem in itself; accordingly, each original result is potentially significant in different fields. Here, we convey some of the (partially) explored topics.

Synchronization. We study synchronization phenomena in coupled pendula, constructing a model which accounts for the flexibility of the coupling structure and its continuous nature. With respect to other discretised finite-dimensional models, this choice allows not only to portray a more realistic coupling structure, but also to adopt a damping model different from the viscous friction, to derive general results for an arbitrary number of pendula, and to give an explanation for the different synchronization regimes.

Waves in a locally periodic medium. The locally periodically loaded string is a well-known model, which belongs to a wider class of systems that describes waves in a locally periodic medium. For this system, we recover a known expression for the eigenvalue equation, in terms of Chebyshev polynomials, providing an alternative derivation of the result. Moreover, we enrich the description of such a system by including a Kelvin-Voigt dissipative term, and also for this case we obtain, for any number of masses, closed-form expressions for the eigenvalue equations and the eigenfunctions, in terms of Chebyshev polynomials of the second kind. Furthermore, we prove that similar expressions are obtained when the equally spaced masses are replaced by harmonic oscillators.

Lagrangian mechanics. The construction of the model is based on a Lagrangian description of the system, considering a particle-field type of interaction. In fact, the model is a "hybrid" system in the sense that it is composed of both discrete and continuous degrees of freedom.

Spectral theory. The analysis conducted for the dynamics of the system relies on the characterisation of the spectrum, and the associated eigenfunctions, of a system of coupled second-order ODEs and hyperbolic PDEs. For our model, a weak formulation of the problem is left to future study. Our description in the conservative case is fully

analytical, while in the dissipative regime, part of our spectral study relies on a numerical investigation.

Part III represents an initial study based on ideas that can be found spread in the literature of unforced synchronization, mostly employed ad hoc to specific problems. Since we were not able to find a precise theory, ours is a first attempt to systematically apply some classical techniques to study these problems in a general framework. However, the analysis in this direction has only been initiated and no conclusive results have been found, and the discussion belongs to the chapter "future perspectives", as further investigation is required.

Part I

A look at synchronization in systems of coupled pendula

Chapter 1

Short review of the literature

The study of the synchronous behaviour of coupled systems started with a fortuitous observation made in 1665 by Christiaan Huygens, who had constructed the first pendulum clock some years before [17]. Huygens's pendulum clock consisted of an oscillating pendulum embedded in a wooden chase, kept in motion by an escapement mechanism. He noticed that when two of those pendula with very closely matched frequencies hung side by side from a common wooden beam supported by two chairs, they would spontaneously adjust their rhythm, and after a transient, they would oscillate synchronously in opposite directions, motion now referred to as 'anti-phase' synchronization. Instead, when they were hanging on a wall or out-distanced, each pendulum would oscillate without influencing the motion of the other one.

Huygens's clocks are one of the mechanical systems which exhibit synchronization phenomena that received the greatest interest. Reproductions and variations of the original experiment are still carried out today, and several models, rich in new details, try to grasp the fundamental features of the synchronization of Huygens's pendulum clocks [39]. A major obstacle in understanding the phenomenon – with the consequence of considering this problem still open ([39]) – is the fact that anti-phase synchronization is not the only behaviour that pendulum clocks manifest. On the contrary, a notable aspect that emerges when we face the literature on this subject is the great variety of possible dynamics that a pair, or more, of coupled pendula manifest. In general, it is still not clear what to expect a priori from a new experiment. Examples of motions recorded following Huygens's observations are in- or anti-phase synchronization, beats, beating death, quenching, clustering, chimera states, ... For an up-to-date review, we refer to, e.g., [14] and references therein.

The focus on pendulum clocks, and more generally on systems of pendula, is motivated not only by the historical significance but also – and possibly foremost – by their central role in mechanics. In fact, being a one-dimensional nonlinear holonomically constrained system in a conservative field, the pendulum provides sufficient material to better understand synchronous behaviours in other mechanical systems. Indeed, phenomena analogous to the above-mentioned types of synchronization in systems of pendulum clocks have been witnessed, for example, in coupled metronomes ([34]). Moreover, several applications

have been developed in the context of control synchronization (see [31]) and, even in this context, pendulum-like systems play a major role.

This chapter presents a partial overview of some of the main models employed in the study of synchronization of mechanical systems and, more specifically, of systems of coupled pendula inspired by Huygens clocks. In doing that, we resolve to provide a proper contextualisation for the system we will address in the following Part. In particular, we organise the collected material in order to point out the principal research lines on this topic, and the shortcomings of the modelling. We evaluate only theoretical studies, while for a review of the experimental evidence we refer to [36].

1.1 Huygens's clocks

First of all, it is instructive to give a detailed look at the Huygens observations, and at the prototypical first model which tried to explain the underlying mechanisms. Indeed, they are paradigmatic for any study of synchronization of coupled mechanical (pendulum-like) oscillators.

1.1.1 Huygens - first observation

Through thorough observations gathered from further experiments, Huygens could provide a quite detailed and comprehensive description of the behaviour of his two pendulum clocks [18]. The key properties can be summarised as follows.

1. The synchronization is consistently always in anti-phase, howsoever the motion is initiated. This means that, after a transient, at each oscillation the pendula reach their maximum amplitudes at the same time, but in opposite direction with respect to the resting configuration.

2. The common oscillation frequency when synchronised differs from the proper one of each pendulum when not interacting, and it is in fact a value in-between.

3. The interaction between the pendula is ascribable to the imperceptible movements of the common wooden support. When the clocks are positioned in different configurations, like laid on the ground back-to-back or side-by-side, the motion of each pendulum is not affected by the other.

4. The synchronous behaviour is robust with respect to small perturbations, namely after being disturbed, the pendula would tend to swing with opposite phases again.

1.1.2 Korteweg - first model

The first attempts at a mathematical description of Huygens's work started in the 20th century with the work of D.J. Korteweg [22]. His analysis is based on the belief that the fundamental properties of Huygens's observations could be fully described by a three-degree-of-freedom system, in which the clocks are modelled by (not necessarily

identical) pendula and the wooden supporting bar by a one-degree-of-freedom linear oscillator. Korteweg does not introduce in this mathematical model either driving forces or dissipative terms, and works in the regime of small oscillations. His analysis, based on the normal modes of oscillation, leads, in particular, to the following conclusions:

1. the generic small oscillation of his system is the linear superposition of three normal modes, two of which corresponding to the in-phase configuration and one corresponding to the anti-phase configuration;

2. in the normal mode corresponding to the anti-phase configuration, the displacement of the supporting bar is small with respect to the amplitude of oscillation of the pendula, and smaller compared to the other two normal modes;

3. the frequency of oscillation associated to the anti-phase normal mode has a value in-between the proper frequency of each pendulum, while the frequencies of the in-phase normal modes are respectively greater/smaller than the proper frequency of both pendula;

4. the motion of a pendulum greatly affects the other whenever their lengths (and hence their proper frequencies) are comparable.

Subsequently, Korteweg remarks that "friction" was certainly not negligible in Huygens's experiment and discusses that, as a matter of fact, the observed emergence of synchronization is ascribable to the great dissipation of energy associated with the motion of the supporting bar. Korteweg observes that, as the parameters change, the three normal modes dissipate energy differently, and the energy supplied by the escapement mechanisms of the clocks might not compensate for the dissipation in those normal modes in which the amplitude of oscillation of the bar is of the same order as that of the pendula. In particular, for values of the parameters corresponding to Huygens's set-up, the anti-phase synchronization of the two pendula could be explained as the only normal mode, out of the three, which was energetically sustainable.

Korteweg's model was able to give an explanation to experimental evidence of other phenomena connected with the anti-phase synchronization observed by Huygens. For example, he was motivated also by the observations by J. Ellicott, among others, who reported that two pendulum clocks laid on the same rail would undergo beating oscillations, namely periodic and alternating variations of the amplitude of the oscillations due to the exchange of energy. According to Korteweg's reasoning, the emergence of beats was justifiable in terms of the superposition of two normal modes having close frequencies and both associated with a small (with respect to the amplitudes of oscillation of the pendula) displacement of the supporting bar.

1.2 Features of the models

Both Huygens's experiment and Korteweg's model found great appeal. Remarkably, even apparently similar experimental setups show that different collective behaviours

may emerge: for example, very close reproductions of Huygens's experiment may exhibit in-phase synchronization ([36]). The very existence of a large number of ad hoc studies of different models seems to indicate the lack of a unifying understanding.

Here, we focus our survey on the research strategies rather than on the types of synchronization attained. More precisely, in this section we collect and present a summary of the main features which characterise the most popular models for two, or more, coupled pendulum-like oscillators. A discussion regarding the outcomes of such models and their agreement with the observations is not included; instead, we provide references for these aspects.

Models of pendula

The first choice for the model is the type of oscillator used to describe the pendula.

The simplest possibility is the *pendulum*, whose linearisation at the stable equilibrium is the *harmonic oscillator*. Instances of studies based on such models of possibly dissipative coupled pendula are the already mentioned Korteweg's [22] and the more recent [46].

Most studies include some sources of energy supply, which prevent the pendula from asymptotically stopping as a result of dissipative contributions. Indeed, to this end, systems that admit a limit cycle are often preferred.

This can be achieved by considering the so-called "self-sustained" oscillators, examples of which are the *Van der Pol oscillator*, the *Duffing oscillator*, and the *Andronov oscillator* [32].

Alternatively, an external driving force can be introduced to model, for example, an impulsive *escapement mechanism* [7], [12], [21], [14].

Degrees of freedom

The number of degrees of freedom of the system can vary depending on either the coupling structure model or the number of pendula considered.

Coupling. The degrees of freedom of the coupling structure may not be included in the model. This can be achieved by adopting different approaches. One way the pendula might interact is by means of a massless structure, for example, an elastic string (as in [28]) or, conversely, a structure with great inertia (as assumed in [32]). More generally, the *direct coupling* may be modelled as a suitable coupling function (see [45]).

Alternatively, the degrees of freedom of the coupling structure may be taken into account. A one-degree-of-freedom coupling, as the one considered by Korteweg, models, for example, a rigid bar that can move in one dimension, and is often referred to as *Huygens type coupling*, e.g., [21]. Some degree of elasticity of the coupling structure has been considered, allowing the pivots of the pendula to move, in four-degree-of-freedom models ([12]), or more ([44]). Finally, a higher number of degrees of freedom have been modelled using finite element methods (see [35]).

To our knowledge, there are no studies in which the coupling is analysed as a continuum.

Number of pendula. Most studies deal with two coupled pendula. Some generalisations to three or more have been considered, e.g., in [21], [20] and [28], and analysed through numerical simulations.

To our knowledge, there are no analytical studies dealing with a generic number of pendula.

Parameters

Both experiments and models reveal a great sensitivity of the emergence of synchronization to the physical parameters. Without dwelling upon how they influence the dynamics, we list here the main ones, as we shall encounter them in our model as well.

i. Mass ratio of pendula and coupling structure.
ii. Stiffness of the structure.
iii. Proper frequency of the pendula.
iv. Damping coefficients.

As these parameters vary, bifurcations emerge (see, e.g., [20]). Moreover, often, some of the parameters are considered to be small; in which cases the analysis proceeds, for example, under the hypothesis of weak coupling or weak damping, as in [7].

1.3 Some comments

From the map outlined in the previous section, one may perceive not only the great variety of models and the complexity of the related analyses, but also some of the issues left unsolved from these studies. We can assert that a major obstacle in constructing a general framework is, as we portrayed, the number of variables entering the models and the difficulty to discern how each contribution affects the overall dynamics. Indeed, as, for example, advanced in [12], despite the fact that several models are rich in details, a defined identification of the underlying mechanisms which influence the collective behaviours of these systems is still lacking. The study we present in this thesis aims to take a step forward in this direction. In this perspective, and on the basis of the evidence that we discussed, we argue that the details of the dissipative contributions are a fundamental factor. Hence, we choose to consider unforced systems only and, accordingly, our analysis will focus on the study of the asymptotic dynamics.

Besides, it might be restrictive to investigate these phenomena starting from a strict definition of synchronization (for one, distinguishing between in- or anti-phase). Indeed, the variety of correlated phenomena suggests that a wider perspective might be preferred. Ultimately, to fix the concept, we can think of synchronicity phenomena, in a quite indefinite fashion, as the ability of an observer to discern, in the dynamics of complex

systems, quasi-periodic behaviours. We will eventually discuss in our analysis specific regimes and their peculiarities.

Finally, as mentioned above, coupled pendula models with many degrees of freedom have been investigated only numerically. We try to fill this gap by analytically examining an infinite degree-of-freedom system, in which the continuous nature of the coupling structure is taken into account, and by deriving results valid for an arbitrary number of pendula.

Part II

Study of a system of pendula hanging from a viscoelastic string

Chapter 2

The hybrid system

In this chapter, we introduce the model of the mechanical system which will be the object of our study in this part of the dissertation. Such a system consists of a viscoelastic string fixed at its ends and of an arbitrary number of identical pendula hanging from it, equally spaced. The characteristics of our model will be detailed in Section 2.3, however, we anticipate that its peculiarity is to be hybrid, in that discrete and continuous components are coupled. Accordingly, the equations of motion governing the dynamics are a system of coupled ODEs and PDEs. Furthermore, our model describes a dissipative system, without forcing, where the viscoelasticity of the string is responsible for the dissipation.

Our study of this system evolves progressively from a Lagrangian formulation of the problem to the description of asymptotic synchronization phenomena for the pendula. In this chapter, we define our model and derive the equations of motion for the infinite-dimensional coupled system. In particular, in Section 2.3.3 we introduce the "horizontal and vertical systems", obtained by linearising the equations about the stable configuration of equilibrium. Their study is the main goal of this work.

2.1 Lagrangian systems

Conservative mechanical systems, both finite- and infinite-dimensional, admit a natural Lagrangian description. In this section, we recall the basic notions of the Lagrangian formulation of mechanics and field theory, mainly following Arnold's exposition [1–3], and [29]. As prototypical examples, we refer to the pendulum and the vibrating string, which, in fact, are the components of the system that we intend to investigate.

2.1.1 Lagrangian formulation for mechanics

Let Q be a d-dimensional connected smooth manifold and TQ its tangent bundle. For any configuration point $q \in Q$, its tangent vector $\dot{q} \in T_qQ$ is the velocity, and the pair $(q, \dot{q}) \in TQ$ is a state in the phase space. Let then g be a Riemannian metric on Q and $V : Q \to \mathbb{R}$ a smooth function. We consider the (autonomous and conservative) mechanical system (Q, g, V) which describes a holonomically constrained d degree-of-freedom system

of material points, with configuration manifold Q, kinetic energy $T(q,\dot{q}) = \frac{1}{2}g_q(\dot{q},\dot{q})$ and potential energy $V(q)$. We take as Lagrangian of the system the smooth scalar function on the phase space $L : TQ \to \mathbb{R}$ defined by $L(q,\dot{q}) := T(q,\dot{q}) - V(q)$. The equations of motion in the lifted local coordinates $(q^1,\dots,q^d,\dot{q}^1,\dots,\dot{q}^d)$ in TQ are the Lagrange equations

$$\left(\frac{d}{dt}\frac{\partial L}{\partial \dot{q}^i}\right)(q,\dot{q},\ddot{q}) - \frac{\partial L}{\partial q^i}(q,\dot{q}) = 0, \quad i = 1,\dots,d, \tag{2.1}$$

which are a system of d second-order ordinary differential equations. A motion is a curve $t \to q(t) \in Q$ solution of (2.1), and the pair $(q(t),\dot{q}(t))$ identifies the state of the system at time t.

For such a system, the energy function $E : TQ \to \mathbb{R}$,

$$E(q,\dot{q}) := T(q,\dot{q}) + V(q), \tag{2.2}$$

is a first integral, namely $\frac{d}{dt}E(q(t),\dot{q}(t)) = 0$ along any motion $t \to q(t) \in Q$.

A state $(q_{eq}, v_{eq}) \in TQ$ is called equilibrium if $t \to q_{eq}$ is a constant solution of (2.1). In particular, $(q_{eq}, 0)$ is an equilibrium if and only if q_{eq} is a critical point for V.

2.1.2 The pendulum

We consider as a basic example of Lagrangian system the pendulum, a heavy material point of mass m constraint to move without friction on a circle of radius l in a vertical plane. The configuration space is diffeomorphic to S^1 and can be parametrised by an angle ϕ measured from the downward vertical. The Lagrangian is then

$$L(\phi,\dot{\phi}) = \frac{1}{2}ml^2\dot{\phi}^2 + mgl\cos\phi,$$

with g the constant gravitational acceleration. The equation of motion is

$$\ddot{\phi} + \omega_p^2 \sin\phi = 0$$

with $\omega_p := \sqrt{\frac{g}{l}}$ the proper frequency of the pendulum.

2.1.3 Lagrangian formulation for fields

Let $D \subset \mathbb{R}^3$ be a bounded, open set with smooth boundary ∂D. Let Q be a Hilbert manifold of functions on $\overline{D}$ and TQ its tangent bundle ([24]). For any configuration $u \in Q$, its tangent vector $u_t \in T_uQ$ is the velocity, and the pair $(u,u_t) \in TQ$ is a state in the phase space. Let then g be a Riemannian metric on Q and $V : Q \to \mathbb{R}$ a smooth functional. We consider the (autonomous and conservative) continuous mechanical system (Q,g,V), with configuration manifold Q, kinetic energy $T(u,u_t) = \frac{1}{2}g_u(u_t,u_t)$ and potential energy $V(u)$, and we take as Lagrangian of the system the smooth functional on the phase space $L : TQ \to \mathbb{R}$ defined by $L(u,u_t) := T(u,u_t) - V(u)$. Let $x = (x^1,x^2,x^3)$ be coordinates on D and let the subscripts denote the partial derivatives of u (e.g.,

$u_{x^i} = \frac{\partial u}{\partial x^i}, u_{x^i x^j} = \frac{\partial^2 u}{\partial x^i \partial x^j}, \dots$). The Lagrangian can be expressed in terms of a so-called Lagrangian density $\mathcal{L}$ as

$$L(u, u_t) = \int_D \mathcal{L}(u, u_x, \dots, u_t, u_{tx}, \dots, x)\, dx.$$

Let $\nabla_\alpha L$ denote the L^2-gradient of L with respect to its arguments $\alpha = u, u_t$; for example, if $\mathcal{L} = \mathcal{L}(u, u_x, u_t)$, $\nabla_u L = \frac{\partial \mathcal{L}}{\partial u} - \frac{d}{dx}\frac{\partial \mathcal{L}}{\partial u_x}$, $\nabla_{u_t} L = \frac{\partial \mathcal{L}}{\partial u_t}$. The equations of motion are the Euler-Lagrange equations

$$\frac{d}{dt}\nabla_{u_t} L(u, u_t) - \nabla_u L(u, u_t) = 0 \qquad \text{in } D, \tag{2.3}$$

to be supplemented by the boundary conditions $u = g$ on ∂D, g being given.

For such a system, the energy function $E : TQ \to \mathbb{R}$,

$$E(u, u_t) := T(u, u_t) + V(u), \tag{2.4}$$

is a conserved quantity.

A configuration $u_{eq} \in Q$ is called equilibrium configuration if $t \to u_{eq}$ is a stationary solution of (2.3) that satisfies the boundary conditions. In particular, $\nabla_u L(u_{eq}, 0) = 0$.

2.1.4 The vibrating string

We consider as an example of a continuous mechanical system a model of a string with the following properties (as in [43], Chap. 5.2): homogeneous, infinitesimally thin, perfectly flexible, and elastic string, with extremities fixed, which lays horizontally and tightly stretched in the gravitational field, and we shall assume it performs small transverse vibrations from the equilibrium configuration, in a vertical plane. By this, we mean the following (standard)

constitutive properties:

- *infinitesimally thin:* the string is a one-dimensional object;
- *homogeneous:* the linear density is constant along the length of the string; ρ will denote the value of the density of the string at rest;
- *perfectly flexible:* the tension is a force which, at any point of the string, acts tangentially, hence there is no resistance to bending;
- *perfectly elastic:* the tension is constant, and τ will denote its magnitude;

static properties:

- *horizontal:* the extrema of the string are fixed at the same level with respect to the vertical direction, at a distance Λ that is the length of the resting string;
- *tightly stretched:* the string is subject only to small changes (with respect to its length) in the slope from the horizontal equilibrium configuration;

dynamical properties:

- *heavy:* gravity acts on any point of the string, with constant acceleration g;
- *small transverse vibrations:* each point of the string moves transversally to the equilibrium configuration, and these displacements are small (with respect to the length of the string). Longitudinal displacements are neglected.

The configuration of the system is a function $u \in H$, that represents the transverse displacement of the string, with H a space of functions $[0, \Lambda] \to \mathbb{R}$ which vanish at 0 and Λ. Let x be the coordinate on $[0, \Lambda]$. The Lagrangian of the system is

$$L(u, u_t) = \int_0^\Lambda \left[\frac{\rho}{2} u_t^2 - \frac{\tau}{2} u_x^2 - \rho g u \right] dx. \tag{2.5}$$

The associated Euler-Lagrange equation – a second-order hyperbolic linear nonhomogeneous PDE with constant coefficients –, supplemented by homogeneous Dirichlet boundary conditions, is the wave equation for the so-called "vibrating string":

$$\begin{cases} \rho u_{tt} - \tau u_{xx} = f \\ u|_0 = u|_\Lambda = 0 \end{cases} \tag{2.6}$$

where $f = -\rho g$.

The equilibrium configuration is

$$u_{eq}(x) = \frac{\rho g}{2\tau}(x^2 - \Lambda x),$$

namely the profile of the string at the equilibrium is a parabola. (The parabolic shape is due to the hypotheses of elasticity and small displacements; the profile is a catenary for an inextensible string [19]). It is convenient to redefine u as $u - u_{eq}$ and work with rescaled coordinate and time $x' = \frac{x}{\Lambda}$, $t' = \sqrt{\frac{\tau}{\rho}} \frac{\pi}{\Lambda} t$, and still denote them x, t. After this rescaling, the vibrating string equation (2.6) becomes

$$\begin{cases} \pi^2 u_{tt} - u_{xx} = 0 \\ u|_0 = u|_1 = 0. \end{cases} \tag{2.7}$$

For any $\ell \in \mathbb{Z}_+$, the ℓ-th normal mode, defined as a family of nonzero solutions of (2.7) of the form

$$u_\ell(x, t) = \mathrm{Re}\left(c_\ell f_\ell^{\mathrm{S}}(x) e^{i\omega_\ell^{\mathrm{S}} t} \right), \quad c_\ell \in \mathbb{C} \setminus \{0\},$$

has frequency

$$\omega_\ell^{\mathrm{S}} = \ell \tag{2.8}$$

and associated eigenfunction

$$f_\ell^{\mathrm{S}}(x) = \sin(\pi\, \omega_\ell^{\mathrm{S}}\, x), \quad x \in [0, 1]. \tag{2.9}$$

The spectrum of the system is $\mathrm{Sp}^{\mathrm{S}} = \{\pm i\omega_\ell^{\mathrm{S}}\}_{\ell \in \mathbb{Z}_+}$, and it consists of countably many eigenvalues equally spaced along the imaginary axis.

The energy of the vibrating string at time t, in rescaled variables, is

$$E_t(u, u_t) = \frac{1}{2}\int_0^1 (u_t^2 + u_x^2)\, dx, \tag{2.10}$$

which is a conserved quantity for system (2.7). Indeed, $\frac{d}{dt}E_t(u, u_t) = 0$ for every solution $t \mapsto u$.

2.2 Models of dissipation

Next, we discuss the modelling of dissipative contributions, which cause the mechanical energy of the system to decrease over time. In general, their laws have to be determined empirically, from physical reasonings and experimental evidence, and several such sources might affect the motion concurrently.

We may generically distinguish between internal and external sources of dissipation, depending on whether they come from the interaction among parts of the system or with external elements, respectively. These contributions are commonly accounted for in the model with the inclusion of suitable additional forces in the Lagrange equations.

The example of a viscously damped pendulum is classical. The system is described by the equation $\ddot{\phi} + \omega_p^2 \sin\phi + \gamma\dot{\phi} = 0$, where the force $-\gamma\dot{\phi}$, with $\gamma > 0$, accounts for the viscous friction of the air acting upon the pendulum. The mechanical energy of this pendulum decays at a rate proportional to its kinetic energy.

More diverse are the models of dissipation for infinite-dimensional systems. For a string, for example, typical sources of dissipation come again from the interaction with an external fluid, but now also from internal friction, due, for example, to deformation or bending. Classical damping models for a string with density ρ, length Λ and displacement u, are the following (see, e.g., [43]):

- *viscous damping*: $-\gamma(x)\rho u_t$;
- *viscoelastic damping*: $\gamma(x)u_{txx}$;

where the damping coefficient γ is positive and might be, in principle, a function of x.

In the following sections, we detail the main properties of these models, one of which will be adopted for our system. In this description we consider $\gamma > 0$ constant, and we refer to [11] for the former model and to [41] for the latter. A combined study of the two is presented, e.g., in [23].

2.2.1 The viscous string

Drag forces act on the string as it moves in a viscous medium (typically the air) and are therefore an external source of dissipation. Such contributions are modelled as a linear term proportional to the velocity of the system, in analogy with viscously damped finite-dimensional systems.

The equation of motion of the viscous string is

$$\pi^2 u_{tt} - u_{xx} + \nu\pi^2 u_t = 0 \tag{2.11}$$

with $\nu > 0$ the damping coefficient.

The energy function (2.10) decreases at a rate that is proportional to the kinetic energy of the string: along any non-stationary solution $t \to u$ of (2.11) with Dirichlet boundary conditions $u|_0 = u|_1 = 0$,

$$\frac{d}{dt}E_t(u, u_t) = -\nu \int_0^1 u_t^2 \, dx.$$

The eigenvalues of the eigenvalue problem associated to (2.11) with $u|_0 = u|_1 = 0$ are the nonzero solutions $\lambda \in \mathbb{C}$ of the equation*

$$\sinh\left(\pi(\lambda^2 + \nu\lambda)^{1/2}\right) = 0.$$

Hence, the spectrum Sp^v_ν of the viscous vibrating string consists of the eigenvalues

$$\lambda^v_{\ell,\pm} = -\frac{\nu}{2} \pm \sqrt{\left(\frac{\nu}{2}\right)^2 - \ell^2}\,, \quad \ell \in \mathbb{Z}_+. \tag{2.12}$$

Remark 2.1. In particular, Sp^v_ν contains finitely many (and possibly zero) negative real eigenvalues

$$r^v_{\ell,\pm} := \lambda^v_{\ell,\pm}, \quad \ell \le \left\lfloor \frac{\nu}{2} \right\rfloor,$$

and a countable infinity of complex conjugate pairs of eigenvalues with nonzero imaginary part and constant real part

$$\lambda^v_\ell := \lambda^v_{\ell,+}\,, \;\; \overline{\lambda}^v_\ell := \lambda^v_{\ell,-}, \quad \ell > \left\lfloor \frac{\nu}{2} \right\rfloor$$

(see Figure 2.1).

2.2.2 The viscoelastic string

The viscoelastic damping models the internal dissipation caused by the friction between the particles composing the string as it bends. The conversion of mechanical energy into heat leads to a decrease in tension that depends on the velocity of the change in slope. For a generic continuum, the *Kelvin-Voigt model* of viscoelasticity introduces a linear term proportional to the elasticity operator that acts on the velocity.

For a viscoelastic string with damping coefficient $\nu > 0$, the Kelvin-Voigt equation is

$$\pi^2 u_{tt} - u_{xx} - \nu u_{txx} = 0. \tag{2.13}$$

*We find it convenient, here and in the following, to make the convention that $(\,)^{1/2}$ denotes the complex square root with nonnegative imaginary part, which is analytic in $\mathbb{C} \setminus \{x \ge 0\}$.

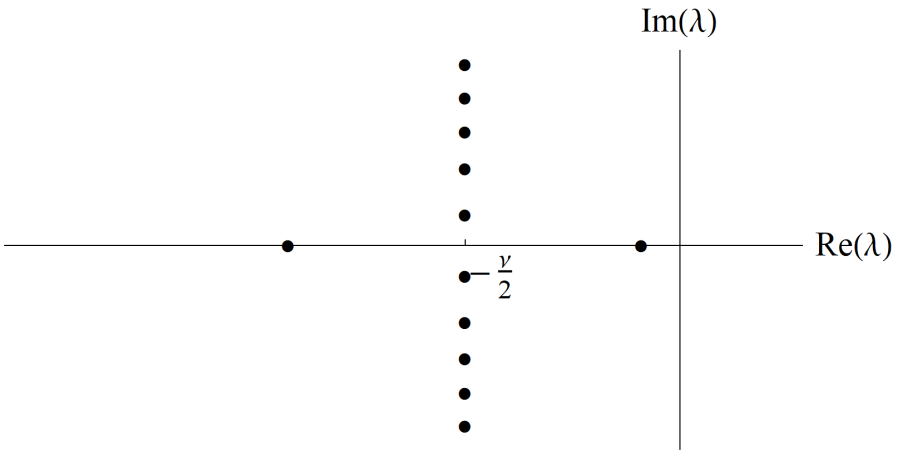

Figure 2.1: The eigenvalues (2.12) of the viscous string. The numerical value used in the generation of the picture is $\nu = 3.5$. The two eigenvalues on the real axis are $r^v_{1,\pm}$, while the countably many nonreal ones are $\lambda^v_\ell, \overline{\lambda}^v_\ell$ with $\ell \geq 2$, having constant real part equal to $-\frac{\nu}{2}$.

The energy function (2.10) is strictly decreasing along any non-stationary solution $t \to u$ of (2.13) with Dirichlet boundary conditions $u|_0 = u|_1 = 0$:

$$\frac{d}{dt} E_t(u, u_t) = -\frac{\nu}{\pi^2} \int_0^1 u_{tx}^2.$$

The eigenvalues of the eigenvalue problem associated to (2.13) with $u|_0 = u|_1 = 0$ are the nonzero solutions $\lambda \in \mathbb{C}$ of the equation

$$\sinh\left(\frac{\pi\lambda}{(1+\nu\lambda)^{1/2}}\right) = 0. \tag{2.14}$$

Hence, the spectrum Sp^{KV}_ν of the vibrating string with Kelvin-Voigt damping consists of the eigenvalues

$$\begin{aligned} \lambda^{\mathrm{KV}}_{\ell,\pm} &= -\frac{\nu\ell^2}{2} \pm \sqrt{\left(\frac{\nu\ell^2}{2}\right)^2 - \ell^2} \\ &= -\frac{\nu(\omega^{\mathrm{S}}_\ell)^2}{2} \pm \sqrt{\left(\frac{\nu(\omega^{\mathrm{S}}_\ell)^2}{2}\right)^2 - (\omega^{\mathrm{S}}_\ell)^2}\,, \quad \ell \in \mathbb{Z}_+, \end{aligned} \tag{2.15}$$

and the associated eigenfunction are

$$f^{\mathrm{KV}}_\ell(x) = \sin(\pi\omega^{\mathrm{S}}_\ell\, x)\,, \quad \ell \in \mathbb{Z}_+. \tag{2.16}$$

Remark 2.2. In particular (see Figure 2.2), the spectrum Sp^{KV}_ν consists of a countable infinity of negative eigenvalues

$$r^{\mathrm{KV}}_{\ell,\pm} := \lambda^{\mathrm{KV}}_{\ell,\pm}, \quad \ell \geq \left\lceil \frac{2}{\nu} \right\rceil,$$

which belong to the interval $(-\infty, -\frac{1}{\nu})$ and accumulate to its boundaries, and of a (possibly zero) finite number, which equals $\lfloor \frac{2}{\nu} \rfloor$, of pairs of nonreal complex conjugate eigenvalues

$$\lambda_\ell^{\mathrm{KV}} := \lambda_{\ell,+}^{KV}\,, \quad \overline{\lambda}_\ell^{\mathrm{KV}} := \lambda_{\ell,-}^{KV}, \quad \ell < \left\lceil \frac{2}{\nu} \right\rceil,$$

which belong to the circle C_ν of centre $(-\frac{1}{\nu}, 0)$ and radius $\frac{1}{\nu}$.

Remark 2.3. An important feature of the Kelvin-Voigt model is that it gives a frequency-dependent damping. In particular, the less damped normal modes are the λ_ℓ^{KV}'s with small ℓ (unless ν is very large and they are absent). For small ν, those with $\ell \ll \frac{2}{\nu}$ have a decay rate $|\mathrm{Re}(\lambda_{\ell,\pm}^{KV})| = \frac{1}{2}\nu\ell^2$ which grows in an approximately quadratic way with their frequency $|\mathrm{Im}(\lambda_{\ell,\pm}^{KV})| = \frac{1}{2}\ell\nu\sqrt{(\frac{2}{\nu})^2 - \ell^2} \approx \ell$.

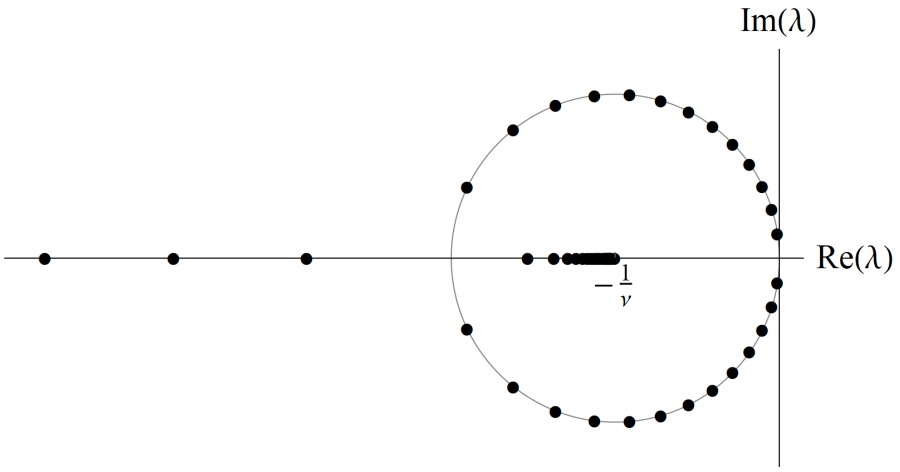

Figure 2.2: The eigenvalues (2.15) of the Kelvin-Voigt viscoelastic string. The numerical value used in the generation of the picture is $\nu = 0.15$. Countably many eigenvalues, $\lambda_{\ell,\pm}^{KV}$ with $\ell \geq 14$, belong to the negative real axis, and $\lfloor \frac{2}{\nu} \rfloor$ pairs of complex conjugate eigenvalues, $\lambda_{\ell,\pm}^{KV}$ with $\ell \leq 13$, belong to C_ν.

2.3 Our model

In this section, we detail the construction of our model for the system considered, which is formed by a vibrating string, modelled according to Section 2.1.4, with the inclusion of a Kelvin-Voigt term (see Section 2.2.2), and $n \geq 1$ identical pendula, as in Section 2.1.2, hanging from n equally spaced points of it, under the action of weight (see Figure 2.3).

We proceed as follows: we provide a Lagrangian description of the coupled 'hybrid' system and we derive the Euler-Lagrange equations for the Lagrangian density which describes our infinite-dimensional system in absence of dissipation; we then add the terms which account for the viscoelasticity of the string; finally, we linearise the system of

equations about the stable equilibrium configuration. The system of equations obtained will be the object of investigation in the upcoming chapters.

We remark that our choice for the damping model is motivated, on one hand, by experimental evidence on decay rates in strings (we refer to [41] for a review), and on the other, is targeted at the explanation of patterns in the asymptotic dynamics of the pendula. We shall comment on this aspect in Chapter 5, when discussing the details of the asymptotic dynamics of the system.

2.3.1 Configurations

Fix a coordinate system $\{O; X, Y, Z\}$ such that the extrema of the string are attached at the origin O and at the point $(\Lambda, 0, 0)$ and the Z-axis is directed as the ascending vertical. For each $t \in \mathbb{R}$, the configuration of the string at time t is described by an embedding of the form

$$[0, \Lambda] \ni x \mapsto \big(x, \psi(x,t), \zeta(x,t)\big) \in \mathbb{R}^3$$

where the "horizontal displacement" ψ and the "vertical displacement" ζ are two functions from $[0, \Lambda] \times \mathbb{R}$ to $\mathbb{R}$ which satisfy the homogeneous Dirichlet boundary conditions $\psi(0,t) = \psi(\Lambda, t) = \zeta(0,t) = \zeta(\Lambda, t) = 0 \ \forall t \in \mathbb{R}$.

We assume that $n \geq 1$ identical pendula of length l are hanging from the string and are constrained to move in vertical planes parallel to the YZ-plane. The pivot of the k-th pendulum is attached to the point of the string with coordinate x given by $\tilde{x}_k := \frac{k\Lambda}{n+1}$, and the position in the space of the k-th pendulum at time t is

$$\big(\tilde{x}_k \, , \, \psi\big(\tilde{x}_k, t\big) + l \sin(\phi_k(t)) \, , \, \zeta\big(\tilde{x}_k, t\big) - l \cos(\phi_k(t))\big)$$

where ϕ_k is the angle formed by the k-th pendulum with the downward vertical ($k = 1, \ldots, n$).

Remark 2.4. This mechanical system is "hybrid" in the sense that it consists of point masses coupled to a continuous system, and being so, its study requires techniques from both mechanics (see Section 2.1.1) and field theory (see Section 2.1.3). The description of similar systems is studied in [5]. To our knowledge, our model is completely new.

2.3.2 The equations of motion

We assume that the forces that act on the system are the weight of the string and the pendula, and the tension of the string. Both these forces are conservative. We assume moreover that internal dissipative forces act on the string, which we hence assume to be viscoelastic. We neglect other sources of dissipation, such as the viscous friction of the air.

We derive the equations of motion of the undamped coupled string-pendula system from a Lagrangian formulation, to which we then add the Kelvin-Voigt dissipation term. Proceeding for now formally, we consider the configuration space

$$\mathcal{M} := \mathbb{T}^n \times H \times H \ni (\phi, \psi, \zeta) = ((\phi_1, \ldots, \phi_n), \psi, \zeta)$$

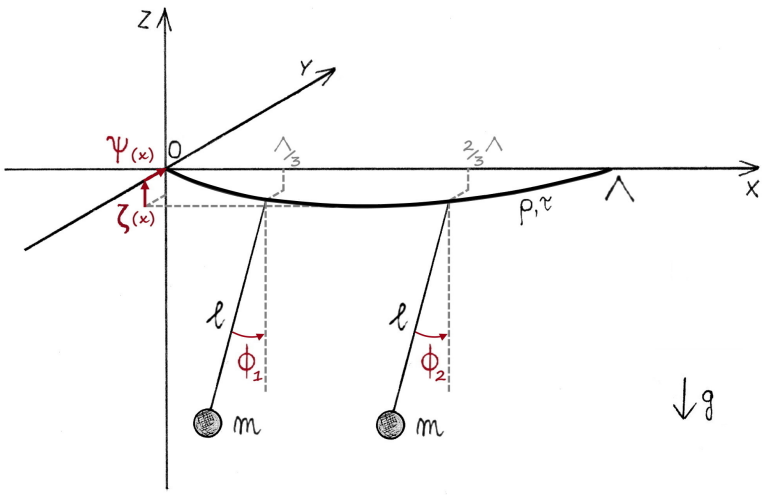

Figure 2.3: The system with $n = 2$ pendula.

where H is a space of functions $[0, \Lambda] \to \mathbb{R}$ that vanish at the extrema, to be better specified.

We choose as Lagrangian for the system the scalar functional in the (formal) tangent bundle $T\mathcal{M}$ given by the difference between the kinetic energy T and the potential energy V of the full (string+pendula) system, namely

$$L(\phi, \psi, \zeta, \dot{\phi}, \psi_t, \zeta_t) = T(\phi, \psi, \zeta, \dot{\phi}, \psi_t, \zeta_t) - V(\phi, \psi, \zeta)$$

with

$$T = \int_0^\Lambda \frac{\rho}{2}\left(\psi_t^2 + \zeta_t^2\right) dx + \frac{m}{2}\sum_{k=1}^{n}\left[l^2\dot{\phi}_k^2 + \left(\psi_t^2 + \zeta_t^2 + 2l\dot{\phi}_k\big(\psi_t\cos\phi_k + \zeta_t\sin\phi_k\big)\right)\Big|_{x=\tilde{x}_k}\right],$$

$$V = \int_0^\Lambda \left[\frac{\tau}{2}\left(\psi_x^2 + \zeta_x^2\right) + \rho g\zeta\right] dx + \sum_{k=1}^{n} mg\big(\zeta|_{x=\tilde{x}_k} - l\cos\phi_k\big).$$

The Lagrangian can be written as $L(\phi, \psi, \zeta, \dot{\phi}, \psi_t, \zeta_t) = \int_0^\Lambda \mathcal{L}(\phi, \psi, \zeta, \dot{\phi}, \psi_t, \zeta_t, \psi_x, \zeta_x)dx$ with Lagrangian density

$$\begin{aligned}\mathcal{L} \;=\; & \frac{\rho}{2}\left(\psi_t^2 + \zeta_t^2\right) - \frac{\tau}{2}\left(\psi_x^2 + \zeta_x^2\right) - \rho g\zeta + \\ & \sum_{k=1}^{n}\left[\frac{m}{2}\left(l^2\dot{\phi}_k^2 + \psi_t^2 + \zeta_t^2 + 2l\dot{\phi}_k\left(\psi_t\cos\phi_k + \zeta_t\sin\phi_k\right)\right) - mg\left(\zeta - l\cos\phi_k\right)\right]\delta_{\tilde{x}_k}\end{aligned} \tag{2.17}$$

where $\delta_{\tilde{x}_k}(x) := \delta(x - \tilde{x}_k)$, with δ the Dirac delta.

We take as equations of motion the Euler-Lagrange equations for the Lagrangian density $\mathcal{L}$ with the inclusion of a Kelvin-Voigt term, with damping coefficient $\gamma \geq 0$, in

the equations for the horizontal and vertical displacement of the string, complemented with the homogeneous Dirichlet boundary conditions, namely the system

$$\begin{aligned}
&\frac{d}{dt}\frac{\partial \mathcal{L}}{\partial \dot{\phi}_k} - \frac{\partial \mathcal{L}}{\partial \phi_k} = 0 \qquad (k = 1, \dots, n)\\
&\frac{d}{dt}\frac{\partial \mathcal{L}}{\partial \psi_t} - \frac{\partial \mathcal{L}}{\partial \psi} + \frac{d}{dx}\frac{\partial \mathcal{L}}{\partial \psi_x} - \gamma \psi_{txx} = 0\\
&\frac{d}{dt}\frac{\partial \mathcal{L}}{\partial \zeta_t} - \frac{\partial \mathcal{L}}{\partial \zeta} + \frac{d}{dx}\frac{\partial \mathcal{L}}{\partial \zeta_x} - \gamma \zeta_{txx} = 0\\
&\psi(0,t) = \psi(\Lambda,t) = \zeta(0,t) = \zeta(\Lambda,t) = 0
\end{aligned} \tag{2.18}$$

in $[0, \Lambda] \times \mathbb{R}$.

To reduce the number of parameters, we work with rescaled space and time coordinates $x' = \frac{x}{\Lambda}$, $t' = \sqrt{\frac{\tau}{\rho}}\frac{\pi}{\Lambda}t$, and still denote them x, t, and with rescaled displacements of the string $\psi' = \frac{\psi}{l}$ and $\zeta' = \frac{\zeta}{l}$, and still denote them ψ, ζ. Hence, we define the dimensionless parameters

$$\alpha := \sqrt{\frac{\rho g}{l\tau}}\,\frac{\Lambda}{\pi}, \qquad \mu := \frac{m}{\Lambda\rho}, \qquad \nu := \frac{\pi\gamma}{\sqrt{\rho\tau}\,\Lambda}, \qquad x_j := \frac{j}{n+1} \quad (j = 0, \dots, n+1). \tag{2.19}$$

Note that α is the ratio between the proper frequency $\sqrt{\frac{g}{l}}$ of the pendulum and the (dimensional) fundamental frequency $\frac{\pi}{\Lambda}\sqrt{\frac{\tau}{\rho}}$ of the vibrating string, while μ is the ratio between the mass of each pendulum and the total mass of the string. We assume $\alpha > 0$, $\mu > 0$, and $\nu \geq 0$. As noticed, after this rescaling of time, the frequencies of the vibrating string are $\omega_\ell^{\mathrm{S}} = \ell$, $\ell \in \mathbb{Z}_+$.

Written in these variables, equations (2.18) are the system

$$\begin{aligned}
&\ddot{\phi}_k + \left(\psi_{tt}\cos\phi_k + \zeta_{tt}\sin\phi_k\right)|_{x=x_k} + \alpha^2 \sin\phi_k = 0 \qquad (k = 1, \dots, n)\\
&\psi_{tt} + \sum_{k=1}^{n} \mu\left(\psi_{tt} + \ddot{\phi}_k\cos\phi_k - \dot{\phi}_k^2\sin\phi_k\right)\delta_{x_k} - \frac{1}{\pi^2}\psi_{xx} - \frac{\nu}{\pi^2}\psi_{txx} = 0\\
&\zeta_{tt} + \sum_{k=1}^{n} \mu\left(\zeta_{tt} + \ddot{\phi}_k\sin\phi_k + \dot{\phi}_k^2\cos\phi_k + \alpha^2\right)\delta_{x_k} - \frac{1}{\pi^2}\zeta_{xx} - \frac{\nu}{\pi^2}\,\zeta_{txx} + \alpha^2 = 0\\
&\psi(0,t) = \psi(1,t) = \zeta(0,t) = \zeta(1,t) = 0
\end{aligned} \tag{2.20}$$

in $[0,1] \times \mathbb{R} \ni (x,t)$, where $\delta_{x_k}(x) = \delta(x - x_k)$.

2.3.3 The linearised system

The equations of motion (2.20) have the equilibrium solution $t \mapsto (\phi_{eq}, \psi_{eq}(x), \zeta_{eq}(x))$ with

$$\begin{aligned}
&\phi_{eq} = (0, \dots, 0)\,, \qquad\qquad \psi_{eq}(x) = 0\,,\\
&\zeta_{eq}(x) = \pi^2\alpha^2\left(\frac{x^2}{2} - \frac{x}{2}(1 + n\mu) + \mu\sum_{k=1}^{n}(x - x_k)\Theta(x - x_k)\right)
\end{aligned} \tag{2.21}$$

where Θ denotes the Heaviside step function. In this equilibrium, all pendula are in their stable vertical position while the string, which lies in the vertical plane, has the profile of an arc of parabola in each interval $x_k \le x \le x_{k+1}$, $k = 0, \dots, n$, with not $\mathcal{C}^1$ matchings at the pendula's hanging positions.

Linearising system (2.20) at the equilibrium configuration (2.21) gives the two systems in $[0,1] \times \mathbb{R}$

$$\begin{aligned} &\ddot{\phi}_k + \psi_{tt}|_{x=x_k} + \alpha^2 \phi_k = 0 \qquad (k = 1, \dots, n) \\ &\psi_{tt} - \frac{1}{\pi^2}\psi_{xx} - \frac{\nu}{\pi^2}\psi_{txx} + \mu \sum_{k=1}^{n} \big(\psi_{tt} + \ddot{\phi}_k\big)\delta_{x_k} = 0 \\ &\psi(0,t) = \psi(1,t) = 0 \end{aligned} \tag{2.22}$$

and

$$\begin{aligned} &\zeta_{tt} - \frac{1}{\pi^2}\zeta_{xx} - \frac{\nu}{\pi^2}\,\zeta_{txx} + \mu \sum_{k=1}^{n} \zeta_{tt}\,\delta_{x_k} = 0 \\ &\zeta(0,t) = \zeta(1,t) = 0 \end{aligned} \tag{2.23}$$

where $\delta_{x_k}(x) = \delta(x - x_k)$ and ϕ, ψ, ζ stand now for the displacements $\phi - \phi_{eq}$, $\psi - \psi_{eq}$ and $\zeta - \zeta_{eq}$ from the equilibrium.

Thus, at the linear level, *the linearised dynamics of the pendula is coupled only to the horizontal displacement of the string, while the vertical displacement of the string decouples from the other degrees of freedom* (i.e., in the regime of small oscillations about the lower equilibrium position, the horizontal displacement of the pendula is an infinitesimum of order 1 while the vertical one is of order 2). Note, moreover, that system (2.22) depends on the three parameters α, μ, ν and system (2.23) depends on the parameters μ, ν. In particular, the second can be regarded as the (singular) limit of the first for $\alpha \to +\infty$, namely as the limit case of zero-length pendula. In fact, it may be shown that system (2.23) describes the motion in a plane of a viscoelastic vibrating string loaded with n identical and equidistant masses.

We call system (2.22) the *horizontal (linear) system* and system (2.23) the *vertical (linear) system*. We shall also refer to the latter as *Rayleigh's periodically loaded string*, as the undamped case for $n = 1$ was first studied by Lord Rayleigh [40].

2.3.4 Solutions of the linearised system

We close this chapter by defining what we mean by the solution of horizontal and vertical systems.

First, we specify the function spaces in which we will work for the study of (2.22) and (2.23):

i. $\mathcal{E}$ is the space of continuous functions $u : [0,1] \to \mathbb{R}$ which are C^2 in $(0,1) \setminus \{x_1, \dots, x_n\}$, have bounded left and right derivatives at $x_1, \dots, x_n$, and satisfy $u(0) = u(1) = 0$.

ii. $\mathcal{S}$ is the space of functions $v : [0,1] \times \mathbb{R} \to \mathbb{R}$, $(x,t) \mapsto v(x,t)$, which are C^2 in t and such that $v(\cdot, t) \in \mathcal{E}$ for every t.

iii. $\mathcal{P}$ is the space of functions of class C^2 from $\mathbb{R}$ to $\mathbb{T}^n$.

iv. $\Sigma^H := \mathcal{P} \times \mathcal{S}$ and $\Sigma^V := \mathcal{S}$.

v. $\mathcal{E}^{\mathbb{C}}$ is the space of continuous complex functions $u : [0,1] \to \mathbb{C}$ which are C^2 in $(0,1)\setminus\{x_1,\dots,x_n\}$, have bounded left and right derivatives at $x_1,\dots,x_n$, and satisfy $u(0) = u(1) = 0$.

vi. $\Sigma^H_{\mathbb{C}}$ and $\Sigma^V_{\mathbb{C}}$ are the spaces of complex functions whose real and imaginary parts belong to Σ^H and Σ^V respectively.

Moreover, we shall adopt the following notation: if $u \in \mathcal{E}$ we write $u'(x_k^{\pm})$ for $\lim_{x\to x_k^{\pm}} u'(x)$ $(k = 1,\dots,n)$. If $(\phi,\psi) \in \Sigma^H$ then $\psi_x(x_k^{\pm},t)$ and $\psi_{tx}(x_k^{\pm},t)$ have a similar meaning, and so also for $\zeta \in \Sigma^V$.

We define as *solution of the horizontal system* (2.22) any function $(\phi,\psi) \in \Sigma^H$ which satisfies

$$\begin{aligned}
&\ddot{\phi}_k(t) + \psi_{tt}(x_k,t) + \alpha^2\phi_k(t) \;=\; 0\\
&\psi_{tt}(x,t) - \frac{1}{\pi^2}\psi_{xx}(x,t) - \frac{\nu}{\pi^2}\psi_{txx}(x,t) \;=\; 0 \qquad\qquad \forall x \in (0,1)\setminus\{x_1,\dots,x_n\}\\
&\mu\big(\psi_{tt}(x_k,t) + \ddot{\phi}_k(t)\big) - \frac{1}{\pi^2}\big(\psi_x + \nu\psi_{tx}\big)(x_k^+,t) + \frac{1}{\pi^2}\big(\psi_x + \nu\psi_{tx}\big)(x_k^-,t) \;=\; 0
\end{aligned} \tag{2.24}$$

for all $t \in \mathbb{R}$ and $k = 1,\dots,n$. Similarly, we define as *solution of the vertical system* (2.23) any function $\zeta \in \Sigma^V$ which satisfies

$$\begin{aligned}
&\zeta_{tt}(x,t) - \frac{1}{\pi^2}\zeta_{xx}(x,t) - \frac{\nu}{\pi^2}\,\zeta_{txx}(x,t) \;=\; 0 \qquad\qquad \forall x \in (0,1)\setminus\{x_1,\dots,x_n\}\\
&\mu\zeta_{tt}(x_k,t) - \frac{1}{\pi^2}\big(\zeta_x + \nu\zeta_{tx}\big)(x_k^+,t) + \frac{1}{\pi^2}\big(\zeta_x + \nu\zeta_{tx}\big)(x_k^-,t) \;=\; 0
\end{aligned} \tag{2.25}$$

for all $t \in \mathbb{R}$ and $k = 1,\dots,n$.

We define as *solution of the linearised system* any function $(\phi,\psi,\zeta) \in \Sigma^H \times \Sigma^V$ with (ϕ,ψ) and ζ solutions of the horizontal and vertical system, respectively. Finally, by *complex* solutions of these systems we mean complex functions whose real and imaginary parts are real solutions.

Remark 2.5. This procedure is classical (see, e.g., [47], Appendix III to Ch. II). For the horizontal system, the jump of the x derivative at each point x_k is computed integrating the function in the second line of (2.22) in the interval $(x_k - \epsilon, x_k + \epsilon)$ and taking $\epsilon \to 0$; same with the first equation of (2.23) for the vertical system.

Chapter 3

The eigenvalue problem

In this chapter, we initiate the study of the solutions of the vertical and horizontal systems. In particular, since the two systems of equations (2.22) and (2.23) are linear, we deal with the associated eigenvalue problem. As we shall discuss, the locally periodic arrangement of the pendula along the string has a remarkable impact on the analysis of the problem. Ultimately, we are able to obtain closed-form expressions for the eigenvalue equations for any number of pendula, as well as for the eigenfunctions, in terms of Chebyshev polynomials of the second kind.

Even if the horizontal and the vertical systems may be investigated as two independent problems, since equations (2.22) and (2.23) are independent of each other, we propose a parallel description, so as to facilitate the comparison of the two. In particular, the results for the vertical system will always be stated first, and those for the horizontal system, which carries the degrees of freedom of the pendula, right after, so as to highlight more easily the peculiarities of the latter.

3.1 Damped normal modes

Among the solutions of the horizontal system (2.24) and the vertical system (2.25), we are interested in the 'damped normal modes', which we define in the following way.

Definition 3.1. i. A *horizontal damped normal mode* with *eigenvalue* $\lambda \in \mathbb{C}$ and *eigenfunction* $(A, f) \in \mathbb{C}^n \times \mathcal{E}^{\mathbb{C}}$ is a family of nonzero complex solutions (ϕ, ψ) of (2.22) of the form

$$(\phi(t), \psi(x,t)) \,=\, \left(cAe^{\lambda t}, cf(x)e^{\lambda t}\right), \qquad c \in \mathbb{C} \setminus \{0\}\,.$$

ii. A *vertical damped normal mode* with *eigenvalue* $\lambda \in \mathbb{C}$ and *eigenfunction* $f \in \mathcal{E}^{\mathbb{C}}$ is a family of nonzero complex solutions ζ of (2.23) of the form

$$\zeta(x,t) \,=\, cf(x)e^{\lambda t}\,, \qquad c \in \mathbb{C} \setminus \{0\}\,.$$

We call *decay rate* the absolute value of the real part of the eigenvalues and *(oscillation) frequency* their positive imaginary part. By *multiplicity* of an eigenvalue of each of the two

types we mean the number of damped normal modes with that eigenvalue and linearly independent eigenfunctions.

The set of all the eigenvalues of the horizontal and vertical damped normal modes, each one repeated as many times as its multiplicity, will be called the *horizontal and vertical spectra*. In order to stress their dependence on the parameters on which the linearised systems depend, we will denote them, respectively, $\mathrm{Sp}^{\mathrm{H}}_{\alpha,\mu,\nu}$ and $\mathrm{Sp}^{\mathrm{V}}_{\mu,\nu}$. Finally, we call *damped small oscillation* for the horizontal and vertical system a linear superposition of the horizontal and vertical damped normal modes, respectively.

For each of the above definitions, we will drop the attribute "damped" whenever $\nu = 0$.

3.1.1 Energy estimates

Preliminarily to the study of the damped normal modes of the system, we make a remark.

Proposition 3.1. *If* $\lambda \in \mathrm{Sp}^{\mathrm{H}}_{\alpha,\mu,\nu}$ *or* $\mathrm{Sp}^{\mathrm{V}}_{\mu,\nu}$, *then* $\mathrm{Re}(\lambda) = 0$ *if* $\nu = 0$ *and* $\mathrm{Re}(\lambda) < 0$ *if* $\nu > 0$.

Proof. We consider the horizontal spectrum; the argument for the vertical spectrum is similar. Define the total energy of the horizontal system at time t of a complex solution (ϕ, ψ) of the horizontal linear system as

$$E^H_t(\phi,\psi) := \frac{1}{2}\sum_{j=0}^{n}\int_{x_j}^{x_{j+1}}\Big(|\psi_t(x,t)|^2 + \frac{|\psi_x(x,t)|^2}{\pi^2}\Big)dx + \frac{\mu}{2}\sum_{k=1}^{n}\Big(|\dot\phi_k(t)+\psi_t(x_k,t)|^2 + \alpha^2|\dot\phi_k^2(t)|^2\Big)\,.$$

Using equations (2.24), the fact that ψ_t vanishes at $x = 0, 1$ and integrating by parts terms containing $\psi_x\psi_{tx}$, $\psi_x\psi_{txx}$ and their complex conjugates gives

$$\frac{d}{dt}E^H_t(\phi,\psi) = -\frac{\nu}{\pi^2}\sum_{j=0}^{n}\int_{x_j}^{x_{j+1}}|\psi_{tx}(x,t)|^2dx\,.$$

For a horizontal damped normal mode $(\phi, \psi) = (Ae^{\lambda t}, f(x)e^{\lambda t})$,

$$\delta := \sum_{j=0}^{n}\int_{x_j}^{x_{j+1}}|\psi_{tx}(x,t)|^2dx = |\lambda e^{\lambda t}|^2\sum_{j=0}^{n}\int_{x_j}^{x_{j+1}}|f'(x)|^2dx > 0$$

because $\lambda \neq 0$ and f is not constant (if it was, then the derivatives of ψ would vanish and the first and last equations (2.24) would give $\phi_k = 0$ for all k, hence $A = 0$ as well). On the other hand, $E^H_t(\phi,\psi) = e^{2t\mathrm{Re}(\lambda)}E_0(\phi,\psi)$ and thus $\frac{d}{dt}E^H_t(\phi,\psi) = 2\mathrm{Re}(\lambda)E^H_t(\phi,\psi)$. We conclude that $2\mathrm{Re}(\lambda)E^H_t(\phi,\psi) = -\nu\frac{\delta}{\pi^2} \leq 0$, with the equality holding if and only if $\nu = 0$. This proves the statement because $E^H_t(\phi,\psi) > 0$ if (ϕ,ψ) is nonzero. □

Proposition 3.1 implies, in particular, that, for any $\nu > 0$, the mechanical energy of the system is dissipated in every damped normal mode, therefore, by LaSalle invariance principle, every such solution tends asymptotically in time to the equilibrium. However, we shall see in Sections 4.3 that, similarly to the case of the viscoelastic string discussed in Section 2.2.2, the decay rates of the eigenvalues of the horizontal and vertical damped normal modes are strongly frequency-dependent, and this will have a crucial impact on the asymptotic dynamics of the system.

3.2 The eigenvalue equations

We derive now equations for the eigenvalues of the horizontal and vertical damped normal modes. In what follows, U_n denotes the Chebyshev polynomials of the second kind of order n; we refer to Appendix A for details on basic facts on these polynomials. We write

$$P_\mu := \frac{\mu}{2}$$

and, for any $\alpha > 0$ and $\mu > 0$, we define

$$P_{\alpha,\mu} : \mathbb{C} \setminus \{\pm i\alpha\} \to \mathbb{C}\,, \qquad P_{\alpha,\mu}(\lambda) = \frac{\mu}{2}\,\frac{\alpha^2}{\alpha^2+\lambda^2},$$

and, for $\nu = 0$,

$$\xi_0 : \mathbb{C} \to \mathbb{C}\,, \qquad \xi_0(\lambda) = \pi\lambda\,,$$

and, for $\nu > 0$,

$$\xi_\nu : \mathbb{C} \setminus \{-\tfrac{1}{\nu}\} \to \mathbb{C}\,, \qquad \xi_\nu(\lambda) = \frac{\pi\lambda}{(1+\nu\lambda)^{1/2}}\,,$$

where $(\,)^{1/2}$ denotes, as above, the complex square root with nonnegative imaginary part, which is analytic in $\mathbb{C} \setminus \{x \geq 0\}$.

Proposition 3.2. *Consider $n \geq 1$, $\alpha > 0$, $\mu > 0$ and $\nu \geq 0$ and a complex number λ.*

i. $\lambda \in \mathrm{Sp}^{\mathrm{V}}_{\mu,\nu}$ if and only if $\lambda \neq 0$, $\lambda \neq -\frac{1}{\nu}$ (if $\nu > 0$) and

$$\sinh\Big(\frac{\xi_\nu(\lambda)}{n+1}\Big)\, U_n\bigg(P_\mu \xi_\nu(\lambda)\sinh\Big(\frac{\xi_\nu(\lambda)}{n+1}\Big) + \cosh\Big(\frac{\xi_\nu(\lambda)}{n+1}\Big)\bigg) = 0. \tag{3.1}$$

ii. $\lambda \in \mathrm{Sp}^{\mathrm{H}}_{\alpha,\mu,\nu}$ if and only if $\lambda \neq 0$, $\lambda \neq -\frac{1}{\nu}$ (if $\nu > 0$) and satisfies any of the following two conditions:

$$\sinh\Big(\frac{\xi_\nu(\lambda)}{n+1}\Big) = 0\,, \tag{3.2a}$$

$$U_n\bigg(P_{\alpha,\mu}(\lambda)\xi_\nu(\lambda)\sinh\Big(\frac{\xi_\nu(\lambda)}{n+1}\Big) + \cosh\Big(\frac{\xi_\nu(\lambda)}{n+1}\Big)\bigg) = 0\,, \quad \lambda \neq \pm i\alpha\,. \tag{3.2b}$$

Proof. (ii.) We consider first the horizontal spectrum. Assume that $(\phi^\lambda,\psi^\lambda) := c(Ae^{\lambda t}, fe^{\lambda t})$, $c \neq 0$, is a horizontal damped normal mode. Write $A = (A_1, \ldots, A_n)$. The function f belongs to $\mathcal{E}^{\mathbb{C}}$. Hence, if we define

$$f_j := f|_{[x_{j-1},x_j]}\,, \qquad j = 1, \ldots, n+1\,,$$

then each $f_j : [x_{j-1}, x_j] \to \mathbb{C}$ is of class C^2 in (x_{j-1}, x_j) and of class C^1 in $[x_{j-1}, x_j]$ (with the derivatives at the extrema interpreted as left and right derivatives) and satisfies

$$f_1(x_0) = 0\,, \qquad f_{n+1}(x_{n+1}) = 0 \tag{3.3}$$

(recall that $x_0 = 0$, $x_{n+1} = 1$) and

$$f_{k+1}(x_k) = f_k(x_k) \qquad \forall k = 1, \dots, n\,. \tag{3.4}$$

The function $(\phi^\lambda, \psi^\lambda)$ satisfies (2.24) if and only if

$$(\alpha^2 + \lambda^2)A_k + \lambda^2 f_k(x_k) = 0\,, \qquad k = 1, \dots, n\,, \tag{3.5a}$$

$$\lambda^2 f_j(x) - \frac{1+\nu\lambda}{\pi^2} f_j''(x) = 0\,, \qquad x \in (x_{j-1}, x_j), \quad j = 1, \dots, n+1\,, \tag{3.5b}$$

$$\mu\lambda^2\big(f_k(x_k) + A_k\big) - \frac{1+\nu\lambda}{\pi^2}\big(f_{k+1}'(x_k^+) - f_k'(x_k^-)\big) = 0\,, \qquad k = 1, \dots n\,. \tag{3.5c}$$

It is simple to check that if $\lambda = 0$ or, when $\nu > 0$, $\lambda = -1/\nu$ then the only solution of equations (3.5) is $A_k = 0$ for all $k = 1, \dots, n$ and $f_j = 0$ for all $j = 1, \dots, n+1$. Thus 0 and (if $\nu > 0$) $-\frac{1}{\nu}$ do not belong to $\mathrm{Sp}^H_{\alpha,\mu,\nu}$ and in the remainder of the proof we exclude these values of λ. Equation (3.5b) is equivalent to

$$f_j(x) = a_j \cosh\big(\xi(x - x_{j-1})\big) + b_j \sinh\big(\xi(x - x_{j-1})\big) \quad \forall x \in [x_{j-1}, x_j],\ \ j = 1, \dots, n+1\,,$$

with $\xi := \xi_\nu(\lambda)$, $a_j := f_j(x_{j-1})$ and $b_j := \frac{1}{\xi} f_j'(x_{j-1}^+)$. Note that $f_j(x_j) = ca_j + sb_j$ and $f_j'(x_j^-) = \xi(sa_j + cb_j)$ with

$$c := \cosh\Big(\frac{\xi_\nu(\lambda)}{n+1}\Big)\,, \qquad s := \sinh\Big(\frac{\xi_\nu(\lambda)}{n+1}\Big)\,.$$

We now impose the conditions on λ and on the A_j's, a_j's and b_j's that come from the fact that A, f satisfies the remaining conditions, namely (3.3), (3.4), (3.5a) and (3.5c), that is

$$a_1 = 0\,, \qquad ca_{n+1} + sb_{n+1} = 0\,, \tag{3.6a}$$

$$a_{k+1} = ca_k + sb_k\,, \qquad k = 1, \dots, n\,, \tag{3.6b}$$

$$(\alpha^2 + \lambda^2)A_k + \lambda^2(ca_k + sb_k) = 0\,, \qquad k = 1, \dots, n\,, \tag{3.6c}$$

$$\mu\xi(a_{k+1} + A_k) - \big(b_{k+1} - sa_k - cb_k\big) = 0\,, \qquad k = 1, \dots, n\,. \tag{3.6d}$$

We distinguish two cases.

(1.) If $\lambda \neq \pm i\alpha$, then (3.6c) are equivalent to

$$A_j = -\frac{\lambda^2}{\alpha^2 + \lambda^2}(ca_j + sb_j)\,, \qquad j = 1, \dots, n\,.$$

Therefore, (3.6b) and (3.6d) can be written

$$\begin{pmatrix} a_{j+1} \\ b_{j+1} \end{pmatrix} = M \begin{pmatrix} a_j \\ b_j \end{pmatrix}\,, \qquad j = 1, \dots, n, \tag{3.7}$$

with the 2×2 "transfer" matrix

$$M := \begin{pmatrix} c & s \\ s + Qc & c + Qs \end{pmatrix}\,, \qquad Q := 2\xi P_{\alpha,\mu}(\lambda) \tag{3.8}$$

This gives, by iteration,

$$\begin{pmatrix} a_{j+1} \\ b_{j+1} \end{pmatrix} = M^j \begin{pmatrix} a_1 \\ b_1 \end{pmatrix}, \qquad j = 1, \dots, n,$$

It remains to impose the two conditions in (3.6a). The first is $a_1 = 0$; but then, since λ is an eigenvalue, $b_1 = \frac{1}{\xi} f'(0^+) \neq 0$ (otherwise all $a_j, b_j = 0$ and $(\phi^\lambda, \psi^\lambda)$ is zero). From the second, the vanishing of $ca_{n+1} + sb_{n+1}$ gives $c(M^n)_{12} + s(M^n)_{22} = 0$.

Since M is a 2×2 matrix with determinant one, its powers are given by (see Appendix B, equation (B.1))

$$M^j = U_{j-1}(y)M - U_{j-2}(y)\mathbb{I}, \qquad j \in \mathbb{N},$$

where $y = \frac{1}{2}\mathrm{Tr}(M)$, $\mathbb{I}$ is the 2×2 unit matrix, $U_{-1} = 0$ and, for $j \geq 0$, the U_j's are the Chebyshev polynomials of the second kind. Thus, $c(M^n)_{12} + s(M^n)_{22} = (cM_{12} + sM_{22})U_{n-1}(y) - sU_{n-2}(y)$. In our case $y = c + \frac{1}{2}Qs$ and $c(M^n)_{12} + s(M^n)_{22} = (2cs + s^2Q)\,U_{n-1}(y) - s\,U_{n-2}(y) = s\,\big(2yU_{n-1}(y) - U_{n-2}(y)\big) = s\,U_n(y)$, where the last equality follows from (A.1). This proves that every eigenvalue $\lambda \neq \pm i\alpha$ is either a zero of s or of $U_n(y)$, as claimed.

Conversely, it is easy to prove that any $\lambda \in \mathbb{C}$ which is $\neq 0$, $\neq i\alpha$ and (if $\nu > 0$) $\neq -\frac{1}{\nu}$ and satisfies $s\,U_n(y) = 0$ belongs to $\mathrm{Sp}^H_{\alpha,\mu,\nu}$.

(2.) If $\lambda = \pm i\alpha$, then (3.5a) is $f_{j+1}(x_j) = 0$ for all $j = 1, \dots, n$. Together with the first equality (3.3) this gives $a_j = 0$ for all $j = 1, \dots, n+1$. Notice that, by Proposition 3.1, $\lambda = \pm i\alpha \in \mathrm{Sp}^H_{\alpha,\mu,\nu}$ implies $\nu = 0$. Equations (3.5c) are satisfied by $A_k = \frac{b_{k+1} - cb_k}{\mu\xi_0(i\alpha)}$ with $c = \cos\left(\frac{\pi\alpha}{n+1}\right)$. The second equality (3.3) and the equalities (3.4) reduce to $s\,b_j = 0$ for $j = 1, \dots, n+1$, which have a nontrivial solution if and only if λ is such that $s = 0$. (The trivial solution would lead to zero A_k's and hence to a zero solution).

(i.) We consider now the vertical system. Assume that $cg(x)e^{\lambda t}$ is a vertical damped normal mode. Proceeding as in i., define $g_j := g|_{[x_{j-1},x_j]}$, $j = 1, \dots, n+1$. The g_j's satisfy conditions similar to the f_j's, specifically (with the f_j's replaced by the g_j's) (3.3), (3.4), (3.5b) and, this is the difference, (3.5c) with all $A_k = 0$. Thus, as above, $\lambda \neq 0$ and (if $\nu > 0$) $\lambda \neq -1/\nu$,

$$g_j(x) = a_j \cosh\big(\xi(x - x_{j-1})\big) + b_j \sinh\big(\xi(x - x_{j-1})\big) \quad \forall x \in [x_{j-1}, x_j], \;\; j = 1, \dots, n+1$$

and instead of (3.6) we have now

$$a_1 = 0\,, \qquad ca_{n+1} + sb_{n+1} = 0\,, \tag{3.9a}$$

$$a_{k+1} = ca_k + sb_k\,, \qquad k = 1, \dots, n\,, \tag{3.9b}$$

$$\mu\xi a_{k+1} - (b_{k+1} - sa_k - cb_k) = 0\,, \qquad k = 1, \dots, n\,. \tag{3.9c}$$

This gives the recurrence (3.7)−(3.8) with $Q = 2\xi P_\mu$ and, by comparison with (3.6), leads to (3.1). □

We will refer to equation (3.1) as the *vertical eigenvalue equation* and to equations (3.2) as the *horizontal eigenvalue equation*. Interestingly, they can be represented in this form for any number of pendula.

Remark 3.1. For $\nu > 0$, equation (3.2) for the horizontal system writes equivalently as

$$\sinh\Big(\frac{\xi_\nu(\lambda)}{n+1}\Big)\, U_n\bigg(P_{\alpha,\mu}(\lambda)\xi_\nu(\lambda)\sinh\Big(\frac{\xi_\nu(\lambda)}{n+1}\Big) + \cosh\Big(\frac{\xi_\nu(\lambda)}{n+1}\Big)\bigg) = 0\,, \quad \lambda \neq \pm i\alpha.$$

Indeed, in virtue of Proposition 3.1, $\lambda = \pm i\alpha$ belongs to $\mathrm{Sp}^H_{\alpha,\mu,\nu}$ only if $\nu = 0$.

In Section 3.2.2, we shall analyse these expressions in greater detail. Here, we note that when $\mu = 0$, namely for massless pendula, we recover the unloaded viscoelastic string, as in Section 2.2.2. Indeed, since, for $\mu = 0$, $P_0 = 0$ and $P_{0,\alpha} = 0$, the left hand sides of equations (3.1) and (3.2) become $\sinh\big(\frac{\xi_\nu(\lambda)}{n+1}\big)\, U_n\big(\cosh\big(\frac{\xi_\nu(\lambda)}{n+1}\big)\big)$. By exploiting the definition (A.3) of Chebyshev polynomials of the second kind, we have $0 = \sinh\big(\frac{\xi_\nu(\lambda)}{n+1}\big)\, U_n\big(\cosh\big(\frac{\xi_\nu(\lambda)}{n+1}\big)\big) = \sinh(\xi_\nu(\lambda))$, which is precisely the eigenvalue equation (2.14) for the viscoelastic string. We consider from now on $\mu > 0$.

Moreover, we remark that the vertical eigenvalue equation (3.1) differs from the horizontal eigenvalue equation (3.2) in that $P_{\alpha,\mu}(\lambda)$ is replaced by P_μ. Indeed, (3.1) (and the vertical system) can be regarded as the (singular) limit for $\alpha \to +\infty$ of (3.2) (and the horizontal system). In fact, as mentioned, equation (2.23) for the vertical system describes a viscoelastic vibrating string loaded with n identical and equidistant masses.

3.2.1 Alternative proof for the vertical eigenvalue equation

We originally obtained equations (3.1) and (3.2) by means of an alternative derivation. At an earlier stage of our study, the possibility of finding explicit expressions for any number of pendula, and in particular the emergence of Chebyshev polynomials, was still not evident to us. We first figured out most formulas inductively, an a-posteriori analysis then allowed us to simplify both the derivation and the final expressions.

Later in our study, we found that our expression (3.1) for the vertical eigenvalue equation was already present in the literature for $\nu = 0$ (see [15, 33]). There, the result was obtained by exploiting the method of the transfer matrix (which we used in the proof of Proposition 3.2). For comparison, we report here our alternative proof for the derivation of (3.1) for $\nu = 0$, since we believe it might provide some useful insights. In particular, we prove the following

Proposition 3.3. *Let $n \geq 1$ and $\alpha > 0$, $\mu > 0$, and consider $\omega > 0$. The conjugate pair $\pm i\omega \in \mathrm{Sp}^{\mathrm{V}}_{\mu,0}$ if and only if ω is a root of*

$$\sin\Big(\frac{\pi\omega}{n+1}\Big)\, U_n\bigg(P_\mu \pi\omega \sin\Big(\frac{\pi\omega}{n+1}\Big) - \cos\Big(\frac{\pi\omega}{n+1}\Big)\bigg) = 0\,. \tag{3.10}$$

Proof. Let $\nu = 0$. Assume that $cf(x)e^{\lambda t}$, $c \neq 0$, is a vertical normal mode. By Proposition 3.1, the eigenvalues are purely imaginary, hence we set $\lambda = i\omega$ (and $\bar\lambda = -i\omega$) with $\omega > 0$. The function f belongs to $\mathcal{E}^{\mathbb{C}}$. Hence, if we define

$$f_j := f|_{[x_{j-1},x_j]}\,, \qquad j = 1, \dots, n+1\,,$$

then each $f_j : [x_{j-1}, x_j] \to \mathbb{C}$ is of class C^2 in (x_{j-1}, x_j) and of class C^1 in $[x_{j-1}, x_j]$ (with the derivatives at the extrema interpreted as left and right derivatives) and satisfies

$$f_1(x_0) = 0\,, \qquad f_{n+1}(x_{n+1}) = 0 \tag{3.11}$$

and

$$f_{k+1}(x_k) = f_k(x_k) \qquad \forall k = 1, \dots, n\,. \tag{3.12}$$

The function $f(x)e^{i\omega t}$ satisfies (2.25) if and only if

$$f_j''(x) + \pi^2\omega^2 f_j(x) = 0\,, \qquad x \in (x_{j-1}, x_j), \quad j = 1, \dots, n+1\,, \tag{3.13a}$$
$$\mu\pi^2\omega^2 f_{k+1}(x_k) + f_{k+1}'(x_k^+) - f_k'(x_k^-) = 0\,, \qquad k = 1, \dots n\,. \tag{3.13b}$$

Equations (3.13a) are equivalent to

$$f_j(x) = a_j \cos(wx) + b_j \sin(wx) \quad \forall x \in [x_{j-1}, x_j], \;\; j = 1, \dots, n+1\,,$$

with $w := \pi\omega$, $a_j := f_j(x_0)$ and $b_j := \frac{1}{w} f_j'(x_0^+)$. Write $P := \mu\pi w$ and, for all $j = 0, \dots, n+1$,

$$c_j := \cos(wx_j)\,, \qquad s_j := \sin(wx_j)\,.$$

We impose that the f_j's satisfy the remaining conditions, namely (3.11), (3.12) and (3.13b), that is $a_1 = 0$ and

$$(a_{k+1} - a_k)c_k - (b_k - b_{k+1})s_k = 0\,, \qquad k = 1, \dots, n\,, \tag{3.14a}$$
$$(a_k - a_{k+1} + Pb_k)s_k - (b_k - b_{k+1} - Pa_k)c_k = 0\,, \qquad k = 1, \dots, n\,, \tag{3.14b}$$
$$a_{n+1}c_{n+1} + b_{n+1}s_{n+1} = 0\,. \tag{3.14c}$$

These are a system of $2n+1$ linear equations for $(b_1, \dots, a_{n+1}, b_{n+1}) =: u$ that we write as $M_n u = 0$ with a $(2n+1) \times (2n+1)$ matrix M_n which depends on n and w. We thus conclude that $\pm i\omega \in \mathrm{Sp}^{\mathrm{H}}_{\mu,0}$ if and only if $\omega = \frac{w}{\pi}$ and $\det M_n = 0$.

Lemma 3.1. *For any $n \geq 0$, $\det M_n$ equals the left-hand side of* (3.10).

Proof. From system (3.14),

$$M_1 = \begin{pmatrix} s_1 & -c_1 & -s_1 \\ Ps_1 - c_1 & -s_1 & c_1 \\ 0 & c_2 & s_2 \end{pmatrix}$$

and, for $n \geq 2$,

$$M_n = \left(\begin{array}{cccccc|cc} & & & & & & 0 & 0 \\ & & & & & & \vdots & \vdots \\ & & & & & & 0 & 0 \\ & & & M_{n-1} & & & & \\ & & & & & & -c_n & -s_n \\ \hline 0 & \cdots & 0 & Pc_n + s_n & Ps_n - c_n & & -s_n & c_n \\ 0 & \cdots & 0 & 0 & 0 & & c_{n+1} & s_{n+1} \end{array}\right). \tag{3.15}$$

Note that, if we define $M_0 := (s_1)$ (a 1×1 matrix), then the recursive formula (3.15) is valid for all $n \geq 1$. Note also that

$$\det M_0 = s_1, \qquad \det M_1 = (Ps_1 - 2c_1)s_1.$$

Assume now $n \geq 2$. Using Laplace expansion along the last row gives $\det M_n$ as a sum $c_{n+1} \det + s_{n+1} \det$ with two matrices and . Using Laplace expansion along the last coloumn to compute det and det gives $\det M_n = -(s_{n+1}s_n + c_{n+1}c_n) \det M_{n+1} + (c_{n+1}s_n) \det \tilde{M}_{n-1}$ where the matrix $\tilde{M}_{n-1}$ differs from M_{n-1} in that its last row is $(0, \ldots, 0, Pc_n + s_n, Ps_n - c_n)$. Hence, with a little trigonometry,

$$\det M_n = -c_1 \det M_{n-1} + s_1 \det \tilde{M}_{n-1}.$$

Since $(0, \ldots, 0, Pc_n + s_n, Ps_n - c_n) = P(0, \ldots, 0, c_n, s_n) + (0, \ldots, 0, s_n, -c_n)$,

$$\det \tilde{M}_{n-1} = P \det M_{n-1} + \det \hat{M}_{n-1}$$

where $\hat{M}_{n-1}$ differs from M_{n-1} only because its last row is $(0, \ldots, 0, s_n, -c_n)$. Hence,

$$\det M_n = (Ps_1 - 2c_1) \det M_{n-1} + (c_1 \det M_{n-1} + s_1 \det \hat{M}_{n-1}) \qquad \forall n \geq 2.$$

We now show that

$$c_1 \det M_k + s_1 \det \hat{M}_k = -\det M_{k-1} \qquad \forall k \geq 1.$$

For $k = 1$ this is verified with a computation. If $k \geq 2$, using the linearity of the determinant as a function of the last row of the matrix, one sees that $c_1 \det M_k + s_1 \det \hat{M}_k = \det \check{M}_k$, where $\check{M}_k$ differs from M_k because its last row is $(0, \ldots, 0, c_1c_{k+1} + s_1s_{k+1}, c_1s_{k+1}, s_{k+1} - s_1c_{k+1}) = (0, \ldots, 0, c_k, s_k)$. Since adding the last row of $\check{M}_k$ to its third-to-last row produces a block lower triangular matrix with diagonal blocks M_{k+1} and $\begin{pmatrix} -s_k & c_k \\ c_k & s_k \end{pmatrix}$, $\det \check{M}_{k-1} = -\det M_{k-1}$. This proves

$$\det M_n = (Ps_1 - 2c_1) \det M_{n-1} + \det M_{n-2}.$$

In particular,

$$\det M_n = s_1 D_n \qquad \forall n \geq 0$$

with the D_n's satisfying the recurrence

$$D_0 = 1, \quad D_1 = 2\left(\frac{P}{2}s_1 - c_1\right), \quad D_n = 2\left(\frac{P}{2}s_1 - c_1\right) D_{n-1} + D_{n+1} \ (n \geq 2).$$

A comparison with Chebyshev recurrence (A.1) shows that $D_n = U_n\big(\frac{P}{2}s_1 - c_1\big)$. This proves the Lemma. □

The statement of Proposition 3.3 follows immediately from that of Lemma 3.1. □

3.2.2 Peculiarities of the eigenvalue equations

In this section we further comment the expressions (3.1) and (3.2) for the eigenvalue equations.

First, we observe that both equations (3.1) and (3.2) factorise. In particular, they share the factor $\sinh\big(\frac{\xi_\nu(\lambda)}{n+1}\big)$ and the remaining factors are expressed in terms of Chebyshev polynomials of the second kind of order n. As we anticipated, this structure of the eigenvalue equations reflects the locally periodic geometry of the system, in particular, it is specific to the fact that we are assuming that the pendula are equally spaced.

Note, indeed, that Chebyshev polynomials U_n naturally emerge in locally periodic systems (see Appendix B.2 for a more general setting and Appendix A.1 for a simple example).

As for the factor $\sinh\big(\frac{\xi_\nu(\lambda)}{n+1}\big)$, we note that the zeroes of this term are those eigenvalues of the viscoelastic string without pendula whose eigenfunctions have nodes at the points of suspension of the pendula (see Section 2.2.2). We will thus call them the (horizontal and vertical) *pure-string eigenvalues* of the vertical and horizontal spectra – and of the Kelvin-Voigt string as well. And we will call (horizontal and vertical) *string-pendula eigenvalues* the other eigenvalues of the vertical and horizontal spectra, which are given by the zeroes of the Chebyshev polynomials.

From Proposition 3.2 and the characterisation (A.4) of the zeroes of $U_n(\cdot)$, we have the following

Corollary 3.1. *For any $n \geq 1$, $\alpha > 0$, $\mu > 0$, $\nu \geq 0$:*

i. The pure-string eigenvalues of $\mathrm{Sp}^{\mathrm{V}}_{\mu,\nu}$ and $\mathrm{Sp}^{\mathrm{H}}_{\alpha,\mu,\nu}$ are the solutions $\lambda \in \mathbb{C}$ of $\sinh\big(\frac{\xi_\nu(\lambda)}{n+1}\big) = 0$, namely of the countably many equations

$$\frac{\xi_\nu(\lambda)}{n+1} = im\pi\,, \qquad m \in \mathbb{Z}\,. \tag{3.16}$$

ii. The string-pendula eigenvalues of $\mathrm{Sp}^{\mathrm{V}}_{\mu,\nu}$ are the solutions $\lambda \in \mathbb{C}$ of the n equations

$$P_\mu\, \xi_\nu(\lambda)\, \sinh\Big(\frac{\xi_\nu(\lambda)}{n+1}\Big) + \cosh\Big(\frac{\xi_\nu(\lambda)}{n+1}\Big) = \cos\Big(\frac{k\pi}{n+1}\Big)\,, \qquad k = 1, \dots, n\,. \tag{3.17}$$

iii. The string-pendula eigenvalues of $\mathrm{Sp}^{\mathrm{H}}_{\alpha,\mu,\nu}$ *are the solutions* $\lambda \in \mathbb{C} \setminus \{\pm i\alpha\}$ *of the* n *equations*

$$P_{\alpha,\mu}(\lambda)\xi_\nu(\lambda)\,\sinh\Big(\frac{\xi_\nu(\lambda)}{n+1}\Big) + \cosh\Big(\frac{\xi_\nu(\lambda)}{n+1}\Big) = \cos\Big(\frac{k\pi}{n+1}\Big)\,, \qquad k = 1,\dots,n\,. \tag{3.18}$$

iv. The sets of pure-string and string-pendula eigenvalues of each of one of the two spectra $\mathrm{Sp}^{\mathrm{V}}_{\mu,\nu}$ *and* $\mathrm{Sp}^{\mathrm{H}}_{\alpha,\mu,\nu}$ *are disjoint.*

Proof. (i.) The zeroes of sinh are $i\pi m$, $m \in \mathbb{Z}$. (ii.) and (iii.) are obvious, given (A.4). (iv.) If λ is a pure-string eigenvalue, then $\frac{\xi_\nu(\lambda)}{n+1} = i\pi m$ for some $m \in \mathbb{Z}$ and equations (3.17) and (3.18) reduce to the n equations $\cos(\pi m) = \cos(\frac{k\pi}{n+1})$, $k = 1,\dots,n$, none of which has solutions. □

Corollary 3.1 implies, in particular, that the string-pendula eigenvalues come in families of n.

As we will see in Chapter 4, the pure-string eigenvalues play an organising role in the vertical and horizontal spectra, dividing them into 'bands' whose consideration will facilitate their description. Moreover, for the horizontal spectrum, we anticipate that another divide enters the structure of the eigenvalues, and that it is given by the special values $\pm i\alpha$. Note that, as we mentioned, being purely imaginary, they can only belong to the horizontal spectrum for $\nu = 0$ and, in that case, only if they are pure-string eigenvalues, namely if

$$\tilde{\alpha} := \frac{\alpha}{n+1} \in \mathbb{Z}_+\,.$$

We will say that α is *resonant* if $\tilde{\alpha} \in \mathbb{Z}_+$ and *nonresonat* otherwise. The reason is that, since α is the ratio between the frequency of oscillation of the pendula and the fundamental frequency of the vibrating string, an integer value of $\frac{\alpha}{n+1}$ means that there is a resonance in which the frequency of each pendulum is a multiple of the vibration frequency of the part of the string between each pair of consecutive pendula.

In Chapter 4 we will study the roots of equations (3.16)—(3.18).

3.3 The eigenfunctions

We determine now expressions for the eigenfunctions of the vertical and horizontal systems in terms of the eigenvalues. Analogously to the eigenvalue equations, we will express them in terms of Chebyshev polynomials, for any number of pendula. Moreover, a peculiarity of the resonant case will emerge.

For comparison, we preliminarily recall that, with our notation, the eigenfunction of the Kelvin-Voigt string relative to an eigenvalue $\lambda \in \mathbb{C}$ is the function

$$f^{KV}_{\nu,\lambda}(x) = \sinh\big(\xi_\nu(\lambda)x\big)\,, \qquad x \in [0,1]\,. \tag{3.19}$$

As above, we write $x_j = \frac{j}{n+1}$, $C_k = \cos\big(\frac{k\pi}{n+1}\big)$, and we make the convention that $U_{-1} = 0$. Notice in particular that $U_n(C_k) = 0\ \forall k = 1,\dots,n$, by property (A.4). We then denote by δ_{ij} the Kronecker delta.

Proposition 3.4. *For any $n \geq 1$, $\alpha > 0$, $\mu > 0$, $\nu \geq 0$:*

i. All eigenvalues in $\mathrm{Sp}^{\mathrm{V}}_{\mu,\nu}$ and $\mathrm{Sp}^{\mathrm{H}}_{\alpha,\mu,\nu}$ have multiplicity 1 except, if present, $\pm i\alpha \in \mathrm{Sp}^{\mathrm{H}}_{\alpha,\mu,0}$ which have multiplicity $n+1$.

ii. The eigenfunction of any vertical pure-string eigenvalue $\lambda \in \mathrm{Sp}^{\mathrm{V}}_{\mu,\nu}$ is $f^{KV}_{\nu,\lambda}$.

iii. The eigenfunction of any vertical string-pendula eigenvalue $\lambda \in \mathrm{Sp}^{\mathrm{V}}_{\mu,\nu}$ solution of the k-th equation (3.17) is the function $f^{\mathrm{V}}_{\nu,k,\lambda} \in \mathcal{E}^{\mathbb{C}}$ such that

$$f^{\mathrm{V}}_{\nu,k,\lambda}(x) = U_{j-1}(C_k)\,\sinh\big(\xi_\nu(\lambda)(x-x_{j-1})\big) - U_{j-2}(C_k)\,\sinh\big(\xi_\nu(\lambda)(x-x_j)\big) \quad (3.20)$$

for $x \in [x_{j-1}, x_j]$, $j = 1, \dots, n+1$.

iv. The eigenfunction of any horizontal pure-string eigenvalue $\lambda \in \mathrm{Sp}^{\mathrm{H}}_{\alpha,\mu,\nu}$ with $\nu > 0$ and of any horizontal pure-string eigenvalue $\lambda \neq \pm i\alpha$ of $\mathrm{Sp}^{\mathrm{H}}_{\alpha,\mu,0}$ is $(0, f^{KV}_{\nu,\lambda})$. If $\pm i\alpha \in \mathrm{Sp}^{\mathrm{H}}_{\alpha,\mu,0}$, then each of them has the $n+1$ independent eigenfunctions $(A^{\mathrm{H}}_{\alpha,l}, f^{\mathrm{H}}_{\alpha,l}) \in \mathbb{R}^n \times \mathcal{E}$, $l = 1, \dots, n+1$, with

$$(A^{\mathrm{H}}_{\alpha,l})_h = \frac{(-1)^{h\frac{\alpha}{n+1}}}{\pi\alpha\mu}(\delta_{hl} + \delta_{h(l-1)}), \quad h = 1, \dots, n, \quad (3.21a)$$

$$f^{\mathrm{H}}_{\alpha,l} = \delta_{lj}\sin(\pi\alpha x), \qquad x \in [x_{j-1}, x_j],\ j = 1, \dots, n+1. \quad (3.21b)$$

v. The eigenfunction of any horizontal string-pendula eigenvalue $\lambda \in \mathrm{Sp}^{\mathrm{H}}_{\alpha,\mu,\nu}$ solution of the k-th equation (3.18) is $(A^{\mathrm{H}}_{\nu,k,\lambda}, f^{\mathrm{H}}_{\nu,k,\lambda}) \in \mathbb{C}^n \times \mathcal{E}^{\mathbb{C}}$ with

$$(A^{\mathrm{H}}_{\nu,k,\lambda})_h = -\frac{\lambda^2}{\alpha^2+\lambda^2}\,U_{h-1}(C_k)\,\sinh\Big(\frac{\xi_\nu(\lambda)}{n+1}\Big), \qquad h = 1, \dots, n, \quad (3.22a)$$

$$f^{\mathrm{H}}_{\nu,k,\lambda}(x) = U_{j-1}(C_k)\,\sinh\big(\xi_\nu(\lambda)(x-x_{j-1})\big) - U_{j-2}(C_k)\,\sinh\big(\xi_\nu(\lambda)(x-x_j)\big) \quad (3.22b)$$

for $x \in [x_{j-1}, x_j]$, $j = 1, \dots, n+1$.

Proof. We adopt the same notation as in the proof of Proposition 3.2, and use some of the results obtained therein. As before, we set $c := \cosh\big(\frac{\xi_\nu(\lambda)}{n+1}\big)$, $s := \sinh\big(\frac{\xi_\nu(\lambda)}{n+1}\big)$, and $C_k := \cos\Big(\frac{k\pi}{n+1}\Big)$.

Consider the vertical system, and assume that $cge^{\lambda t}$, $c \neq 0$, is a vertical damped normal mode. Recall that we wrote $g_j := g|_{[x_{j-1},x_j]}$, $j = 1, \dots, n+1$, as

$$g_j(x) = a_j\cosh\big(\xi_\nu(\lambda)(x-x_{j-1})\big) + b_j\sinh\big(\xi_\nu(\lambda)(x-x_{j-1})\big),$$

and that $a_1, b_1, \dots, a_{n+1}, b_{n+1}$ satisfy (3.9).

ii. Let $\lambda \in \mathrm{Sp}^{V}_{\mu,\nu}$ be a pure-string eigenvalue. Then, $s = 0$ and, from (3.9), $a_j = 0$ and $b_{j+1} = -cb_j$ for all $j = 1, \dots, n+1$. Hence, $g(x) = \sinh(\xi_\nu(\lambda)x)$.

iii. Let $\lambda \in \mathrm{Sp}^V_{\mu,\nu}$ be a string-pendula eigenvalue. From the expression of the transfer matrix (3.8), with $Q := 2\xi P_\mu$, and using the relation (B.1) for its powers, we have, for $j = 1, \dots, n$,

$$\begin{pmatrix} a_{j+1} \\ b_{j+1} \end{pmatrix} = \begin{pmatrix} cU_{j-1}(C_k) - U_{j-2}(C_k) & sU_{j-1}(C_k) \\ (s+Qc)U_{j-1}(C_k) & (c+Qs)U_{j-1}(C_k) - U_{j-2}(C_k) \end{pmatrix} \begin{pmatrix} a_1 \\ b_1 \end{pmatrix}, \quad (3.23)$$

where we used (3.17). Therefore, since $a_1 = 0$, for $j \geq 1$,

$$\begin{aligned} a_{j+1} &= sU_{j-1}(C_k) \\ b_{j+1} &= (c+Qs)U_{j-1}(C_k) - U_{j-2}(C_k) = U_j(C_k) - cU_{j-1}(C_k), \end{aligned}$$

where we set $b_1 \equiv 1$ (an arbitrary constant), and used in the last equality the recurrence (A.1) for the Chebyshev polynomials. Therefore, $g_1(x) = s$ and, for $j \geq 1$, $g_{j+1}(x) = (sU_{j-1}(C_k)) \cosh\big(\xi_\nu(\lambda)(x - x_{j-1})\big) + (U_j(C_k) - cU_{j-1}(C_k)) \sinh\big(\xi_\nu(\lambda)(x - x_{j-1})\big)$. Finally, using standard formulas for the sum of hyperbolic functions, we find expression (3.20).

Consider now the horizontal system, assume that $c\big(Ae^{\lambda t}, fe^{\lambda t}\big)$, $c \neq 0$, is a horizontal damped normal mode. Recall that we wrote $f_j := f|_{[x_{j-1}, x_j]}$, $j = 1, \dots, n+1$, as

$$f_j(x) = a_j \cosh\big(\xi_\nu(\lambda)(x - x_{j-1})\big) + b_j \sinh\big(\xi_\nu(\lambda)(x - x_{j-1})\big),$$

and that $A_1, \dots, A_n$, $a_1, b_1, \dots, a_{n+1}, b_{n+1}$ satisfy (3.6).

iv. Let $\lambda \in \mathrm{Sp}^H_{\alpha,\mu,\nu}$ be a pure-string eigenvalue. Then, $s = 0$ and, from (3.6), provided $\lambda \neq \pm i\alpha$, $A_j = 0$ for all $j = 1, \dots, n$, $a_j = 0$ and $b_{j+1} = -cb_j$ for all $j = 1, \dots, n+1$. Hence, set $b_1 \equiv 1$, $A = 0$ and $f(x) = \sinh(\xi_\nu(\lambda)x)$. We consider now the resonant case. Fix $\nu = 0$ and assume $\lambda = \pm i\alpha$ with $\alpha = \tilde{\alpha}(n+1)$, for some $\tilde{\alpha} \in \mathbb{Z}_+$. By item ii.2. in the proof of Proposition 3.2, $a_j = 0$ for all $j = 1, \dots, n+1$, and therefore $f_j(x) = ib_j(-1)^{\tilde{\alpha}(j+1)} \sin(\pi\alpha x)$. Moreover, $A_h = \frac{i}{\mu\alpha\pi}\big((-1)^{\tilde{\alpha}} b_h - b_{h+1}\big)$, $h = 1, \dots, n$. Thus, we have $n+1$ linearly independent eigenfunctions obtained by setting all b_j's to zero except for one at the time, namely of the form (3.21).

v. Let $\lambda \in \mathrm{Sp}^H_{\alpha,\mu,\nu}$ be a string-pendula eigenvalue. Then, from (3.6), $A_j = -\frac{\lambda^2}{\alpha^2+\lambda^2} f_j(x_j)$, $j = 1, \dots, n$. The computation is then analogous to the one in item iii., with the only difference that in this case $Q := 2\xi P_{\alpha,\mu}(\lambda)$.

i. follows from the items above. □

We shall draw the profiles of the eigenfunctions in Section 4.2, after having determined the eigenvalues in $\mathrm{Sp}^{\mathrm{V}}_{\mu,0}$ and $\mathrm{Sp}^{\mathrm{H}}_{\alpha,\mu,0}$. We can, however, already make some comments on the eigenfunctions described in Proposition 3.4.

As we had anticipated, the eigenfunctions associated to both the horizontal and vertical pure-string eigenvalues correspond to the configurations in which the string vibrates as it were alone and unloaded and the pendula stay still.

We note moreover that, conversely, the situation in which the pendula oscillate while the string lies in the resting configuration is never attained. Indeed, in virtue of Corollary 3.1 item iv., the expressions (3.22b) never vanish for string-pendula eigenvalues.

Furthermore, we observe that any horizontal damped normal mode with string-pendula eigenvalue λ, the ratios $\frac{(A^{\mathrm{H}}_{\nu,k,\lambda})_h}{(A^{\mathrm{H}}_{\nu,k,\lambda})_{h'}}$ are fixed by k, since, from expression (3.22a), they equal $\frac{U_{h-1}(C_k)}{U_{h'-1}(C_k)}$ for every $h, h' = 1, \dots, n$. In particular, these ratios depend on n only. We will come back to this aspect in Chapter 5, where we focus on the dynamics of the pendula.

It is also worth highlighting the following symmetry property for the $(A^{\mathrm{H}}_{\nu,k,\lambda})_h$'s. We first notice that, exploiting definition (A.3) for the Chebyshev polynomials, for any $n \geq 1$ and $h, k = 1, \dots, n$, we have

$$\begin{aligned}\sin\left(\frac{\pi k}{n+1}\right) U_{n-h}(C_k) &= \sin\left((n-h+1)\frac{\pi k}{n+1}\right) \\ &= (-1)^{k+1} \sin\left(h\frac{\pi k}{n+1}\right) \\ &= (-1)^{k+1} \sin\left(\frac{\pi k}{n+1}\right) U_{h-1}(C_k).\end{aligned}$$

Therefore, fixed $n \geq 1$, for any horizontal string-pendula eigenvalue, solution of the k-th equation (3.18), the following parity rule holds:

$$(A^{\mathrm{H}}_{\nu,k,\lambda})_{n-h+1} = (-1)^{k+1} (A^{\mathrm{H}}_{\nu,k,\lambda})_h \qquad \forall h = 1, \dots, n. \tag{3.24}$$

Finally, we underline the peculiarity of the non-generic case in which α is resonant. In such circumstances, which we recall might be attained only for $\nu = 0$, by (3.21), each j-th piece of string is independent of the others, and so are the amplitudes of each pendulum. In particular, it could happen (depending on the initial conditions) that the string is at rest in some of the intervals $[x_{j-1}, x_j]$ and the remaining parts of the system are in motion (we refer to Figure 4.8 in the next chapter).

Chapter 4

The vertical and horizontal spectra

In this chapter, we present a detailed description of the spectra of the vertical and horizontal systems, in the undamped and damped cases. They consist of the eigenvalues $\lambda \in \mathbb{C}$, roots of the eigenvalue equations (3.1) and (3.2). Therefore, this study is based on the investigation of the solutions of these transcendental complex equations. In the (undamped) conservative limit, we are able to analytically characterise the frequencies of oscillation from graphical analyses. As for the dissipative regime, we provide explicit expressions for the eigenvalues of the vertical system, while for the horizontal system we partly resort to a numerical study.

4.1 The vertical and horizontal conservative spectra

We begin our spectral study from the conservative case, i.e. when $\nu = 0$. First, it is convenient to rename the eigenvalues of the unloaded string, whose spectrum will be a reference for the undamped system. Indeed, it is useful to group them in bands (even though these bands have no dynamical meaning for the string without pendula), since, as we anticipated in Section 3.2.2, the eigenvalues of the vertical and horizontal systems form families. Thus, we define $\omega^{\mathrm{S}}_{0,0} := 0$ (which is not a frequency) and rename the equally spaced frequencies $\omega^{\mathrm{S}}_m = m$, $m \in \mathbb{Z}_+$, of the vibrating string (see Section 2.1.4) as

$$\omega^{\mathrm{S}}_{\ell,k} := \omega^{\mathrm{S}}_{(n+1)\ell+k}\,, \qquad \ell \in \mathbb{N}\,,\ k = 0, \dots, n$$

The pure-string eigenvalues are then the $\pm i\omega^{\mathrm{S}}_{\ell,0}$'s, $\ell \in \mathbb{Z}_+$. We define the "vibrating string bands" as $B^{\mathrm{S}}_0 := \{\pm i\omega^{\mathrm{S}}_{0,1}, \dots, \pm i\omega^{\mathrm{S}}_{0,n}\}$ and, for $\ell \geq 1$, $B^{\mathrm{S}}_\ell := \{\pm i\omega^{\mathrm{S}}_{\ell,0}, \dots, \pm i\omega^{\mathrm{S}}_{\ell,n}\}$. All bands, except B^{S}_0, contain a conjugate pair of pure-string eigenvalues and n conjugate pairs of eigenvalues with frequencies to their closest right.

4.1.1 The vertical conservative spectrum

We characterise first the vertical conservative spectrum $\mathrm{Sp}^{\mathrm{V}}_{\mu,0}$, for $\mu > 0$.

Proposition 4.1. *Consider any $n \geq 1$ and $\mu > 0$. $\mathrm{Sp}^{\mathrm{V}}_{\mu,0}$ consists of countably many bands B^{V}_ℓ, $\ell \in \mathbb{N}$, each formed by the two pure-string eigenvalues $\pm i\omega^{\mathrm{S}}_{\ell,0} =: \pm i\omega^{\mathrm{V}}_{\ell,0}$ (unless $\ell = 0$) and by n pairs of conjugate purely imaginary eigenvalues $\pm i\omega^{\mathrm{V}}_{\ell,k}$, $k = 1, \ldots, n$, with*

$$\omega^{\mathrm{S}}_{\ell,0} < \omega^{\mathrm{V}}_{\ell,1} < \ldots < \omega^{\mathrm{V}}_{\ell,n} < \omega^{\mathrm{S}}_{\ell+1,0}\,.$$

(See Figure 4.1.)

For each $\ell \geq 0$ and $k = 1, \ldots, n$, $\lim_{\mu\to 0} \omega^{\mathrm{V}}_{\ell,k} = \omega^{\mathrm{S}}_{\ell,k}$ and $\lim_{\mu\to+\infty} \omega^{\mathrm{V}}_{\ell,k} = (\omega^{\mathrm{S}}_{\ell,0})^+$.

The bands become narrower with ℓ: for all $k = 1, \ldots, n$, $\lim_{\ell\to+\infty} \omega^{\mathrm{V}}_{\ell,k} = \omega^{\mathrm{S}}_{\ell,0}$.

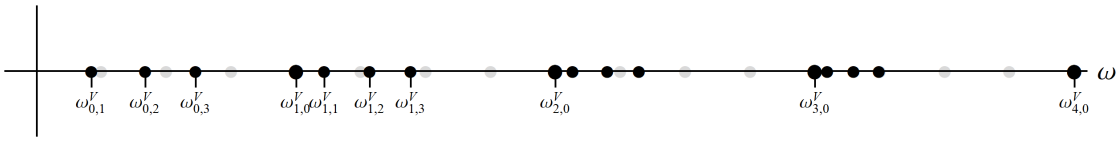

Figure 4.1: The frequencies $\omega^{\mathrm{V}}_{\ell,k}$ of the eigenvalues in the spectrum $\mathrm{Sp}^{\mathrm{V}}_{\mu,0}$ (black dots, for $n = 3$). The frequencies of the first two bands, B^{V}_ℓ ($\ell = 0, 1$), and the pure-string frequencies, $\omega^{\mathrm{S}}_{\ell,0}$, are explicitly labelled, and the latter are marked with a thicker point. To facilitate a comparison, the grey dots represent the frequencies of the (unloaded) vibrating string. The numerical value used in the generation of the picture is $\mu = 0.1$.

Proof. By Proposition 3.1, the eigenvalues are purely imaginary, and come in conjugate pairs. We thus determine those of the form $\lambda = i\omega$ with $\omega \in \mathbb{R}_+$. Since $\xi_0(\lambda) = \pi\lambda$, the eigenvalue equation (3.1) is (3.10). We thus write $\tilde{\omega} := \frac{\omega}{n+1}$, $\tilde{P}_\mu = \frac{\mu(n+1)}{2}$ and as above $C_k = \cos\left(\frac{k\pi}{n+1}\right)$, and look for the positive solutions of

$$\tilde{P}_\mu \pi\tilde{\omega} \sin(\pi\tilde{\omega}) = \cos(\pi\tilde{\omega}) + C_k, \qquad k = 1, \ldots, n\,. \tag{4.1}$$

Since $\tilde{P}_\mu > 0$ and $|C_k| < 1$, each equation (4.1) has exactly one solution $\tilde{\omega}^V_{\ell,k}$ in each interval $(\ell, \ell+1)$, $\ell \in \mathbb{N}$. (An elementary graphical analysis, see Figure 4.2, shows that this is the case if $C_k = 0$ and that, if $C_k \neq 0$, then there is at least one solution in each such interval. But the derivative $\pi^2\tilde{P}_\mu\tilde{\omega}\cos(\pi\tilde{\omega}) + \pi(1+\tilde{P}_\mu)\sin(\pi\tilde{\omega})$ of the function $\tilde{P}_\mu\pi\tilde{\omega}\sin(\pi\tilde{\omega}) - \cos(\pi\tilde{\omega}) - C_k$ is independent of C_k and a similar graphical analysis shows that it has exactly one zero in each interval $(\ell, \ell+1)$; the conclusion then follows from Rolle's theorem). Figure 4.2 also shows that, for ℓ even $\tilde{\omega}^V_{\ell,1} < \ldots < \tilde{\omega}^V_{\ell,n}$ while for ℓ odd $\tilde{\omega}^V_{\ell,n} < \ldots < \tilde{\omega}^V_{\ell,1}$. This proves the band structure of the $\omega^{\mathrm{V}}_{\ell,k} := (n+1)\tilde{\omega}^V_{\ell,k}$. For ℓ odd, we reorder the $\omega^{\mathrm{V}}_{\ell,k}$ so as to have them increasing with k.

A glance at Figure 4.2 shows that, as ℓ increases, the bands become narrower and approach their lowest, pure string, frequency.

The limit behaviours are proven by observing that the solid line in Figure 4.2 becomes steeper if μ increases and flatter if μ decreases.

□

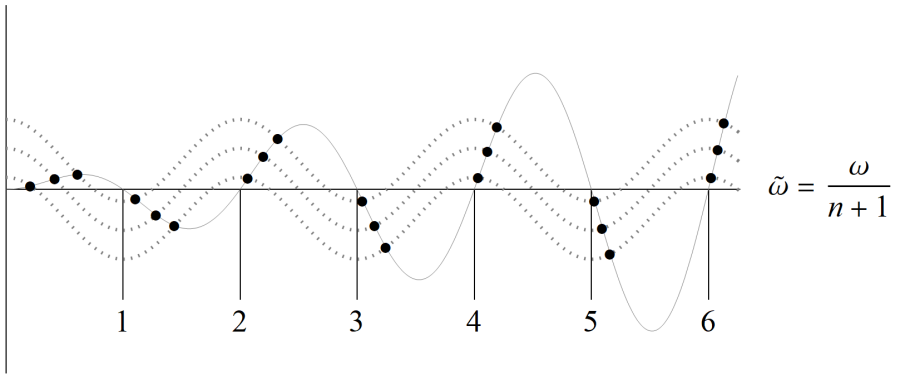

Figure 4.2: Determination of the rescaled string-pendula frequencies $\tilde{\omega}^V_{\ell,k} = \frac{\omega^{\rm V}_{\ell,k}}{n+1}$ of $\mathrm{Sp}^{\rm V}_{\mu,0}$ (for $n = 3$) as intersection between the graphs of the function at the l.h.s. (solid curve) and of the n functions at the r.h.s. (dashed curves) of equation (4.1).

The band structure of $\mathrm{Sp}^{\rm V}_{\mu,0}$ has already been described in Proposition 4.1 and is clearly visible in Figure 4.1. Figure 4.2, where the frequencies are the intersection points of a graph of a function that depends linearly on μ and of a function independent of μ, makes it evident that the eigenvalues depend continuously on μ. Thus, the vertical spectrum $\mathrm{Sp}^{\rm V}_{\mu,0}$ can be seen as a continuous deformation of the spectrum of the (unloaded) vibrating string. As μ increases, the pure-string frequencies $\omega^{\rm S}_{\ell,0}$ remain fixed while the other frequencies $\omega^{\rm V}_{\ell,k}$ move toward the immediately lower pure-string frequency $\omega^{\rm S}_{\ell,0}$ (or zero, if $\ell = 0$). In this way, well-defined bands are formed, which are μ-deformations of the (artificial) bands of $\mathrm{Sp}^{\rm S}$ introduced above.

4.1.2 The horizontal conservative spectrum

We determine now the spectrum of the horizontal conservative system $\mathrm{Sp}^{\rm H}_{\alpha,\mu,0}$, for $\alpha > 0$ and $\mu > 0$. As above, we define $\tilde{\alpha} := \frac{\alpha}{n+1}$ and say that α is *nonresonant* if $\tilde{\alpha} \notin \mathbb{Z}_+$ and *resonant* otherwise.

Proposition 4.2. *For any $n \geq 1$, $\alpha > 0$ and $\mu > 0$, $\mathrm{Sp}^{\rm H}_{\alpha,\mu,0}$ consists of the countably many pure-string eigenvalues $\pm i\omega^{\rm S}_{\ell,0} =: \pm i\omega^{\rm H}_{\ell,0}$, $\ell \in \mathbb{Z}_+$, and, for each $\ell \in \mathbb{N}$ if α is nonresonant and $\ell \in \mathbb{N} \setminus \{\tilde{\alpha}\}$ if α is resonant, of $2n$ purely imaginary eigenvalues $\pm i\omega^{\rm H}_{\ell,k}$, $k = 1, \ldots, n$, which satisfy*

$$\omega^{\rm S}_{\ell,0} < \omega^{\rm H}_{\ell,1} < \ldots < \omega^{\rm H}_{\ell,n} < \min(\alpha, \omega^{\rm S}_{\ell+1,0}) \qquad \text{if} \quad \ell < \tilde{\alpha} \tag{4.2a}$$

$$\max(\alpha, \omega^{\rm S}_{\ell-1,0}) < \omega^{\rm H}_{\ell,1} < \ldots < \omega^{\rm H}_{\ell,n} < \omega^{\rm S}_{\ell,0} \qquad \text{if} \quad \ell > \tilde{\alpha}\,. \tag{4.2b}$$

(See Figure 4.3).

Moreover, for each $k = 1, \ldots, n$, $\omega^{\rm H}_{\ell,k} \to \omega^{\rm S}_{\ell,k}$ as $\ell \to +\infty$, and, for any $\ell \in \mathbb{N}$ ($\ell \in \mathbb{N} \setminus \{\tilde{\alpha}\}$ if α resonant), $\omega^{\rm H}_{\ell,k} \to (\omega^{\rm S}_{\ell,0})^+$ (resp. $(\omega^{\rm S}_{\ell,0})^-$) for $\ell < \tilde{\alpha}$ (resp. $\ell > \tilde{\alpha}$) as $\mu \to +\infty$. ($\mathrm{Sp}^{\rm H}_{\alpha,\mu,0}$ has a band structure which is described after the proof.)

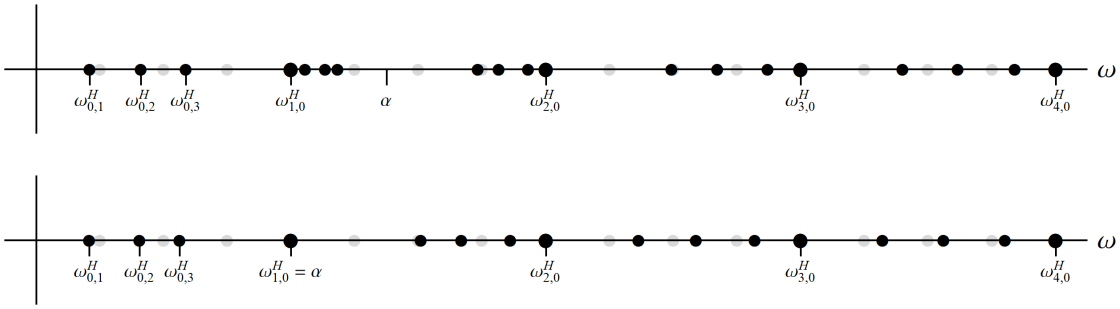

Figure 4.3: The frequencies $\omega^{\mathrm{H}}_{\ell,k}$ of the eigenvalues in the spectrum $\mathrm{Sp}^{\mathrm{H}}_{\alpha,\mu,0}$ (black dots, for $n = 3$). The frequencies of the first band, B^{H}_0, and the pure-string frequencies, $\omega^{\mathrm{S}}_{\ell,0}$, are explicitly labelled, and the latter are marked with a thicker point. To facilitate a comparison, the grey dots represent the frequencies of the vibrating string. Top: Nonresonant case $\frac{\alpha}{n+1} \notin \mathbb{Z}$. Bottom: Resonant case $\frac{\alpha}{n+1} \in \mathbb{Z}$. The numerical values used in the generation of the two pictures are $\mu = 0.1$ and, respectively, $\alpha = 5.5$ and $\alpha = 4$.

Proof. By Proposition 3.1, the eigenvalues are purely imaginary and come in conjugate pairs. Thus, we determine those of the form $\lambda = i\omega$ with $\omega \in \mathbb{R}_+$. Since $\xi_0(\lambda) = \pi\lambda$, by Corollary 3.1, the solutions of (3.16) are the pure-string eigenvalues $\pm i\omega^{\mathrm{H}}_{\ell,0}$, while the string-pendula eigenvalues are the solutions of the n equations (3.18). Thus, we write $\tilde\omega := \frac{\omega}{n+1}$ and $C_k = \cos\Big(\frac{k\pi}{n+1}\Big)$, and look for the positive solutions $\tilde\omega \neq \tilde\alpha$ of the n equations

$$f(\tilde\omega)\sin(\pi\tilde\omega) = \cos(\pi\tilde\omega) + C_k\,, \qquad k = 1, \dots, n\,, \tag{4.3}$$

with $f : \mathbb{R} \setminus \{\tilde\alpha\} \to \mathbb{R}$ given by

$$f(\tilde\omega) = \frac{\pi\mu\tilde\alpha^2}{2(n+1)}\frac{\tilde\omega}{\tilde\alpha^2 - \tilde\omega^2}.$$

If $\tilde\alpha \notin \mathbb{Z}_+$ then the function f has a vertical asymptote at $\tilde\omega = \tilde\alpha$. If $\tilde\alpha \in \mathbb{Z}_+$, instead, f extends to a continuous function on $\mathbb{R}$ which in $\tilde\omega = \tilde\alpha$ has a strict maximum $\frac{\pi}{2}$ if $\tilde\alpha$ is odd and a strict minimum $-\frac{\pi}{2}$ if $\tilde\alpha$ is even. Note also that, in all cases, the factor $\frac{\tilde\omega}{\tilde\alpha^2-\tilde\omega^2}$ changes sign at $\tilde\omega > \tilde\alpha$.

A graphical analysis, similar to that of the proof of Proposition 4.1, shows that, if $\tilde\alpha \notin \mathbb{Z}_+$, then, for each $k = 1, \dots, n$, the solutions of equation (4.3) form a sequence $\tilde\omega^H_{\ell,k}$, $\ell \in \mathbb{N}$, with $\tilde\omega^H_{\ell,k} \in (\ell, \ell+1)$ if $\ell < \tilde\alpha$ and $\tilde\omega^H_{\ell,k} \in (\ell-1, \ell)$ if $\ell > \tilde\alpha$ and, moreover, $\tilde\omega^H_{\ell,k} \neq \tilde\omega^H_{\ell,k+1}$ for all ℓ and k and $\tilde\omega^H_{\lfloor\tilde\alpha\rfloor,k} < \tilde\alpha < \tilde\omega^H_{\lceil\tilde\alpha\rceil,k}$ for all k. For each ℓ we reorder the $\tilde\omega^H_{\ell,k}$ so as to have them increasing with k. See Figure 4.4 top.

If $\tilde\alpha \in \mathbb{Z}_+$ the situation is analogous except that, for each k, equation (4.3) has a sequence of solutions which can be labelled $\tilde\omega^H_{\ell,k}$ with $\ell \in \mathbb{N}\setminus\{\tilde\alpha\}$ and satisfy $\ell < \tilde\omega^H_{\ell,k} < \ell+1$ if $\ell < \tilde\alpha$ and $\ell - 1 < \tilde\omega^H_{\ell,k} < \ell$ if $\ell > \tilde\alpha$, etc. (see Figure 4.4 bottom).

The limit behaviours are proven by observing that the solid line in Figure 4.4 becomes steeper if μ increases, and vice versa it flattens for $\ell \to +\infty$. □

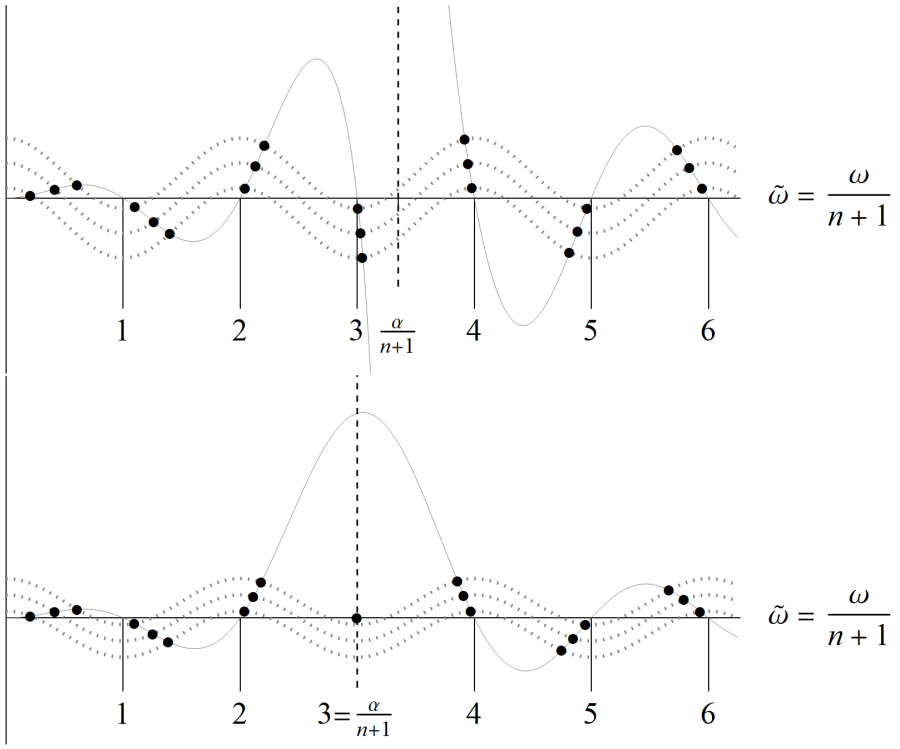

Figure 4.4: Determination of the rescaled string-pendula frequencies $\tilde{\omega}^H_{\ell,k} = \frac{\omega^{\mathrm{H}}_{\ell,k}}{n+1}$ of $\mathrm{Sp}^{\mathrm{H}}_{\alpha,\mu,0}$ (for $n = 3$) as intersection between the graphs of the function at the l.h.s. (solid curve) and of the n functions at the r.h.s. (dashed curves) of equation (4.3). Top: Nonresonant case $\frac{\alpha}{n+1} \notin \mathbb{Z}$. Bottom: Resonant case $\frac{\alpha}{n+1} \in \mathbb{Z}$. The numerical values used in the generation of the two pictures are $\mu = 0.1$ and, respectively, $\alpha = 13.5$ and $\alpha = 12$.

Band structure. The undamped horizontal spectrum is illustrated in Figure 4.3 and has a band structure with bands B^{H}_ℓ, $\ell \in \mathbb{N}$, formed by all the eigenvalues $\pm i\omega^{\mathrm{H}}_{\ell,k}$ with that ℓ, which is similar to that of the undamped vertical spectrum, but with two qualitative differences. First, when α is resonant, namely $\frac{\alpha}{n+1} =: \bar{\ell} \in \mathbb{Z}_+$, then the $(\bar{\ell}+1)$-th band $B^{\mathrm{H}}_{\bar{\ell}}$ consists of the single pair of pure-string eigenvalues $\omega^{\mathrm{H}}_{\bar{\ell},k} = (n+1)\bar{\ell}$. In such a case, as seen in Proposition 3.4, each such eigenvalue has multiplicity $n+1$. This may be related to the fact that, as a glance at Figure 4.4 shows, when $\alpha \to (n+1)\bar{\ell}$ with $\bar{\ell} \in \mathbb{Z}_+$, all the $n+1$ frequencies $\omega^{\mathrm{H}}_{\bar{\ell},k}$ of the eigenvalues in the band $B^{\mathrm{H}}_{\bar{\ell}}$ collapse to $(n+1)\bar{\ell}$. Second, the bands B^{H}_ℓ on the left of α, with $0 \le \ell < \tilde{\alpha}$, and those on the right of α, with $\ell > \tilde{\alpha}$, are arranged in different ways: the pure-string frequency $\omega^{\mathrm{S}}_{\ell,0}$ (or $\omega^{\mathrm{S}}_{0,0} = 0$ if $\ell = 0$) of the former is the smallest frequency of the band, while it is the largest in the latter.

By comparing $\mathrm{Sp}^{\mathrm{V}}_{\mu,0}$ and $\mathrm{Sp}^{\mathrm{H}}_{\alpha,\mu,0}$ (and Figures 4.1 and 4.3), we can notice some additional differences in the band structure of the two. In particular, we remark that, first, while in $\mathrm{Sp}^{\mathrm{H}}_{\alpha,\mu,0}$ the narrowest bands are those close to $\frac{\alpha}{n+1}$, in $\mathrm{Sp}^{\mathrm{V}}_{\mu,0}$ the bands B_ℓ's get thinner as ℓ increases, and second, as already mentioned, all the frequencies of the eigenvalues in $\mathrm{Sp}^{\mathrm{V}}_{\mu,0}$ approach those of pure string from the right, while the opposite

happens in $\mathrm{Sp}^{\mathrm{H}}_{\alpha,\mu,0}$ for those frequencies larger than $\frac{\alpha}{n+1}$. Both these properties can be understood by thinking of $\mathrm{Sp}^{\mathrm{V}}_{\mu,0}$ as a limit case of $\mathrm{Sp}^{\mathrm{H}}_{\alpha,\mu,0}$ for $\alpha \to +\infty$.

Dependence on μ. Clearly, for any given $\ell \in \mathbb{N}$, when $\mu \to +\infty$ all $\omega^{\mathrm{H}}_{\ell,k} \to \omega^{\mathrm{S}}_{\ell,0}$ (the solid curve in Figure 4.4 becomes steeper and steeper). The behaviour for $\mu \to 0$ of the string-pendula frequencies is more complex, and in one feature depends on whether α is resonant or not. If α is resonant, when $\mu \to 0$ the solid curve in Figure 4.4 (bottom) becomes flatter and flatter and each $\omega^{\mathrm{H}}_{\ell,k}$ tends to $\omega^{\mathrm{S}}_{\ell,k}$ if $\ell < \frac{\alpha}{n+1}$ and to $\omega^{\mathrm{S}}_{\ell-1,k}$ if $\ell > \frac{\alpha}{n+1}$. If α is nonresonant, then when $\mu \to 0$ the solid curve in Figure 4.4 (top) becomes flatter and flatter, retaining however the asymptote at $\tilde{\omega} = \tilde{\alpha}$. This implies that the frequencies $\omega^{\mathrm{H}}_{\ell,k}$ with $\ell = \lfloor \frac{\alpha}{n+1} \rfloor$ remain at the left of $\frac{\alpha}{n+1}$ and those with $\ell = \lceil \frac{\alpha}{n+1} \rceil$ remain at the right of $\frac{\alpha}{n+1}$. As a consequence, all the $\omega^{\mathrm{H}}_{\ell,k}$ have the same limit behaviours as in the resonant case, except those with $\ell = \lfloor \frac{\alpha}{n+1} \rfloor$ and those with $\ell = \lceil \frac{\alpha}{n+1} \rceil$. Of these $2n$ frequencies, n tend to the $\omega^{\mathrm{S}}_{\lfloor \frac{\alpha}{n+1} \rfloor,k}$'s and n tend to α (which ones tend to the formers and which to the latter depends on the actual value of $\frac{\alpha}{n+1}$).

4.2 The eigenfunctions of the conservative system

Now that we have determined the eigenvalues in $\mathrm{Sp}^{\mathrm{V}}_{\mu,0}$ and $\mathrm{Sp}^{\mathrm{H}}_{\alpha,\mu,0}$, we can complete our description of the eigenfunctions, obtained in Section 3.3, for the undamped vertical and horizontal systems.

4.2.1 The vertical eigenfunctions

The vertical system describes a vibrating string, in the vertical plane XZ, periodically loaded with n identical point masses located at $(x_h, f(x_h))$, with $x_h = \frac{h}{n+1}$ and $h = 1, \ldots, n$. By Propositions 3.4 and 4.1, for any pure-string eigenvalue $i\omega^{\mathrm{V}}_{\ell,0}$ ($\ell \in \mathbb{Z}_+$), $f(x_h)$ is $f^{KV}_{0,i\omega^{\mathrm{V}}_{\ell,0}}(x_h) = 0$, while for any string-pendula eigenvalue $i\omega^{\mathrm{V}}_{\ell,k}$ ($\ell \in \mathbb{N}, k = 1, \ldots, n$), by equation (3.20), $f(x_h)$ is

$$f^{\mathrm{V}}_{0,k,i\omega^{\mathrm{V}}_{\ell,k}}(x_h) = \sin\left(\frac{\pi\omega^{\mathrm{V}}_{\ell,k}}{n+1}\right) U_{h-1}(C_k), \qquad h = 1, \ldots, n. \tag{4.4}$$

As expected, for small μ's, the vibrating string profiles, and especially the low-frequency normal modes, are weakly deformed by the masses. Vice versa, large values of μ and high-frequency normal modes correspond to configurations in which the masses undergo very small amplitude oscillations. Indeed, as μ or ℓ tend to $+\infty$, $\omega^{\mathrm{V}}_{\ell,k} \to \omega^{\mathrm{V}}_{\ell,0}$ and, by (4.4), $f^{\mathrm{V}}_{0,k,i\omega^{\mathrm{V}}_{\ell,k}}(x_h) \to 0$ for every $h = 1, \ldots, n$.

Figure 4.5 shows the profiles corresponding to the first few vertical normal modes, from which the characteristics of the eigenfunctions under discussion emerge.

4.2.2 The horizontal eigenfunctions

The horizontal system is more interesting.

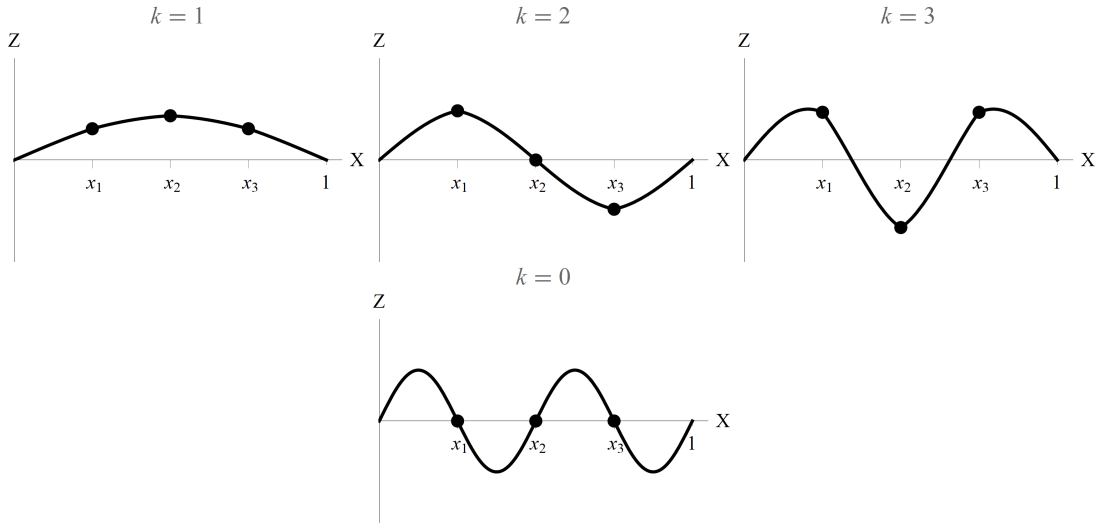

Figure 4.5: The profiles of the vertical eigenfunctions for $\nu = 0$, in the XZ-plane, associated to the eigenvalues in the first band B^{V}_{ℓ}, $\ell = 0$ (top) and to the first pure-string eigenvalues $\pm i\omega^{\mathrm{V}}_{1,0}$, $\ell = 1, k = 0$ (bottom), for $n = 3$. The numerical value used in the generation of the pictures is $\mu = 0.1$.

By Proposition 3.4, we already know that the pendula are at rest in the equilibrium configuration in any pure-string normal mode. Conversely, by equation (3.22), they undergo large amplitude oscillations, compared to the displacement of the string, for string-pendula normal modes with frequencies close to α. Expression (4.2) suggests that this occurs, aside from when α is resonant, for those eigenvalues in the bands $B^{\mathrm{H}}_{\lfloor\tilde{\alpha}\rfloor}$ and $B^{\mathrm{H}}_{\lceil\tilde{\alpha}\rceil}$. Proposition 4.2 also indicates that for high-frequency normal modes the string is weakly affected by the pendula. We recall, moreover, that the ratio between the oscillation amplitudes of the pendula is independent of the parameters α, μ, and that for any string-pendula normal mode with frequency $\omega^{\mathrm{H}}_{\ell,k}$, the relation (3.24) holds.

The (special) resonant case requires a separate discussion. Indeed, for specific values of the parameter α, specifically for $\alpha = \tilde{\alpha}(n+1)$ with $\tilde{\alpha} \in \mathbb{Z}_+$, the pair $\pm i\alpha$ belongs to $\mathrm{Sp}^{\mathrm{H}}_{\alpha,\mu,0}$. When this is the case, there are $n+1$ horizontal normal modes that have frequency α, the eigenfunctions of which are (3.21). For any such eigenfunction, only one piece of string of length $\frac{1}{n+1}$ and the pendula at its extremities have nonzero amplitude of oscillation, while the remaining parts of the system are at rest.

To conclude, we remark that the parameter μ enters in a similar way as in the vertical system, namely as μ increases the profile of the string is more deformed and the amplitudes of the pendula become smaller, with however the difference that, by Proposition 4.2, for any $\mu > 0$, every string-pendula normal mode has a frequency $\omega^{\mathrm{H}}_{\ell,k}$ which is higher than $\omega^{\mathrm{S}}_{\ell,k}$ for $\ell > \frac{\alpha}{n+1}$ $(\forall k = 1, \ldots, n)$.

Figures 4.6—4.8 show the profiles corresponding to some of the horizontal normal modes, for different values of α, from which the characteristics of the eigenfunctions under discussion emerge.

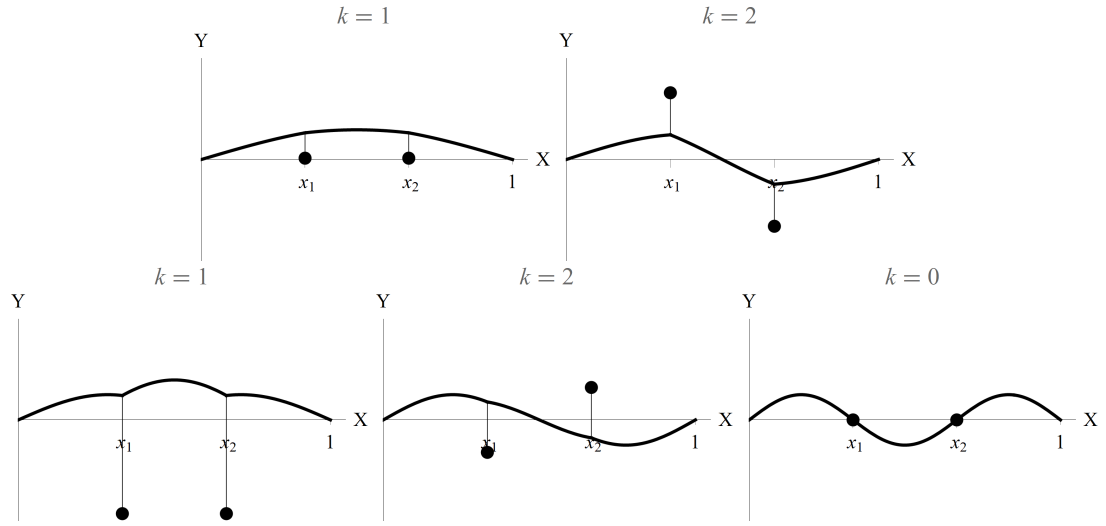

Figure 4.6: The profiles of the horizontal eigenfunctions for $\nu = 0$, projected on the XY-plane, associated to the first two bands B^{H}_ℓ, $\ell = 0$ (top) and $\ell = 1$ (bottom), for $n = 2$. The numerical values used in the generation of the pictures are $\mu = 0.1$ and $\alpha = 1.5$.

4.3 The vertical and horizontal dissipative spectra

We now study the spectra of the vertical and horizontal systems for $\nu > 0$.

First, it is useful to rename the eigenvalues of the (unloaded) viscoelastic string so as to group them in bands as we did for the conservative case. For the Kelvin-Voigt string we define $\lambda^{KV}_{0,0,\pm} := 0$ (which is not an eigenvalue) and, for all $\ell \in \mathbb{N}$ and $k \in \{1, \dots, n\}$,

$$\lambda^{KV}_{\ell,k,\pm} := \lambda^{KV}_{(n+1)\ell+k,\pm}\,,$$

with the $\lambda^{KV}_{\ell,\pm}$'s defined in (2.15). The pure-string eigenvalues are the $\lambda^{KV}_{\ell,0}$'s, $\ell \in \mathbb{Z}_+$. Next, we distinguish the nonreal eigenvalues from the real ones defining

$$\begin{aligned} \lambda^{KV}_{\ell,k} &:= \lambda^{KV}_{(n+1)\ell+k,+} \qquad \text{if} \quad (n+1)\ell + k < \tfrac{2}{\nu} \\ r^{KV}_{\ell,k,\pm} &:= \lambda^{KV}_{(n+1)\ell+k,\pm} \qquad \text{if} \quad (n+1)\ell + k \geq \tfrac{2}{\nu} \end{aligned}$$

so that, for all the ℓ, k's for which they are defined,

$$\lambda^{KV}_{\ell,k}\,, \overline{\lambda^{KV}_{\ell,k}} \in C^*_\nu := C_\nu \setminus \{-\tfrac{2}{\nu}\}\,, \qquad r^{KV}_{\ell,k,\pm} \in \mathbb{R}\,,$$

where C_ν, as before, is the circle of centre $(-\frac{1}{\nu}, 0)$ and radius $\frac{1}{\nu}$. For each $\ell \geq 0$, we define the $(\ell+1)$-th "Kelvin-Voigt band" B^{KV}_ℓ as formed by all the eigenvalues $\lambda^{KV}_{\ell,k}\,, \overline{\lambda^{KV}_{\ell,k}}\,, r^{KV}_{\ell,k,\pm}$. Thus, all bands consist of $2n$ string-pendula eigenvalues and those with $\ell \geq 1$ also of two pure-string eigenvalues, either $\lambda^{KV}_{\ell,0}$ and $\overline{\lambda^{KV}_{\ell,0}}$ or $r^{KV}_{\ell,0,+}$ and $r^{KV}_{\ell,0,-}$.

For reasons that will appear clear later, we will be particularly interested in the bands contained in C^*_ν and – except in the special case in which $\frac{2}{(n+1)\nu}$ is an integer, so that $-\frac{2}{\nu}$

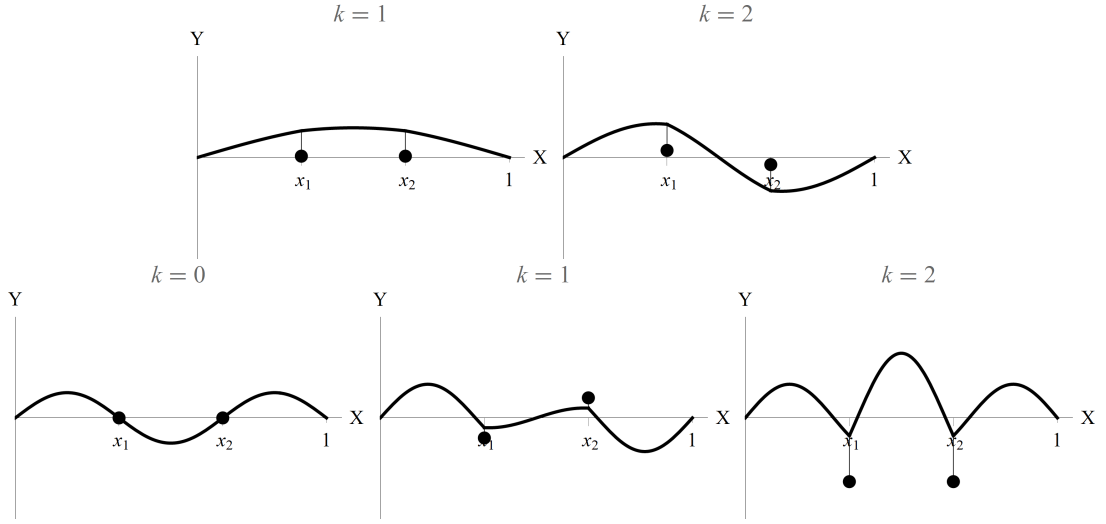

Figure 4.7: The profiles of the horizontal eigenfunctions for $\nu = 0$, projected on the XY-plane, associated to the first two bands B^{H}_ℓ, $\ell = 0$ (top) and $\ell = 1$ (bottom), for $n = 2$. The numerical values used in the generation of the pictures are $\mu = 0.1$ and $\alpha = 4$.

is a pure-string eigenvalue – to the first band which has (some) real eigenvalues. These are the first $\bar{\ell}$ bands $B^{\mathrm{KV}}_0, \ldots, B^{\mathrm{KV}}_{\bar{\ell}-1}$, with

$$\bar{\ell} := \left\lceil \frac{2}{(n+1)\nu} \right\rceil \geq 1 \,. \tag{4.5}$$

Indeed, if $\frac{2}{(n+1)\nu} \in \mathbb{Z}_+$ then $r^{\mathrm{KV}}_{\bar{\ell},0,\pm} = -\frac{2}{\nu}$, the bands $B^{\mathrm{KV}}_0, \ldots, B^{\mathrm{KV}}_{\bar{\ell}-1}$ are entirely contained in C^*_ν and all other bands have only real eigenvalues. If $\frac{2}{(n+1)\nu} < 1$ then $\lambda^{\mathrm{KV}}_{1,0,\pm} = r^{\mathrm{KV}}_{1,0,\pm} \in \mathbb{R}$ and only B^{KV}_0 may have eigenvalues in C^*_ν (if it does and how many depends on ν). Similarly, if $1 < \frac{2}{(n+1)\nu} \notin \mathbb{Z}_+$ then $\lambda^{\mathrm{KV}}_{\bar{\ell},0,\pm} = r^{\mathrm{KV}}_{\bar{\ell},0,\pm} \in \mathbb{R}$, the bands $B^{\mathrm{KV}}_0, \ldots, B^{\mathrm{KV}}_{\bar{\ell}-2}$ are contained entirely in C^*_ν while $B^{\mathrm{KV}}_{\bar{\ell}-1}$ has its pure-string eigenvalue $\lambda^{\mathrm{KV}}_{\bar{\ell}-1,0}$ in C^*_ν and, depending on ν, all, some or none of its string-pendula eigenvalues in C^*_ν.

4.3.1 The vertical spectrum

In this section, we determine the spectrum of the vertical system. As we shall see in Lemma 4.1, there is a relation between this spectrum and the one we studied in Section 4.1.1 for the conservative case. Indeed, the knowledge of the undamped one allows us to understand the structure of the damped one.

Proposition 4.3. *Consider any $n \geq 1$, $\alpha > 0$, and $\mu > 0$. For any $\nu > 0$, $\mathrm{Sp}^{\mathrm{V}}_{\mu,\nu}$ contains all the pure-string eigenvalues of the Kelvin-Voigt spectrum $\mathrm{Sp}^{\mathrm{KV}}_\nu$ and consists of a finite (possibly zero) number of pairs of complex conjugate eigenvalues which belong to the circle C^*_ν and countably many real eigenvalues which belong to the interval $(-\infty, -\frac{1}{\nu})$ and accumulate at $-\infty$ and at $-\frac{1}{\nu}$. ($\mathrm{Sp}^{\mathrm{V}}_{\mu,\nu}$ has a band structure, which is described after the proof).*

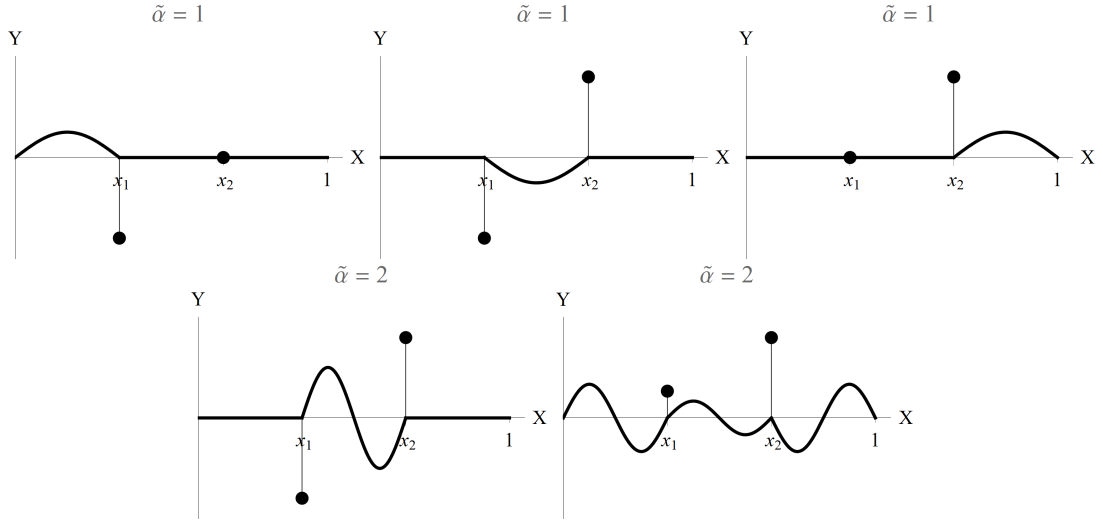

Figure 4.8: The profiles of the horizontal eigenfunctions for $\nu = 0$, projected on the XY-plane, associated to the first (top) and second (bottom) resonance, for $n = 2$. The numerical values used in the generation of the pictures are $\mu = 0.1$, and $\alpha = 3$ (top row), $\alpha = 6$ (bottom row).

Proof. If $\nu > 0$, then, by Proposition 3.1, the eigenvalues are not purely imaginary. However:

Lemma 4.1. *Assume $\nu > 0$. Then, for any $\mu > 0$, $\lambda \in \mathrm{Sp}^{\mathrm{V}}_{\mu,\nu}$ if and only if $\lambda \neq -\frac{1}{\nu}$ and $\frac{\xi_\nu(\lambda)}{\pi} \in \mathrm{Sp}^{\mathrm{V}}_{\mu,0}$.*

Proof. By item i. of Proposition 3.2, $\lambda \in \mathrm{Sp}^{\mathrm{V}}_{\mu,\nu}$ if and only if $\lambda \neq 0$, $\lambda \neq -\frac{1}{\nu}$ and

$$\sinh\Big(\frac{\pi\hat\xi}{n+1}\Big)\, U_n\Big(P_\mu \pi\hat\xi \sinh\Big(\frac{\pi\hat\xi}{n+1}\Big) + \cosh\Big(\frac{\pi\hat\xi}{n+1}\Big)\Big) = 0 \tag{4.6}$$

with $\hat\xi := \frac{\xi_\nu(\lambda)}{\pi} = \frac{\lambda}{(1+\nu\lambda)^{1/2}}$. It is easy to verify that, for all $\lambda \neq -\frac{1}{\nu}$, $\hat\xi \neq -\frac{1}{\nu}$ (indeed, $\hat\xi = -\frac{1}{\nu}$ for $\lambda = \frac{1\pm\sqrt{5}}{2\nu}$). Therefore, observing that $\hat\xi = 0$ if and only if $\lambda = 0$ and recalling that $\xi_0(\lambda) = \pi\lambda$, item i. of Proposition 3.2 implies that the two conditions $\lambda = 0$ and (4.6) are equivalent to $\hat\xi \in \mathrm{Sp}^{\mathrm{V}}_{\mu,0}$. □

This has two consequences. First, for any $\lambda \in \mathrm{Sp}^{\mathrm{V}}_{\mu,\nu}$, $\frac{\xi_\nu(\lambda)}{\pi} = \frac{\lambda}{(1+\nu\lambda)^{1/2}}$ is purely imaginary. Therefore, $\frac{\lambda^2}{1+\nu\lambda}$ is real and hence $(\lambda-\bar\lambda)(\lambda+\bar\lambda+\nu\lambda\bar\lambda) = 0$. This implies that, in the complex plane, the eigenvalues lie either on the real axis or on the circle C_ν, or at their intersection.

Second, provided that $\omega^{\mathrm{V}}_{\ell,k}$, $\ell \in \mathbb{N}$ and $k = 0, \dots, n$, denote the frequencies of the (undamped) loaded string as in Proposition 4.1, it follows that $\lambda \in \mathrm{Sp}^{\mathrm{V}}_{\mu,\nu}$ if and only if $\lambda \neq -\frac{1}{\nu}$ and $\xi_\nu(\lambda) = \pm i\pi\omega^{V}_{\ell,k}$ for some $\ell \in \mathbb{N}$, $k = 0, \dots, n$ (except, as always, $\ell = k = 0$),

namely $\lambda = \lambda^{\mathrm{V}}_{\ell,k,\pm}$ with

$$\lambda^{\mathrm{V}}_{\ell,k,\pm} = -\frac{\nu(\omega^{\mathrm{V}}_{\ell,k})^2}{2} \pm \sqrt{\left(\frac{\nu(\omega^{\mathrm{V}}_{\ell,k})^2}{2}\right)^2 - (\omega^{V}_{\ell,k})^2}. \tag{4.7}$$

Thus, since the $\omega^{\mathrm{V}}_{\ell,k}$'s grow unbounded with ℓ, there is a finite (possibly zero) number of pairs of nonreal eigenvalues $\lambda^{\mathrm{V}}_{\ell,k} = \lambda^{\mathrm{V}}_{\ell,k,+}$, $\overline{\lambda^{\mathrm{V}}_{\ell,k}} = \lambda^{\mathrm{V}}_{\ell,k,-}$ which belong to C^*_ν (those with ℓ, k such that $\omega^{\mathrm{V}}_{\ell,k} < \frac{2}{\nu}$) and countably many real eigenvalues $r^{\mathrm{V}}_{\ell,k,\pm} = \lambda^{\mathrm{V}}_{\ell,k,\pm}$ (those with ℓ, k such that $\omega^{\mathrm{V}}_{\ell,k} \geq \frac{2}{\nu}$; they are all distinct, except possibly two in $-\frac{2}{\nu}$, because $r^{\mathrm{V}}_{\ell,k,+} \geq -\frac{2}{\nu}$ strictly increases and $r^{\mathrm{V}}_{\ell,k,-} \leq -\frac{2}{\nu}$ strictly decreases with $\omega^{\mathrm{V}}_{\ell,k}$). Since all $\omega^{\mathrm{V}}_{\ell,k} \to +\infty$ when $\ell \to +\infty$, it is easily seen that in such a limit all $r^{\mathrm{V}}_{\ell,k,-} \to -\infty$ and all $r^{\mathrm{V}}_{\ell,k,-} \to -\frac{1}{\nu}$. □

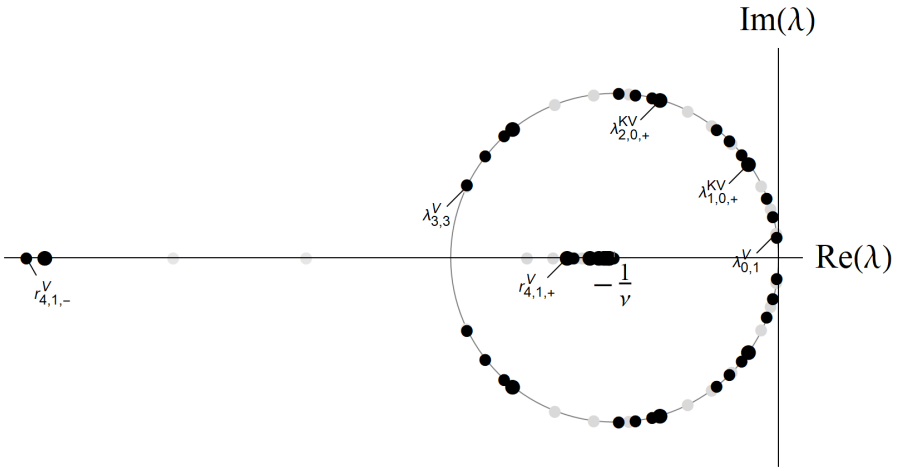

Figure 4.9: The eigenvalues (4.7) of the vertical spectrum $\mathrm{Sp}^{\mathrm{V}}_{\mu,\nu}$ (black dots). To facilitate a comparison, the grey dots represent the frequencies of the Kelvin-Voigt viscoelastic string. The numerical values used in the generation of the picture are $n = 3$, $\mu = 0.1$ and $\nu = 0.15$. Countably many eigenvalues, $r^{\mathrm{V}}_{\ell,k,\pm}$ with $\ell \geq 4$ and $k = 0, \ldots, 3$, belong to the negative real axis, and four bands of conjugate pairs of eigenvalues, $\lambda^{\mathrm{V}}_{\ell,k}, \overline{\lambda^{\mathrm{V}}_{\ell,k}}$ with $\ell = 0, \ldots, 3$ and $k = 0, \ldots, 3$ (except $\ell = k = 0$), belong to the circle C_ν.

Figure 4.9 illustrates the vertical spectrum $\mathrm{Sp}^{\mathrm{V}}_{\mu,\nu}$ and compares it with the spectrum Sp^{KV}_{ν} of the Kelvin-Voigt string.

Similarly to the undamped case, for each $\nu > 0$, the vertical spectrum $\mathrm{Sp}^{\mathrm{V}}_{\mu,\nu}$ can be seen as a continuous μ-deformation of the Kelvin-Voigt spectrum Sp^{KV}_{ν}. Indeed, since $\omega^{\mathrm{V}}_{\ell,0} = \omega^{\mathrm{S}}_{\ell,0}$, $\lambda^{\mathrm{V}}_{\ell,0,\pm} = \lambda^{\mathrm{KV}}_{\ell,0,\pm}$ are the pure-string eigenvalues, and, for $k \neq 0$, the $\lambda^{\mathrm{V}}_{\ell,k,\pm}$'s depend continuously on μ and tend to the $\lambda^{KV}_{\ell,k,\pm}$'s for $\mu \to 0$. This follows from (4.7), the continuity of the $\omega^{\mathrm{V}}_{\ell,k}$'s on μ and the fact that all $\omega^{\mathrm{V}}_{\ell,k} \to \omega^{\mathrm{S}}_{\ell,k}$ as $\mu \to 0$. Similarly, all $\lambda^{\mathrm{V}}_{\ell,k,\pm}$ tend to the pure-string eigenvalues $\lambda^{\mathrm{V}}_{\ell,0,\pm} = \lambda^{\mathrm{KV}}_{\ell,0,\pm}$ for $\mu \to +\infty$.

Furthermore, the fact that the $\omega^{\mathrm{V}}_{\ell,k}$'s are arranged in bands implies that $\mathrm{Sp}^{\mathrm{V}}_{\mu,\nu}$ also has a band structure, with bands formed by the $\lambda^{\mathrm{V}}_{\ell,k,\pm}$ with the same ℓ. The bands are separated

by the pure-string eigenvalues because the vertical eigenvalues $\lambda^{\mathrm{V}}_{\ell,k,\pm}$ are ordered in the same way as the real Kelvin-Voigt eigenvalues $\lambda^{KV}_{\ell,k,\pm}$. (This follows from the monotonicity properties of the real eigenvalues $r^{\mathrm{V}}_{\ell,k,\pm}$ as functions of the $\omega^{\mathrm{V}}_{\ell,k}$ mentioned above, just after formula (4.7), and from the fact that, for those in C^*_ν, $\mathrm{Re}(\lambda^{\mathrm{V}}_{\ell,k}) = -\frac{1}{2}\nu(\omega^{\mathrm{V}}_{\ell,k})^2$). The bands in $\mathrm{Sp}^{\mathrm{V}}_{\mu,\nu}$ are μ-deformations of the bands of the Kelvin-Voigt spectrum in which, as μ increases, the string-pendula eigenvalues of the Kelvin-Voigt band B^{KV}_ℓ move closer to the pure-string eigenvalues $\lambda^{KV}_{\ell,0,\pm}$ of that band (or to 0, if $\ell = 0$). In doing so, all Kelvin-Voigt bands in $\mathbb{R}$ remain in $\mathbb{R}$ and those in C^*_ν remain in C^*_ν, with the only possible exception, when $-\frac{2}{\nu}$ is not a pure-string eigenvalue, of the real eigenvalues of the band denoted $B^{KV}_{\ell-1}$ in Section 3.2.2, see (4.5), which move towards each other along the real axis until they meet in $-\frac{2}{\nu}$ and enter C^*_ν.

We also note that the fact that, when $\mu \to +\infty$, the vertical eigenvalues move towards the pure-string Kelvin-Voigt eigenvalues has a simple mechanical explanation. If the pendula are very massive and the energy of the oscillations of the system is fixed, then necessarily the oscillation amplitudes of the pendula must be very small. In the limit $\mu \to +\infty$ the pendula should remain still, which is exactly what happens in the pure-string normal modes. We anticipate that we will find this limit behaviour also in the horizontal spectrum, where, however, there will be also a different possibility.

Finally, we note that, as in the Kelvin-Voigt viscoelastic string, for ν not too large, the least damped normal mode is that with eigenvalue $\lambda^{\mathrm{V}}_{0,1}$, followed by that with eigenvalue $\lambda^{\mathrm{V}}_{0,2}$ (or $\lambda^{\mathrm{V}}_{1,0}$ if $n = 1$), etc.

4.3.2 The horizontal spectrum

We now consider the horizontal system (2.22). For the horizontal spectrum, the fact that the argument of the Chebyshev polynomials in (3.2b) contain the function $P_{\alpha,\mu}$ of λ, and not a constant, has the consequence that, unlike the vertical spectrum, it is no longer true that $\lambda \in \mathrm{Sp}^{\mathrm{H}}_{\alpha,\mu,\nu}$ if and only if $\xi_\nu \in \pi\mathrm{Sp}^{\mathrm{H}}_{\alpha,\mu,0}$. Correspondingly, the study of the horizontal spectrum in the presence of damping is significantly more complicated. In fact, it is not difficult to obtain an analytic comprehension of the real component of the spectrum, but for the component of the spectrum outside the real axis, we will have to resort to a combination of a continuation argument from the case $\mu = 0$ and numerical investigation.

Some analytical continuation results on the horizontal spectrum

We give here some preliminary analytical results on the horizontal spectrum.

By a smooth (resp. continuous) *μ-continuation to* $\mathrm{Sp}^{\mathrm{H}}_{\alpha,\mu,\nu}$ of a complex number λ_0 we mean a smooth (resp. continuous) curve $\mu \mapsto \lambda(\mu) \in \mathbb{C}$ which is defined for μ in a neighbourhood of 0, satisfies $\lambda(0) = \lambda_0$ and is such that, for each $\mu > 0$, $\lambda(\mu) \in \mathrm{Sp}^{\mathrm{H}}_{\alpha,\mu,\nu}$, and there is a neighbourhood of $\lambda(\mu)$ in $\mathbb{C}$ which does not contain other points of $\mathrm{Sp}^{\mathrm{H}}_{\alpha,\mu,\nu}$. (Note that this implies that λ is not constant).

Proposition 4.4. *Fix $n \geq 1$, $\alpha > 0$, and $\nu \geq 0$.*

i. For any $\mu > 0$, $\mathrm{Sp}^{\mathrm{H}}_{\alpha,\mu,\nu}$ contains all the pure-string eigenvalues $\lambda^{KV}_{\ell,0,\pm}$, $\ell \in \mathbb{Z}_+$.

ii. With the only possible exception of $-\frac{2}{\nu}$ (if it is present in Sp^{KV}_{ν}), each string-pendula eigenvalue $\lambda^{KV}_{\ell,k,\pm}$ ($\ell \in \mathbb{N}$, $k = 1, \dots, n$) of the Kelvin-Voigt string has a smooth μ-continuation $\lambda^{\mathrm{H}}_{\ell,k,\pm}$ to $\mathrm{Sp}^{\mathrm{H}}_{\alpha,\mu,\nu}$.

iii. Each of the two numbers $\pm i\alpha$ has n distinct smooth μ-continuations to $\mathrm{Sp}^{\mathrm{H}}_{\alpha,\mu,\nu}$, unless $\nu = 0$ and α is resonant.

Proof. (i.) This is already known from (3.16).

(ii.) We now consider the function

$$f(\mu,\lambda) := U_n\left(P_{\alpha,\mu}(\lambda)\xi_\nu(\lambda)\sinh\Big(\frac{\xi_\nu(\lambda)}{n+1}\Big) + \cosh\Big(\frac{\xi_\nu(\lambda)}{n+1}\Big)\right), \qquad \lambda \neq \pm i\alpha\,,$$

and prove that, for any α and μ:

1) the zeroes of $f(0,\lambda)$ which satisfy $\sinh\big(\frac{\xi_\nu(\lambda)}{n+1}\big) \neq 0$ are exactly the string-pendula eigenvalues of the Kelvin-Voigt string, and

2) each of them, if different from $-\frac{2}{\nu}$, has a μ-continuation to $\mathrm{Sp}^{\mathrm{H}}_{\alpha,\mu,\nu}$.

Recall that the eigenvalues of the Kelvin-Voigt string are the zeroes of $\sinh\big(\xi_\nu(\lambda)\big)$. The first statement follows from the fact that, using (A.3), $\sinh\big(\xi_\nu(\lambda)\big) = -i\sin(i\xi_\nu(\lambda)) = -i\sin\big(\frac{i\xi_\nu(\lambda)}{n+1}\big)\,U_n\Big(\cos\big(\frac{i\xi_\nu(\lambda)}{n+1}\big)\Big) = \sinh\big(\frac{\xi_\nu(\lambda)}{n+1}\big)\,U_n\big(\cosh\big(\frac{\xi_\nu(\lambda)}{n+1}\big)\big) = \sinh\big(\frac{\xi_\nu(\lambda)}{n+1}\big)\,f(0,\lambda)$. The second follows from the implicit function theorem, because

$$\frac{\partial f}{\partial\lambda}(0,\lambda) = \frac{\partial}{\partial\lambda}U_n\Big(\cosh\Big(\frac{\xi_\nu(\lambda)}{n+1}\Big)\Big) = U_n'\Big(\cosh\Big(\frac{\xi_\nu(\lambda)}{n+1}\Big)\Big)\sinh\Big(\frac{\xi_\nu(\lambda)}{n+1}\Big)\frac{\pi}{2(n+1)}\frac{2+\nu\lambda}{(1+\nu\lambda)^{3/2}}$$

which, if λ is a zero of $U_n\big(\cosh\big(\frac{\xi_\nu(\lambda)}{n+1}\big)\big)$ which satisfies $\sinh\big(\frac{\xi_\nu(\lambda)}{n+1}\big) \neq 0$, is zero if and only if $\lambda = -\frac{2}{\nu}$ (see (A.5)).

(iii.) We consider now the n functions

$$f_k(\mu,\lambda) := \frac{1}{2}\mu\alpha^2\xi_\nu(\lambda)\sinh\Big(\frac{\xi_\nu(\lambda)}{n+1}\Big) + \big(\alpha^2+\lambda^2\big)\Big(\cosh\Big(\frac{\xi_\nu(\lambda)}{n+1}\Big) - C_k\Big)\,, \qquad k = 1,\dots,n\,,$$

with, as usual, $C_k = \cos\big(\frac{k\pi}{n+1}\big)$. Each $f_k(0,\lambda)$ has the zero $\lambda = i\alpha$. Since, for each k,

$$\frac{\partial f_k}{\partial\lambda}(0,i\alpha) = 2i\alpha\Big(\cosh\Big(\frac{\xi_\nu(i\alpha)}{n+1}\Big) - C_k\Big) = 2i\alpha\Big(\cos\Big(\frac{\pi\alpha}{(n+1)(1+i\alpha\nu)^{1/2}}\Big) - C_k\Big)$$

is nonzero (just note that if $\nu \neq 0$ then $(1+i\alpha\nu)^{1/2} \notin \mathbb{R}$ for $\alpha \neq 0$ while, if $\nu = 0$, $\cos(\frac{\pi\alpha}{n+1}) \neq C_k$ for $\frac{\alpha}{n+1} \notin \mathbb{Z}$) the implicit function theorem grants the existence of a smooth curve $\mu \mapsto \lambda_k(\mu)$ through $i\alpha$ such that $f_k(\mu,\lambda_k(\mu)) = 0$ for all μ. Since, for $\mu = 0$ and $\frac{\alpha}{n+1} \in \mathbb{Z}$,

$$\frac{\partial f_k}{\partial\mu}(0,i\alpha) = \frac{1}{2}\alpha^2\sinh\Big(\frac{\xi_\nu(i\alpha)}{n+1}\Big) = \frac{1}{2}i\alpha^2\sin\Big(\frac{\pi\alpha}{(n+1)(1+i\alpha\nu)^{1/2}}\Big) \neq 0\,,$$

for μ small enough, $\lambda_k(\mu) \neq i\alpha$. Thus, for μ small enough $\lambda_k(\mu)$ is also a zero of $\frac{1}{\alpha^2+\lambda^2} f(\mu, \lambda)$ and hence belongs to $\mathrm{Sp}^{\mathrm{H}}_{\alpha,\mu,\nu}$. It only remains to prove that the n continuations $\lambda_1, \ldots, \lambda_n$ are, for small μ, pairwise distinct. This follows from the fact that the n derivatives $\frac{\partial f_k}{\partial \mu}(0, i\alpha)$ are all equal and nonzero while the n derivatives $\frac{\partial f_k}{\partial \lambda}(0, i\alpha)$ are pairwise distinct because $C_k \neq C_h$ if $k \neq h$; therefore, the n derivatives $\frac{\partial \lambda_k}{\partial \mu}(0) = -\frac{\frac{\partial f_k}{\partial \lambda}(0,i\alpha)}{\frac{\partial f_k}{\partial \mu}(0,i\alpha)}$ are nonzero and pairwise distinct. The argument for $-i\alpha$ is the same. □

The existence of the n μ-continuations of $\pm i\alpha$ requires some comments because $\pm i\alpha$ do not belong to the Kelvin-Voigt spectrum. Recall that α is the (rescaled) frequency of the small oscillations of the pendula. For small μ the pendula are very light compared to the string and, intuitively the system can oscillate with the string staying almost at rest and the pendula oscillating with a frequency close to α. For this reason, we will call the μ-continuations of $\pm i\alpha$ "almost-pure-pendula". We will denote by $\lambda_1^{\mathrm{H}}, \ldots, \lambda_n^{\mathrm{H}}$ these μ-continuations of $i\alpha$ (hence those of $-i\alpha$ are $\overline{\lambda_1^{\mathrm{H}}}, \ldots, \overline{\lambda_n^{\mathrm{H}}}$).

It should be noted that, for small μ, the decay rate of the almost-pure-pendula eigenvalues is close to 0. Hence, it may happen that, for small μ, the corresponding normal modes are the less dissipated among those of the horizontal spectrum. We will come back to this later.

On the real component of the horizontal spectrum

Real eigenvalues of the horizontal spectrum come from both equations (3.2a) and (3.2b). We do not try to give a detailed description of their distributions (our main interest is for the nonreal eigenvalues) and only note that:

Proposition 4.5. *For any $n \geq 1$, $\alpha > 0$, $\mu > 0$ and $\nu > 0$, $\mathrm{Sp}^{\mathrm{H}}_{\alpha,\mu,\nu}$ contains countably many negative numbers which belong to the open interval $(-\infty, -\frac{1}{\nu})$ and accumulate to its boundaries.*

Proof. The real pure-string frequencies coincide with those of the Kelvin-Voigt system. Hence, they are countably many, belong to the interval $(-\infty, -\frac{1}{\mu})$ and accumulate to its boundaries. We only need to prove that the real string-pendula frequencies are at most countably many and are all $< -\frac{1}{\nu}$. They are the real solutions of the n equations (3.18), and, by Proposition 3.1, they are all negative. To prove that they are in fact $< -\frac{1}{\nu}$ note that, if $-\frac{1}{\nu} < \lambda < 0$, then $\xi_\nu(\lambda) = \frac{\pi\lambda}{\sqrt{1+\nu\lambda}} < 0$, the sum at the left-hand side of (3.18) is > 1 (the first summand is > 0, the second is > 1) and, since $\cos(\frac{k\pi}{n+1}) < 1$, λ is not a solution of (3.18). For $\lambda < -\frac{1}{\nu}$, the left-hand side of (3.18) is a real analytic function of $\lambda \in (-\infty, -\frac{1}{\nu})$ and thus (3.18) has at most countably many solutions. □

Numerical investigation of the non-real component of the horizontal spectrum

Proposition 4.4 gives some information on the nonreal component of $\mathrm{Sp}^{\mathrm{H}}_{\alpha,\mu,\nu}$: it contains all the Kelvin-Voigt pure-string eigenvalues in C^*_ν and, at least for small μ, a μ-continuation of every other nonreal Kelvin-Voigt eigenvalue and n distinct μ-continuations of $\pm i\alpha$ (a

continuous μ-continuation of a nonreal complex number is certainly nonreal for sufficiently small μ).

Nevertheless, several questions remain open: Are these continuations *global*, that is, defined for all $\mu > 0$? Do they remain in C^*_ν, as in the damped vertical spectrum? Are there other nonreal eigenvalues, besides those in such continuations? The latter is not a trivial question because, for instance, the argument of the Chebyshev polynomial in the eigenvalue equation has, besides poles at $\pm i\alpha$ from which n continuations come out, also an essential singularity at $-\frac{1}{\nu}$: does it contribute any zeroes? And, most of all, what is the global structure of the spectrum?

We tried to provide answers to these questions through a numerical study of the solutions of the eigenvalue equation (3.2b). We report here those indications that we drew from such a numerical analysis that appear to us as reasonably certain. Together, they provide a reasonably clear picture of the spectrum.

1. The global structure of $\mathrm{Sp}^{\mathrm{H}}_{\alpha,\mu,\nu}\backslash\mathbb{R}$. Recall that, with $\bar\ell := \lceil \frac{2}{(n+1)\nu} \rceil \geq 1$, the Kelvin-Voigt spectrum has all its first $\bar\ell - 1$ bands in C^*_ν. The ℓ-th band $B^{\mathrm{KV}}_{\bar\ell-1}$ is contained in C^*_ν if $-\frac{2}{\nu}$ is a pure-string eigenvalue ($\frac{2}{(n+1)\nu} \in \mathbb{Z}$) but otherwise might have some real eigenvalue. (Specifically, in $B_{\bar\ell-1}$ there are $2b \geq 0$ distinct string-pendula real eigenvalues, counting $-\frac{2}{\nu}$ twice if it is a string-pendula eigenvalue ($\frac{2}{(n+1)\nu} \notin \mathbb{Z}$, $\frac{2}{\nu} \in \mathbb{Z}$), with $b = \lceil \frac{2}{(n+1)\nu} \rceil - \lceil \frac{2}{\nu} \rceil$). These real eigenvalues of $B_{\bar\ell-1}$ are important because they happen to have μ-continuations that, at some point, leave the real axis. Indeed, our first numerical conclusions are the following.

N.1 For all $\alpha, \nu > 0$:

1. *All the string-pendula Kelving-Voigt eigenvalues which belong to C^*_ν have a global μ-continuation to $\mathrm{Sp}^{\mathrm{H}}_{\alpha,\mu,\nu}$.*
2. *Each of the two points $\pm i\alpha$ has n distinct global μ-continuations to $\mathrm{Sp}^{\mathrm{H}}_{\alpha,\mu,\nu}$.*
3. *If $-\frac{2}{\nu}$ is a string-pendula Kelvin-Voigt eigenvalue ($\frac{2}{\nu} \in \mathbb{Z}$, $\frac{2}{(n+1)\nu} \notin \mathbb{Z}$), then it has two complex conjugate global μ-continuations to $\mathrm{Sp}^{\mathrm{H}}_{\alpha,\mu,\nu}$.*
4. *If $-\frac{2}{\nu}$ is not a pure-string Kelvin-Voigt eigenvalue ($\frac{2}{(n+1)\nu} \notin \mathbb{Z}$), then the two Kelvin-Voigt eigenvalues of each real pair $r^{\mathrm{KV}}_{\bar\ell-1,k,\pm} \neq -\frac{2}{\nu}$ have global (only continuous at $\mu = \mu_k$) μ-continuations that move towards each other along the real axis until, at a value $\mu_k > 0$, they collide at a point $r_k < -\frac{2}{\nu}$ and leave the real axis, forming a complex conjugate pair.*

There is a total of $2n(\bar\ell + 1)$ of these μ-continuations, which of course form complex conjugate pairs (except those of item 4. when real).

N.2 All these μ-continuations are pairwise distinct and have no intersection points with C^*_ν and (except those in item 4. for $\mu \leq \mu_k$) with $\mathbb{R}$.

N.3 For $\mu \to +\infty$, exactly n complex conjugate pairs of these μ-continuations go to infinity in the complex plane, n complex conjugate pairs go to zero, and all others tend to a pure-string eigenvalue in C^*_ν.

N.4 For all $\alpha, \mu, \nu > 0$, $\mathrm{Sp}^{\mathrm{H}}_{\alpha,\mu,\nu} \setminus \mathbb{R}$ consists of the pure-string Kelvin-Voigt eigenvalues in C^*_ν, of a point in each of the μ-continuations of the Kelvin-Voigt eigenvalues 1.-3. above and, for μ not too small ($\mu > \mu_k$ for each k), also of a point in each of the two μ-continuations of each pair of real eigenvalues of the band $B^{\mathrm{KV}}_{\ell-1}$.

An illustration of this global structure is given in Figure 4.10 which, for given α and ν, shows the μ-continuations as images of curves $\mu \mapsto \lambda(\mu) \in \mathbb{C}$ for $\mu \in [0, \mu_{\max}]$ with increasing values of $\mu_{\max}$.* We note that Figure 4.10, and the following figures, show intersections between the curves traced by different continuations; however, in all cases we checked, the different continuations reach the intersection points at different values of μ and therefore appear to retain their identity.

As we have already noticed, in the limit $\mu \to 0$, the n almost-pure-pendula μ-continuations of $\pm i\alpha$ can be thought of as oscillations of the pendula alone. Thus, the previous numerical conclusions seem to indicate that *globally, the nonreal component of the spectrum is a μ-continuation of the two limiting cases of the string without the pendula and of the pendula without the string.*

We describe now some finer details of the spectrum, for some (but not all) of which we may provide some explanation.

2. The limit $\mu \to \infty$ and the band that goes to infinity. The presence of a band formed by n eigenvalues which go to infinity as $\mu \to +\infty$ was quite unexpected to us. Dynamically, for large μ, namely for very massive pendula, these normal modes describe high-frequency oscillations of the pendula which are damped very quickly (as we note below, both the frequency and the decay rate grow with μ as $\sim \mu^{2/3}$, with a coefficient $\sim \nu^{-1/3}$). Interestingly, the numerics indicates that, for $\mu \to +\infty$, these continuations are asymptotic to a straight line (see Figure 4.11) which, moreover, appears to be independent of all parameters. Only the 'speed' $\frac{\partial \lambda}{\partial \mu}$ with which the eigenvalues move along the continuations as $\mu \to +\infty$ appears to depend on ν. As we now show, assuming that an asymptotic line exists, a simple asymptotic analysis accounts for almost all these facts.

Assume that there exists a smooth curve $\mathbb{R}_+ \ni \mu \to \lambda^{\mathrm{H}}_\infty(\mu) \in \mathrm{Sp}^{\mathrm{H}}_{\alpha,\mu,\nu}$ which solves one of the n equations (3.18) and goes to ∞ for $\mu \to +\infty$. For large μ, $P_{\alpha,\mu}(\lambda^{\mathrm{H}}_\infty(\mu)) = \frac{1}{2}\mu\frac{\alpha^2}{\alpha^2+\lambda^{\mathrm{H}}_\infty(\mu)^2} \sim \frac{1}{2}\mu\lambda^{\mathrm{H}}_\infty(\mu)^{-2}$, $\xi_\nu(\lambda^{\mathrm{H}}_\infty(\mu)) \sim \frac{\pi}{\sqrt{\nu}}\lambda^{\mathrm{H}}_\infty(\mu)^{1/2}$, $\sinh\big(\frac{\xi_\nu(\lambda^{\mathrm{H}}_\infty(\mu))}{n+1}\big) \sim \cosh\big(\frac{\xi_\nu(\lambda^{\mathrm{H}}_\infty(\mu))}{n+1}\big) \sim$

*The figure is produced in the following way. Given $\alpha, \mu, \nu > 0$, the string-pendula eigenvalues are the solutions $\lambda \in \mathbb{C}$ of the n equations $a(\lambda)\mu + b_k(\lambda) = 0$ with $a(\lambda) := \frac{1}{2}\frac{\alpha^2}{\alpha^2+\lambda^2}\xi_\nu(\lambda)\sinh(\frac{\xi_\nu(\lambda)}{n+1}) \neq 0$ and $b_k(\lambda) := \cosh(\frac{\xi_\nu(\lambda)}{n+1}) - \cos(\frac{k\pi}{n+1})$, that is, $\frac{b_k(\lambda)}{a(\lambda)} = -\mu$. Given that μ is real, for each k, this complex equation is equivalent to the system of two equations $\rho(\lambda) := \frac{\mathrm{Re}(b_k(\lambda))\mathrm{Re}(a(\lambda))+\mathrm{Im}(b_k(\lambda))\mathrm{Im}(a(\lambda))}{|a(\lambda)|^2} = -\mu$, $\iota(\lambda) := \mathrm{Re}(b_k(\lambda))\mathrm{Im}(a(\lambda)) - \mathrm{Im}(b_k(\lambda))\mathrm{Re}(a(\lambda)) = 0$. Thus, given $\alpha, \nu, \mu_{\max} > 0$ we used the standard plotting capabilities of *Mathematica* to plot the zero set of $\iota(\lambda) = 0$ in the region where $0 \leq \rho(\lambda) \leq \mu_{\max}$.

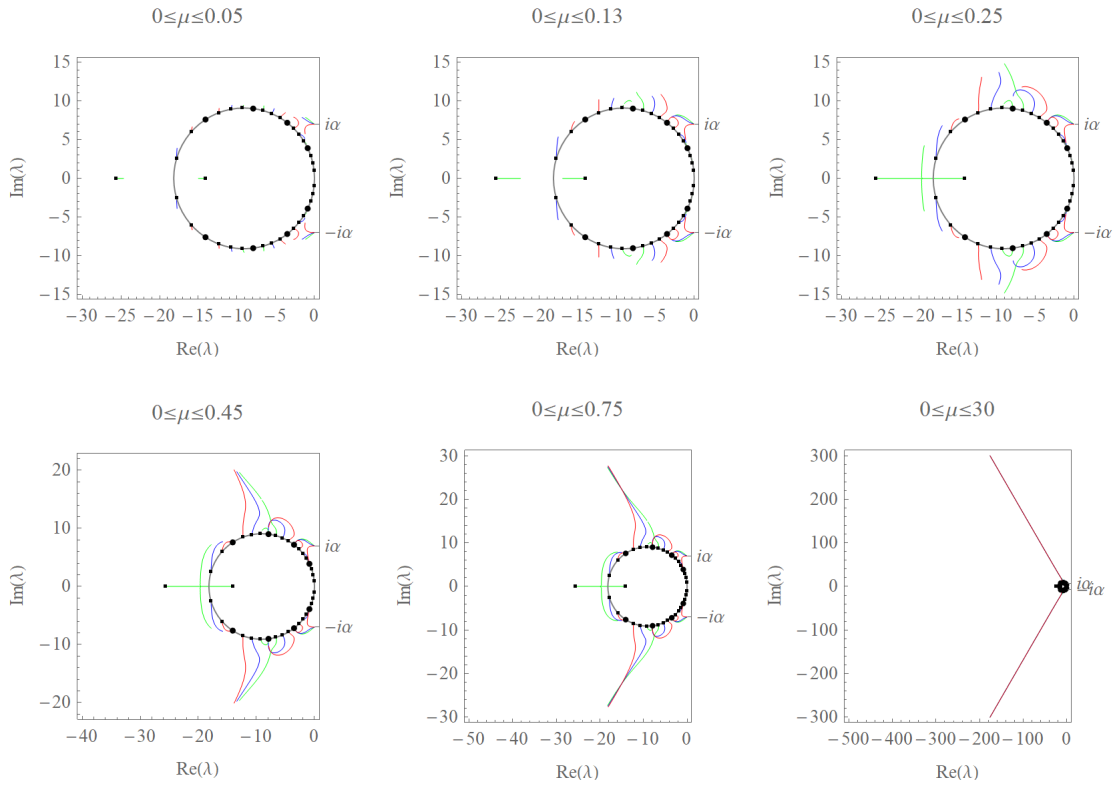

Figure 4.10: A numerically computed illustration of the global structure of the horizontal spectrum $\mathrm{Sp}^{\mathrm{H}}_{\alpha,\mu,\nu}$, for fixed $\alpha > 0$ and $\nu > 0$ and increasing values of μ. The dots denote the eigenvalues $\lambda^{KV}_{\ell,k}$, $k = 1, \dots, n$, of the first bands of the Kelvin-Voigt string—those which have some eigenvalue on the circle C_ν. The thicker dots mark the pure-string eigenvalues $\lambda^{KV}_{\ell,0}$. Each figure shows the curve described by the continuation of each $\lambda^{KV}_{\ell,k}$ for μ between 0 and a maximum value which is specified in the legend. (Values used: $n = 3$, $\alpha = 4$, $\nu = 0.11$).

$\frac{1}{2}\exp\left(\frac{\pi}{(n+1)\sqrt{\nu}}\lambda^{\mathrm{H}}_\infty(\mu)^{1/2}\right)$, and equation (3.18) can only be satisfied if

$$\left(\frac{\pi\,\mu\lambda^{\mathrm{H}}_\infty(\mu)^{-3/2}}{2\sqrt{\nu}} + 1\right)\exp\left(\frac{\pi\,\lambda^{\mathrm{H}}_\infty(\mu)^{1/2}}{(n+1)\sqrt{\nu}}\right) \;\sim\; \mu^0$$

which requires the asymptotic vanishing of the first factor. Assume now that, moreover, $\lambda^{\mathrm{H}}_\infty(\mu)$ is asymptotic to the straight line $\mathbb{R}e^{i\theta} + a$ with some $\theta \in [0, 2\pi)$ and $a \in \mathbb{C}$. Then, for large μ, $\lambda^{\mathrm{H}}_\infty(\mu) \sim z(\mu)e^{i\theta}$ with a function $z : \mathbb{R} \to \mathbb{R}$ such that $\lim_{\mu\to+\infty} z(\mu) = +\infty$ and

$$\frac{\pi}{2\sqrt{\nu}}\,\mu\lambda^{\mathrm{H}}_\infty(\mu)^{-3/2} + 1 \;\sim\; \frac{\pi}{2\sqrt{\nu}}\,\mu z(\mu)^{-3/2}e^{-i\frac{3}{2}\theta} + 1$$

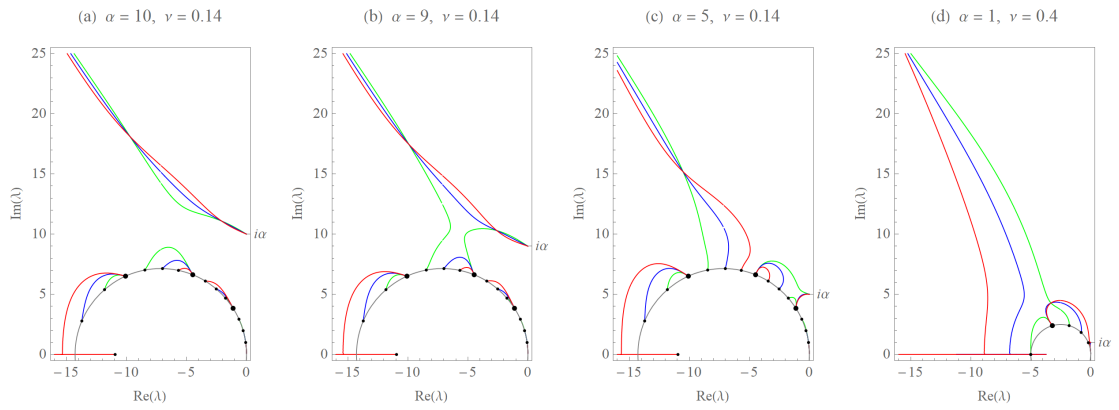

Figure 4.11: Illustrating the four possible 'origins' (as $\mu \to 0$) of the eigenvalues that go to infinity. The curves refer to $n = 3$ and have the same meaning as in Figure 4.10.

vanishes only if $z(\mu) \sim \left(\frac{\pi}{2\sqrt{\nu}}\,\mu\right)^{2/3}$, $\theta = \frac{2\pi}{3}$. Hence,

$$\lambda^{\mathrm{H}}_{\infty}(\mu) \;\sim\; a \;+\; \left(\frac{\pi}{2\sqrt{\nu}}\,\mu\right)^{\frac{2}{3}} e^{i\frac{2\pi}{3}}$$

and *the asymptotic line forms an angle of* $-\frac{\pi}{6}$ *with the imaginary axis, independent of all parameters.* For large μ, the eigenvalues move along such an asymptotic line with 'speed' $\left|\frac{\partial\lambda^{\mathrm{H}}_{\infty}}{\partial\mu}\right| \sim (\nu\,\mu)^{-1/3}$. We add that, numerically, it seems that the asymptotic line passes through 0, namely $a = 0$.

Finally, we note that the numerics also indicates that, for ν not too large, so that there are at least two complete Kelvin-Voigt bands in C^*_ν, the eigenvalues in the band which go to infinity are continuations of: (a) eigenvalues of the Kelvin-Voigt string near the top of the circle C_ν if α is smaller than a threshold which is $\sim \frac{1}{\nu}$; (b) $\pm i\alpha$ if α is larger than this threshold; (c) a mix of the two when α is near the threshold. Instead, for ν large, some or all eigenvalues which go to infinity may also (d) come from the first real Kelvin-Voigt eigenvalues outside C_ν. See Figure 4.11.

3. Structure and reorganisation of the bands. Next, we say a few words about the finer structure of the spectrum, and particularly how it is affected by the changes of the parameters α and ν, which produce bifurcations and rearrangements of the bands. We only consider cases with ν not too large, so that there are at least a couple of bands of the Kelvin-Voigt spectrum in C_ν. For definiteness, we consider only the upper half-plane $\mathrm{Im}(\lambda) > 0$.

First, we note that, for α not too large, up to $\sim \frac{1}{\nu}$, the two bands formed by the μ-continuations λ^{H}_k of $i\alpha$ and by the eigenvalues which go to infinity coming out of the top of C_ν are well identified and divide the spectrum into three parts which have different asymptotic behaviours for $\mu \to +\infty$: the eigenvalues external to these two bands move

towards the (less damped) pure-string eigenvalue to their right (or to 0, see below), while the eigenvalues between them move towards the (more strongly damped) pure-string eigenvalue to their left. For α in a range near $\sim \frac{1}{\nu}$, the two bands coalesce and reorganise. See again Figures 4.10 and 4.11.

Second, as α and ν change, the asymptotic behaviour for $\mu \to +\infty$ of the almost-pure-pendula μ-continuations λ_k^{H} $(k = 1, \ldots, n)$ undergoes a number of bifurcations. If α is resonant, namely $\frac{\alpha}{n+1} =: \tilde{\alpha} \in \mathbb{Z}_+$, then for any $\nu > 0$ each λ_k^{H} is asymptotic to a pure-string eigenvalue, which depends on k and ν. Specifically, for small ν all $\lambda_k^{\mathrm{H}} \to \lambda^{KV}_{\tilde{\alpha},0,+}$, but as ν increases they become, one after the other, asymptotic first to $\lambda^{\mathrm{KV}}_{\tilde{\alpha}+1,0,+}$ (or to infinity), then to $\lambda^{\mathrm{KV}}_{\tilde{\alpha}+2,0,+}$ (or to infinity), etc., and finally, when $\nu \sim \frac{1}{\alpha}$, they first mix with the band which goes to infinity and then, eventually, go to infinity. The asymptotic behaviour of the almost-pure-pendula eigenvalues when α is nonresonant is similar, but with an important difference: for sufficiently small α, namely for approximatively $\alpha < \mathrm{Im}(\lambda^{\mathrm{H}}_{0,1,+})$, all λ_k^{H}'s tend to 0. As α increases, one after the other they begin 'jumping' to $\lambda^{KV}_{1,0,+}$, $\lambda^{KV}_{2,0,+}$, etc., and eventually to infinity, just as in the resonant case. See Figure 4.12.

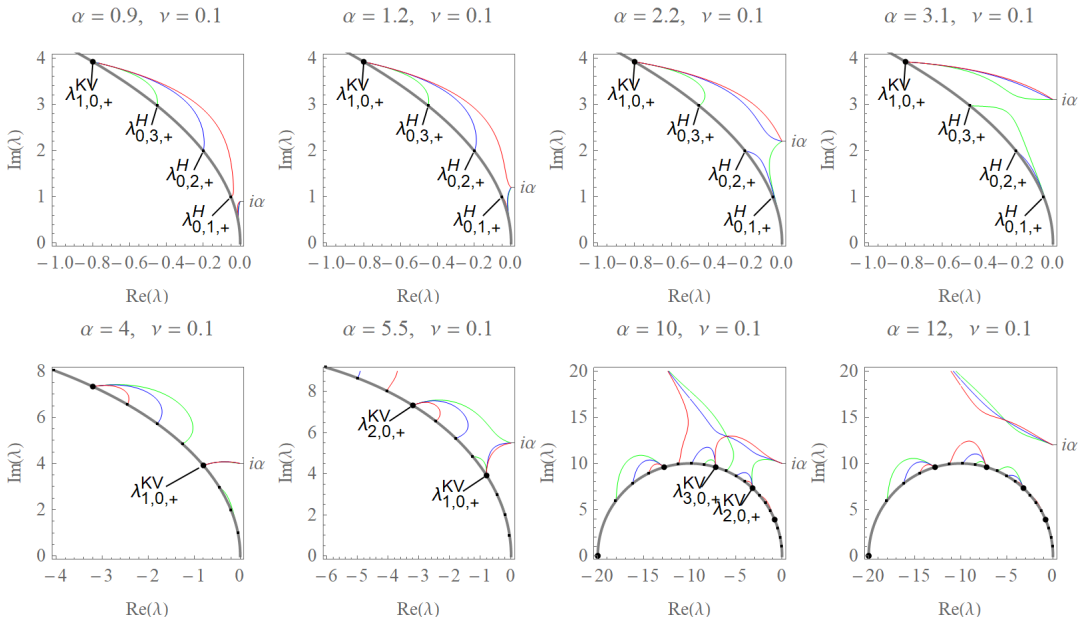

Figure 4.12: The asymptotic behaviour as $\mu \to +\infty$ of the almost-pure-pendula. The limit point of each one changes from 0 to infinity as α grows (at fixed ν; or equivalently, as ν decreases at fixed α). The curves refer to $n = 3$ and have the same meaning as in Figure 4.10. The resonant values of α are the multiples of 4.

Chapter 5

Analysis of synchronization of the two-pendula system

We finalise the analysis of our model by studying synchronization phenomena in the asymptotic dynamics of the pendula, for $n = 2$. We hence focus on the horizontal damped normal modes, with the goal to answer the following question:

Q1. What does the long-term asymptotic dynamics of the pendula look like (in particular, one with respect to the other)?

To this end, we investigate, by means of a numerical study, the dependence of the decay rates of the eigenvalues in $\mathrm{Sp}^{\mathrm{H}}_{\alpha,\mu,\nu}$ on the parameters α and μ. We do that in the regime of weak dissipation. Ultimately, we discuss the emergence of synchronous behaviours for the pendula.

We note that similar reasonings could be easily extended to the case $n > 2$. Besides, (in virtue of Proposition 3.1) as the amplitudes of the pendula become small, we expect the full asymptotic dynamics of the pendula to be well-described – after a sufficiently long transient – by such a linearised analysis.

5.1 On the Kelvin-Voigt model

We preliminarily highlight the following key peculiarity of the Kelvin-Voigt model for the dissipation of the string with respect to the viscous model (see Sections 2.2.1 and 2.2.2 for the details). While all the nonreal eigenvalues of the viscous string have the same, constant, decay rate, the decay rates of the eigenvalues of the Kelvin-Voigt string are frequency-dependent. This implies that the damped small oscillations of the viscoelastic string will evolve with multiple timescales and asymptotically will be dominated by the few least-damped normal modes. The inclusion of a viscous term would add a constant (the same one for every nonreal eigenvalue) to the decay rate of each eigenvalue and, as a consequence, all damped normal modes would tend to the equilibrium at the same rate.

A similar reasoning can be extended to the coupled string-pendula system. In particular, we observe that, by adopting a viscoelastic string, the eigenvalues $\lambda^{\mathrm{V}}_{\ell,k,\pm}$'s of the vertical system inherit from the Kelvin-Voigt model the dependence on the frequencies of the corresponding conservative system, $\omega^{\mathrm{V}}_{\ell,k}$'s, with $\ell \in \mathbb{N}$ and $k = 0, 1, 2$ (compare equation (4.7) with (2.15)). In particular, for small ν and for any $\mu > 0$, the eigenvalues with $\ell \ll \frac{2}{\nu}$ have decay rate $|\mathrm{Re}(\lambda^{\mathrm{V}}_{\ell,k,\pm})| \propto (\omega^{\mathrm{V}}_{\ell,k})^2$, and therefore,

$$\min_{\ell,k} |\mathrm{Re}(\lambda^{\mathrm{V}}_{\ell,k,\pm})| = |\mathrm{Re}(\lambda^{\mathrm{V}}_{0,1,\pm})|.$$

The dissipative horizontal system presents, on the other hand, some peculiarities. Indeed, the analysis conducted in Section 4.3.2 suggests that, for a nonreal eigenvalue in $\mathrm{Sp}^{\mathrm{H}}_{\alpha,\mu,\nu}$, the decay rate does not depend monotonically on the frequency, but rather in a complicated way, which depends on the parameters of the system. In what follows, we discuss the implications of this fact on the variety of asymptotic behaviours of the pendula.

5.2 The least-damped horizontal normal mode

Since, for our model, the long-term dynamics is dominated by the few least-damped normal modes, the eigenvalues of which are the closest to the imaginary axis, our study first tries to answer the following question.

Q2. Which is the least-damped horizontal normal mode?

First, we further discuss the results for the horizontal spectrum that we obtained in the previous chapter, with now a greater focus on the real parts of the eigenvalues.

The numerical investigation that we conducted in Section 4.3.2 evidenced that, on the one hand, for any α, μ, ν not too large,

$$|\mathrm{Re}(\lambda^{\mathrm{H}}_{0,1,\pm})| < |\mathrm{Re}(\lambda^{\mathrm{H}}_{0,2,\pm})| < |\mathrm{Re}(\lambda^{KV}_{1,0,\pm})| < \min_{\ell\in\mathbb{Z}_+,\, k=1,2} |\mathrm{Re}(\lambda^{\mathrm{H}}_{\ell,k,\pm})|\,,$$

on the other, the almost-pure-pendula eigenvalues λ^{H}_k's (and $\overline{\lambda^{\mathrm{H}}_k}$'s) may have decay rates smaller than the $\lambda^{\mathrm{H}}_{0,k,\pm}$'s. Moreover, when this is the case, which one of the λ^{H}_k's (and $\overline{\lambda^{\mathrm{H}}_k}$'s) has the smallest decay rate depends on μ. See again Figures 4.10 and 4.12.

In particular, since the λ^{H}_k's are μ-continuations of $i\alpha$ (see Proposition 4.4), for μ sufficiently small, $|\mathrm{Re}(\lambda^{\mathrm{H}}_k)|$ is close to zero for both $k = 1, 2$. Thus, for μ small enough, for any value of α, the eigenvalues with the smallest decay rates are $\lambda^{\mathrm{H}}_1, \overline{\lambda^{\mathrm{H}}_1}$ and $\lambda^{\mathrm{H}}_2, \overline{\lambda^{\mathrm{H}}_2}$.

On the opposite, for $\mu \to +\infty$, we know (see N.3) that some μ-continuations tend to zero and some others to a pure-string eigenvalue (either to their right or their left). More specifically, for any α, precisely two conjugate pairs, among the $\lambda^{\mathrm{H}}_{0,k,\pm}$'s and the $\lambda^{\mathrm{H}}_k, \overline{\lambda^{\mathrm{H}}_k}$'s, tend to 0. In particular, whether each of the $\lambda^{\mathrm{H}}_{0,k,\pm}$'s tends to $\lambda^{\mathrm{H}}_{1,0,\pm}$ or to zero depends on α. We observe (Figure 4.12) that $\lambda^{\mathrm{H}}_{0,k,\pm} \to 0$ $(k = 1, 2)$ for every α greater than approximately $\mathrm{Im}(\lambda^{KV}_{1,0,\pm})$; decreasing α, $\lambda^{\mathrm{H}}_{0,2,\pm} \to \lambda^{KV}_{1,0,\pm}$ while $\lambda^{\mathrm{H}}_{0,1,\pm}$ and one complex pair

among the $\lambda_k^{\mathrm{H}}, \overline{\lambda_k^{\mathrm{H}}}$'s tend to zero; eventually, for α smaller than approximately $\mathrm{Im}(\lambda_{0,1,+}^{\mathrm{H}})$, all the almost-pure-pendula tend to zero.

Now, since for the other ranges of the parameters α and μ, to identify the eigenvalues with the smallest decay rate may be more demanding, we slightly simplify question *Q2* by recalling that we are ultimately interested in the relative sign of the amplitudes of the pendula for the least-damped normal modes (see *Q1*).

Hence, we start from the following observation. We recall that, as discussed in Section 3.3, for every string-pendula eigenvalue $\lambda \in \mathrm{Sp}_{\alpha,\mu,\nu}^{\mathrm{H}}$ (i.e. $\lambda_{\ell,k,\pm}^{\mathrm{H}}$ or $\lambda_k^{\mathrm{H}}, \overline{\lambda_k^{\mathrm{H}}}$, $\ell \in \mathbb{N}$ and $k = 1, 2$), the ratio between the pendula components of the corresponding eigenfunction is independent of all the parameters, and depends on k only. Namely, we have

$$\frac{(A_{\nu,k,\lambda}^{\mathrm{H}})_2}{(A_{\nu,k,\lambda}^{\mathrm{H}})_1} = \frac{U_1(C_k)}{U_0(C_k)} = 2C_k = (-1)^{k+1}, \quad k = 1, 2,$$

where we now used the fact that $n = 2$, together with the recurrence definition (A.1) of the Chebyshev polynomial and $C_1 = \cos(\frac{\pi}{3}) = \frac{1}{2}$, $C_2 = \cos(\frac{2\pi}{3}) = -\frac{1}{2}$. Hence, for any $\alpha, \mu, \nu > 0$, $(A_{\nu,k,\lambda}^{\mathrm{H}})_2 = (-1)^{k+1}(A_{\nu,k,\lambda}^{\mathrm{H}})_1$.

Therefore, instead of *Q2*, we try to answer the following question.

$Q2_{bis}$. Which is the index k of the horizontal least-damped normal mode?

We investigate this aspect in the regime of weak dissipation, that is, we now assume that ν is small. This approach, on the one hand, simplifies the numerics, on the other, enables us to rely on the well-defined ordering of the spectrum of the undamped horizontal system. We refer, in particular, to Section 4.1.2.

5.2.1 Weakly dissipative regime

First, similarly to the approach of Section 4.3.2, we resort to a continuation argument, now from the case $\nu = 0$. Hence, we say that a smooth curve $\nu \mapsto \hat{\lambda}(\nu) \in \mathbb{C}$ is a smooth *ν-continuation to* $\mathrm{Sp}_{\alpha,\mu,\nu}^{\mathrm{H}}$ of a complex number λ_0 if it is defined for ν in a neighbourhood of 0, satisfies $\hat{\lambda}(0) = \lambda_0$ and is such that, for each $\nu > 0$, $\hat{\lambda}(\nu) \in \mathrm{Sp}_{\alpha,\mu,\nu}^{\mathrm{H}}$ and there is a neighbourhood of $\hat{\lambda}(\nu)$ in $\mathbb{C}$ which does not contain other points of $\mathrm{Sp}_{\alpha,\mu,\nu}^{\mathrm{H}}$.

In this case, since the dependence in ν of the eigenvalue equation (3.2b) is more complicated than its dependence in μ, we need to verify the continuability condition numerically. Specifically, we have the following evidence.

Almost-Proposition 5.1. *For every $\alpha > 0$ and $\mu > 0$ not too large,*

i. each string-pendula eigenvalue $\pm i\omega_{\ell,k}^{\mathrm{H}} \in \mathrm{Sp}_{\alpha,\mu,0}^{\mathrm{H}}$, with $k = 1, 2$, and $\ell \in \mathbb{N}$ not too large, has a smooth ν-continuation to $\mathrm{Sp}_{\alpha,\mu,\nu}^{\mathrm{H}}$, which, at first order in ν, has

frequency $\omega^{\mathrm{H}}_{\ell,k}$ *and decay rate*

$$\varepsilon_\nu(\omega^{\mathrm{H}}_{\ell,k}) = \frac{\nu(\omega^{\mathrm{H}}_{\ell,k})^2}{2} + \frac{3\nu\omega^4\alpha^2\mu\sin\left(\frac{\pi\omega}{3}\right)}{\pi\omega(\alpha^2-\omega^2)\alpha^2\mu\cos\left(\frac{\pi\omega}{3}\right) + (2(\alpha^2-\omega^2)^2 + 3(\alpha^2+\omega^2)\alpha^2\mu)\sin\left(\frac{\pi\omega}{3}\right)}\Big|_{\omega=\omega^{\mathrm{H}}_{\ell,k}}; \quad (5.1)$$

ii. if α *is resonant, each of the two numbers* $\pm i\alpha$ *has two distinct smooth* ν*-continuations to* $\mathrm{Sp}^{\mathrm{H}}_{\alpha,\mu,\nu}$*, which, at first order in* ν*, have frequency* α *and decay rate*

$$\varepsilon^r_{\nu,k}(\alpha) = \frac{\nu\alpha^4\mu\pi^2}{24\left(1+(-1)^{k-\frac{\alpha}{3}} + \frac{\alpha^2\mu\pi^2}{12}\right)}, \quad k=1,2. \quad (5.2)$$

Almost-Proof. (i.) We consider the n functions

$$f_k(\nu,\lambda) := P_{\alpha,\mu}(\lambda)\xi_\nu(\lambda)\sinh\left(\frac{\xi_\nu(\lambda)}{n+1}\right) + \cosh\left(\frac{\xi_\nu(\lambda)}{n+1}\right) - \cos\left(\frac{k\pi}{n+1}\right), \qquad \lambda \neq \pm i\alpha\,,$$

with $k=1,2$. The zeroes of each $f_k(0,\lambda)$ are the string-pendula eigenvalues of the undamped horizontal system with frequencies $\omega^{\mathrm{H}}_{\ell,k}$, $\ell\in\mathbb{N}$ (see Proposition 4.2).

The ν-continuability of the eigenvalues $\pm i\omega^H_{\ell,k} \in \mathrm{Sp}^H_{\alpha,\mu,0}$ ($\ell\in\mathbb{N}$, $k=1,2$) to $\mathrm{Sp}^{\mathrm{H}}_{\alpha,\mu,\nu}$ follows from the implicit function theorem, provided

$$\frac{\partial f_k}{\partial\lambda}(0,\pm i\omega) = \frac{\mu\alpha^2\pi i}{2(\alpha^2-\omega^2)}\left(\frac{\alpha^2+\omega^2}{\alpha^2-\omega^2}\sin\left(\frac{\pi\omega}{n+1}\right) + \frac{\pi\omega}{n+1}\cos\left(\frac{\pi\omega}{n+1}\right)\right) + \frac{\pi i}{n+1}\sin\left(\frac{\pi\omega}{n+1}\right)$$

never vanishes for $\omega=\omega^H_{\ell,k}$, $\ell\in\mathbb{N}$, $k=1,2$. We we verified numerically that this term is different from zero for $\omega^H_{\ell,k}$'s with ℓ up to 4, for $\alpha\in[0,4]$ and $\mu\in[0,2]$ (see Figure 5.1 below).* Hence, for the range of values for which we are confident that the above derivative is not zero, by the implicit function theorem we have that each of the eigenvalues $\pm i\omega^{\mathrm{H}}_{\ell,k}$ has a smooth ν-continuation to $\mathrm{Sp}^{\mathrm{H}}_{\alpha,\mu,\nu}$. At the first order in ν, such ν-continuations are $\pm i\omega^{\mathrm{H}}_{\ell,k} - \varepsilon_\nu(\omega^{\mathrm{H}}_{\ell,k})$, where

$$\varepsilon_\nu(\omega^{\mathrm{H}}_{\ell,k}) := \nu\frac{\frac{\partial f_k}{\partial\nu}(0,\pm i\omega^{\mathrm{H}}_{\ell,k})}{\frac{\partial f_k}{\partial\lambda}(0,\pm i\omega^{\mathrm{H}}_{\ell,k})},$$

which is expression (5.1). We note that $\varepsilon_\nu(\omega^{\mathrm{H}}_{\ell,k})>0$ and therefore it is the decay rate, at the first order in ν, of the eigenvalue of frequency $\omega^{\mathrm{H}}_{\ell,k}$.

*This is the only non-rigorous part of this 'almost' proof. As one of the referees indicated, the result may be made rigorous by employing interval arithmetic. The computation would indeed allow one to prove the statement within a limited but significant range of the parameters and for a reasonable number of eigenvalues.

(ii.) If α is resonant, $\frac{\alpha}{(n+1)} \in \mathbb{Z}_+$. We consider now the two functions

$$\tilde{f}_k(\nu,\lambda) = \frac{\mu}{2}\alpha^2\xi_\nu(\lambda)\sinh\Big(\frac{\xi_\nu(\lambda)}{n+1}\Big) + (\alpha^2+\lambda^2)\Big(\cosh\Big(\frac{\xi_\nu(\lambda)}{n+1}\Big) - \cos\Big(\frac{k\pi}{n+1}\Big)\Big),\ k=1,2.$$

For $\nu = 0$ and α resonant, each f_k has the zeros $\lambda = \pm i\alpha$. Since, for each $k = 1, 2$,

$$\frac{\partial\tilde{f}_k}{\partial\lambda}(0,\pm i\alpha) = \pm i\alpha(-1)^{\frac{\alpha}{(n+1)}}\Big(\frac{\mu}{2}\frac{\pi^2\alpha^2}{n+1} + 2 - 2(-1)^{\frac{\alpha}{(n+1)}}C_k\Big)$$

is nonzero, the implicit function theorem grants the existence of a smooth curve $\nu \mapsto \lambda_k(\nu)$ through $i\alpha$ such that $\tilde{f}_k(\nu, \lambda_k(\mu)) = 0$ for all ν. At the first order in ν, such ν-continuations are $\pm i\alpha - \varepsilon^r_{\nu,k}(\alpha)$, where

$$\varepsilon^r_{\nu,k}(\alpha) := \nu\frac{\frac{\partial\tilde{f}_k}{\partial\nu}(0,\pm i\alpha)}{\frac{\partial\tilde{f}_k}{\partial\lambda}(0,\pm i\alpha)},$$

which is (5.2). Since $\varepsilon^r_{\nu,k}(\alpha) > 0$, they are the decay rates, at the first order in ν, of the two pairs of eigenvalues of frequency α. □

We remark that, as expected, while for $\mu = 0$, $\varepsilon_\nu(\omega) \propto \omega^2$ (namely we recover the decay rate, for low frequencies, of the Kelvin-Voigt string), for $\mu > 0$, $\omega \to \varepsilon_\nu(\omega)$ is not a monotone function. Hereafter, we investigate numerically this aspect.

We compare the (first-order) decay rates as functions of the parameters α and μ, for a fixed $\nu > 0$ small. Our analysis focuses on a window of parameters with $\alpha \in [0, 4]$ and $\mu \in [0, 2]$, and frequencies of string-pendula eigenvalues of the undamped horizontal spectrum in the first two bands B^{H}_ℓ, $\ell = 0, 1$. Preliminarily, we warn that, except for some cases, we do not have (nor, necessarily, need) information about which eigenvalue in $\mathrm{Sp}^{\mathrm{H}}_{\alpha,\mu,\nu}$ corresponds to each ν-continuation.

Figure 5.1 shows the contour plots, in the parameter space (α, μ), of the $\varepsilon_\nu(\omega^{\mathrm{H}}_{\ell,k})$'s for $k = 1, 2$ and $\ell = 0, 1$. From comparison of the four plots, we note the following qualitative properties.

First, for a wide range of values of the parameters (specifically, for μ and α not too small), the decay rates $\varepsilon_\nu(\omega^{\mathrm{H}}_{0,k})$, $k = 1, 2$, are significantly smaller than the $\varepsilon_\nu(\omega^{\mathrm{H}}_{1,k})$'s. Therefore, for these parameters, the lowest-frequency damped normal modes are the least damped. This is in agreement with our preliminary discussion, where we observed that for every α the first band would tend to zero as μ grows. In particular, if α is not too small, we know that (see Figure 4.12) such damped normal modes are those corresponding to the string-pendula eigenvalues $\lambda^{\mathrm{H}}_{0,1,\pm}$, $\lambda^{\mathrm{H}}_{0,2,\pm}$.

Second, Figure 5.1 also agrees with the fact that, as discussed in Section 4.3.2, the eigenvalues with frequency close to α have the smallest decay rates when μ is small enough (see Figure 4.10, top-left). In fact, for μ small, these ν-continuations correspond to the almost-pure-pendula eigenvalues, λ^{H}_k and $\overline{\lambda^{\mathrm{H}}_k}$ ($k = 1, 2$). We remark that, in these cases, the longer-lasting damped normal modes may not have the lowest frequencies. In fact, they have frequencies $\sim \alpha$, which may be large.

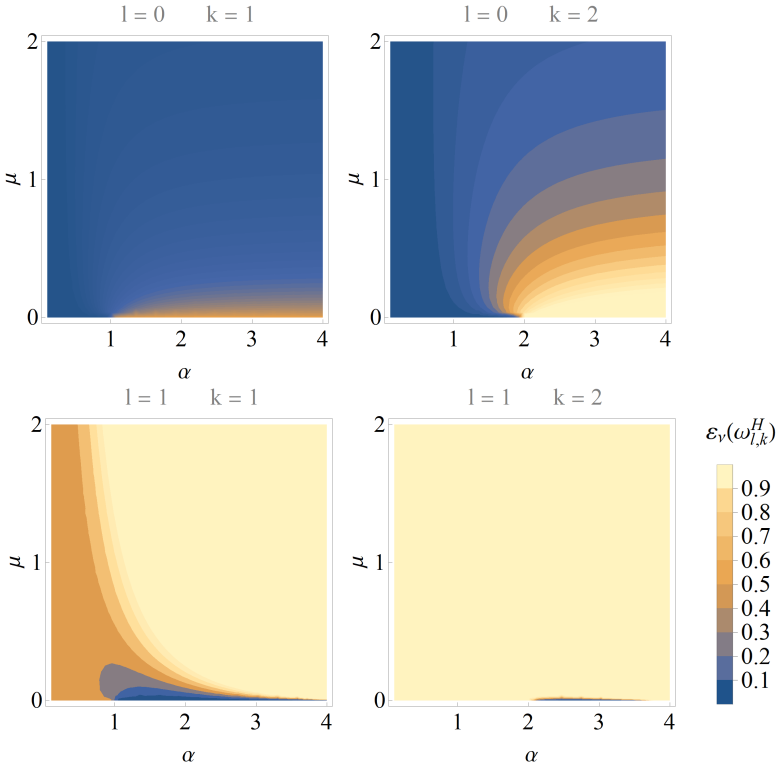

Figure 5.1: Contour plots, in the parameter space (α, μ), for a fixed small value of ν, of the decay rates, at the first order in ν, of the horizontal string-pendula eigenvalues in $\mathrm{Sp}^{\mathrm{H}}_{\alpha,\mu,\nu}$, $\varepsilon_\nu(\omega^{\mathrm{H}}_{\ell,k})$ for $\ell = 0, 1$ and $k = 1, 2$. Darker shades correspond to small decay rates. The numerical values used in the generation of the picture are $n = 2$ and $\nu = 0.01$.

This analysis, in addition, allows us to associate each decay rate with a precise index k, and, correspondingly, the relative sign of the pendula component of the eigenfunction corresponding to the least-damped normal mode. This information is highlighted in Figure 5.2, where only $\min_{\ell,k} \varepsilon_\nu(\omega^{\mathrm{H}}_{\ell,k})$ is taken into account and different colours correspond to different $\varepsilon_\nu(\omega^{\mathrm{H}}_{\ell,k})$ for $\ell = 0, 1$, $k = 1, 2$. The relative sign of the pendula component of the eigenfunctions, namely $(A^{\mathrm{H}}_{\nu,k,\lambda})_1$ and $(A^{\mathrm{H}}_{\nu,k,\lambda})_2$, associated to eigenvalues with the (first-order) decay rate $\varepsilon_\nu(\omega^{\mathrm{H}}_{\ell,k})$, is marked in the legend of Figure 5.2. From this, it emerges that the orange region corresponds to the anti-phase configuration, whereas the two pendula have concordant amplitudes in all the other regions displayed.

5.3 Asymptotic dynamics

Figure 5.2 provides an answer to question $Q2_{bis}$ (and $Q2$). However, such information may be too coarse-grained. Indeed, to describe the asymptotic dynamics – and answer $Q1$ – satisfactorily, it might not suffice to determine the very least damped normal mode, since, in principle, various damped normal modes could have comparable decay rates.

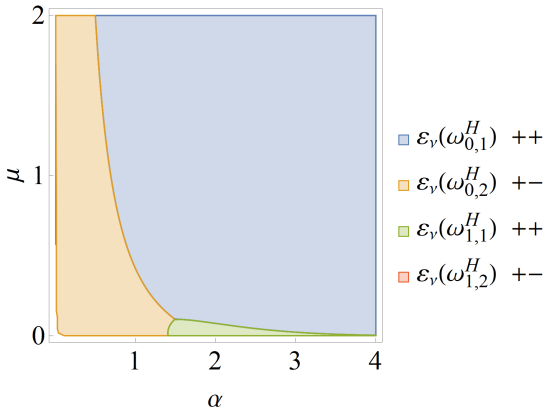

Figure 5.2: Region plots of $\min_{\ell,k} \varepsilon_\nu(\omega^{\mathrm{H}}_{\ell,k})$ for $\ell = 0, 1$ and $k = 1, 2$, in the parameter space (α, μ). Each colour marks the region in the parameter space in which the eigenvalue with the smallest decay rate (at the first order in ν) is the one with frequency $\omega^{\mathrm{H}}_{\ell,k}$ described in the legend (for example, for values of parameters corresponding to the region coloured in blue, the eigenvalue with minimal decay rate is the one with the indexes $\ell = 0$ and $k = 1$). In the legend, the signature "++" and "+−" reminds that for $k = 1$ (resp. $k = 2$) the pendula are concordant (resp. discordant). The numerical values used in the generation of the picture are $n = 2$ and $\nu = 0.01$.

Hence, we now try to estimate the separation in the spectrum $\mathrm{Sp}^{\mathrm{H}}_{\alpha,\mu,\nu}$ between 'slowly-' and 'fast-decaying' eigenvalues, and we study its dependence on the parameters α and μ. To this end, we order the $\varepsilon_\nu(\omega^{\mathrm{H}}_{\ell,k})$'s ($\ell \in \mathbb{N}$, $k = 1, 2$) increasingly and relabel them $\min_{\ell,k} \varepsilon_\nu(\omega^{\mathrm{H}}_{\ell,k}) =: \varepsilon^1 < \varepsilon^2 < \ldots$, and define the quantity

$$g^j := e^{\left(\varepsilon^j - \varepsilon^{j+1}\right)}, \quad j \in \mathbb{Z}_+,$$

which quantifies the 'gap' in the (first-order) decay rates of the eigenvalues between two nearest neighbours. By definition, it satisfies $0 < g^j < 1$ $\forall j$, and small values of the g^j's correspond to wide gaps, and vice versa.

Figure 5.3 shows the contour plots of the gaps g^1 and g^2 for the first three least-damped normal modes, at variance of the parameters α and μ, for a fixed ν small. We note the following aspects.

First, from a comparison of the two plots, we deduce that, for a wide range of values of the parameters, two damped normal modes have decay rates considerably smaller than the others. An exception emerges for values of α between, approximately, 1 and 2, and μ small, in which case the damped small oscillation is a superposition of three damped normal modes.

Second, the plot for $j = 1$ in Figure 5.3 shows that the decay rates of the first two least-damped normal modes are always comparable and small for values of α below 1 (yellow-shaded region), as well as for μ large. Instead, the first gap is quite large in the blue-shaded region (α greater than approximately 2 and $\mu < 1$).

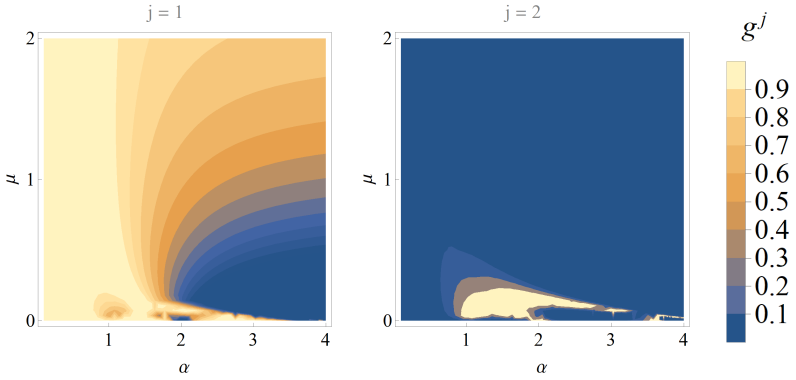

Figure 5.3: Contour plots of g^j, for $j = 1, 2$, in the parameter space (α, μ). g^1 (resp., g^2) quantifies the difference in the decay rates, at the first order in ν, of the first two (resp., third and second) least-damped horizontal normal modes. Darker shades indicate a wide gap, and, correspondingly, an appreciable dichotomy in the decaying rate of the damped normal modes. The numerical values used in the generation of the picture are $n = 2$ and $\nu = 0.01$.

5.3.1 Regimes of synchronization

Finally, we summarise the collected numerical evidence and discuss the regimes of synchronization for the two-pendula system predicted by our model.

In the hypothesis of weak dissipation, we evidenced that the long-term behaviour of the pendula strongly depends on the parameters α and μ. Specifically, the asymptotic dynamics is dominated by the two least-damped normal modes (Figures 5.1 and 5.3), as the others decay much more quickly. Therefore, after a transient, the damped small oscillation will be well-approximated by a superposition of these two modes only.

Figure 5.3 suggests that for values of α lower than approximatively 1, the two above-mentioned damped normal modes will tend to the equilibrium configuration at an almost identical rate. Moreover, since we observed that, for these values of the parameters, they are associated to the almost-pure-pendula eigenvalues, which are μ-continuations of $\pm i\alpha$, for μ small, their frequencies are both close to α. Therefore, we deduce that, for this range of the parameters, the pendula undergo a beating behaviour. We also remark that this implies, in particular, that anti-phase synchronization will not be observable, unless for very small amplitudes (cf. Figure 5.2).

On the other side, Figure 5.3 indicates that, for some ranges of the parameters (blue-shaded region), the decay rate of one of the two least-damped normal modes is considerably smaller than the other: after some time, only one damped normal mode will contribute to the dynamics. Hence, as Figure 5.2 suggests, the two pendula will asymptotically synchronise in phase, with slowly decaying amplitudes of oscillation.

By recalling the physical meaning of the parameters α and μ (introduced in (2.19)), we can conclude that long pendula hanging from a light (compared to the pendula) and stretched string undergo a beating behaviour, while a mass ratio smaller than 1 (i.e. a string heavier than the pendula) and a proper frequency of the pendula greater than the fundamental frequency of the string favour in-phase synchronization of the pendula.

Figure 5.4 summarises – in a schematic way – the asymptotic dynamics of the two-pendula system.

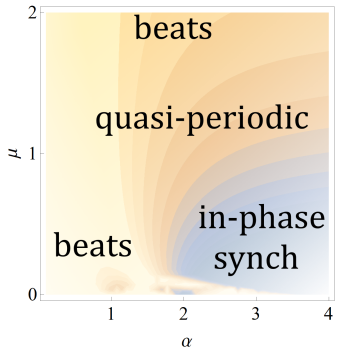

Figure 5.4: Scheme of the asymptotic dynamics, for weak dissipation, of the two-pendula system. Depending on the parameters α (frequency-ratio pendulum/string) and μ (mass-ratio pendulum/string), the two pendula might undergo a beating motion, exhibit a quasi-periodic behaviour with slowly-decaying amplitudes, or synchronise in phase.

Appendix A

Chebyshev polynomials

We recall here a few basic facts about the Chebyshev polynomials of the second kind (see, e.g., [30] for more details). These are the (complex) polynomials U_n defined by the recurrence

$$U_0(x) := 1, \qquad U_1(x) := 2x, \qquad U_n(x) := 2xU_{n-1}(x) - U_{n-2}(x) \quad \forall n \geq 2, x \in \mathbb{C}. \tag{A.1}$$

Clearly, U_n has degree n and is real on real arguments. Moreover, U_n is even if n is even and odd if n is odd. Recurrence (A.1) can also be written in the matrix form

$$\det \begin{pmatrix} 2x & -1 & 0 & 0 & \dots & 0 \\ -1 & 2x & -1 & 0 & \dots & 0 \\ 0 & -1 & 2x-1 & \dots & \dots & \\ \dots & \dots & \dots & \dots & \dots & \dots \\ 0 & 0 & \dots & -1 & 2x & -1 \\ 0 & 0 & 0 & \dots & -1 & 2x \end{pmatrix} = 0. \tag{A.2}$$

An equivalent definition, for real arguments, is

$$\sin(\theta)\, U_{n-1}(\cos\theta) = \sin(n\theta), \quad n \geq 1. \tag{A.3}$$

For each $n \geq 1$, U_n has n simple roots given by

$$C_k := \cos\left(\frac{k}{n+1}\pi\right), \qquad k = 1, \dots, n, \tag{A.4}$$

and which all belong to the interval $(-1, 1)$.

Explicit expressions are known. For instance,

$$U_n(x) = \sum_{k=0}^{\lfloor \frac{n}{2} \rfloor} (-1)^k \binom{n-k}{k} (2x)^{n-2k}, \qquad n \geq 1.$$

The derivative of U_n is $U_n'(x) = \frac{n+1}{x^2-1} T_{n+1}(x) - \frac{x}{x^2-1} U_n(x)$ where, for each $n \geq 0$, T_n is the Chebyshev polynomial of the first kind of order n and satisfies $T_n(\cos(x)) = \cos(nx)$ for all $x \in \mathbb{R}$. Hence, at a zero C_k of U_n,

$$U_n'(C_k) = \frac{n+1}{C_k^2 - 1} T_{n+1}(C_k) = \frac{n+1}{C_k^2 - 1} \cos(k\pi) \neq 0\,. \tag{A.5}$$

A.1 The beaded string

Here, we briefly describe the "beaded string" with equally-spaced masses, which is a well-known example of system in which the Chebyshev polynomials naturally emerge (see e.g. [48]). Such system consists of a finite number of point masses suspended on a massless thread, and can be regarded as a finite-dimensional limit case of the loaded string for negligible mass density. For this system, both the eigenvalues and the eigenvectors can be expressed in terms of Chebyshev polynomials of the second kind.

We follow Rayleigh [40], and we consider n identical masses m which are equidistantly distributed along a string of length $\Lambda = (n+1)a$ and tension τ. Let u_j denote the displacement of the j-th mass from its equilibrium configuration, for small transverse displacements, the Lagrangian of the system is

$$L(u, \dot{u}) = \sum_{j=1}^{n} \Big[\frac{m}{2} \dot{u}_j^2 - \frac{\tau}{2a} (u_{j+1} - u_j)^2 \Big]$$

with $u_0 = u_{n+1} \equiv 0$. Thus, the equations of motion write

$$m\ddot{u}_j + \frac{\tau}{a}(u_j - u_{j-1} + u_j - u_{j+1}) = 0, \quad j = 1, \dots, n$$

with $u_0 = u_{n+1} = 0$. The frequencies of the small oscillations of the system are the $\omega > 0$ solutions of

$$\det \begin{pmatrix} 2z & -1 & 0 & 0 & \dots & 0 \\ -1 & 2z & -1 & 0 & \dots & 0 \\ 0 & -1 & 2z & -1 & \dots & \dots \\ \dots & \dots & \dots & \dots & \dots & \dots \\ 0 & 0 & \dots & -1 & 2z & -1 \\ 0 & 0 & 0 & \dots & -1 & 2z \end{pmatrix} = 0$$

with $z := 1 - \omega^2 \frac{ma}{2\tau}$. By property (A.1), the determinant is the Chebyshev polynomial of the second kind with argument z. Its roots are therefore equal to $\cos\left(\frac{k\pi}{n+1}\right)$, $k = 1, \dots, n$, namely

$$\omega_k = 2\sqrt{\frac{\tau}{ma}} \sin\left(\frac{k\pi}{2(n+1)}\right), \quad k = 1, \dots, n.$$

The associated eigenvectors are the $A^{(k)} = (A_1^{(k)}, \dots, A_n^{(k)})$, $k = 1, \dots, n$, which satisfy the recurrence

$$A_0^{(k)} = A_{n+1}^{(k)} = 0, \qquad A_{j-1}^{(k)} - 2zA_j^{(k)} + A_{j+1}^{(k)} = 0, \quad j = 1, \dots, n$$

which, by relation (A.1), gives

$$A_j^{(k)} = \sin\left(j \frac{k\pi}{(n+1)}\right), \quad j = 1, \dots, n.$$

Appendix B

Transfer matrix method

The *transfer matrix method* is a classical technique employed in the study of the propagation of waves in layered media. Examples of such systems are numerous in solid-state physics, as well in optics or acoustic. We refer to the classical manual [10]. Here, to fix the ideas, we formulate the theory for mechanical waves, for which the layers are identified by different densities, following, e.g., [15].

We restrict to one-dimensional systems and, in particular, we shall particularise the study to locally periodic systems.

B.1 The transfer matrix

Consider a one-dimensional travelling wave and assume that at the position $x = 0$ the system presents a discontinuity. To fix the ideas, think of a piecewise-homogeneous string, or an electromagnetic wave travelling through a piecewise-constant potential. A wave with frequency ω and wavelength k has the form

$$u(x,t) = \begin{cases} a_- e^{i(kx-\omega t)} + b_- e^{-i(kx+\omega t)}, & x < 0 \\ a_+ e^{i(kx-\omega t)} + b_+ e^{-i(kx+\omega t)}, & x > 0 \end{cases}$$

with $a_\pm, b_\pm \in \mathbb{C}$ constrained by suitable interface conditions at $x = 0$. Typically, these are continuity conditions of u and u_x and they inherit the linearity from the evolution equation.

The *transfer matrix* M expresses the coefficients of the wave on the left-hand side of the discontinuity in terms of the coefficients of the wave on the right-hand side:

$$\begin{pmatrix} a_+ \\ b_+ \end{pmatrix} = M \begin{pmatrix} a_- \\ b_- \end{pmatrix}.$$

For a multilayered system, the computation above repeats at every interface. The coefficients of the outcoming wave, which crossed j layers, are expressed in terms of the

coefficients of the incoming wave as

$$\begin{pmatrix} a_{j+1} \\ b_{j+1} \end{pmatrix} = \underbrace{M_j M_{j-1} \dots M_1}_{M} \begin{pmatrix} a_1 \\ b_1 \end{pmatrix}$$

with the transfer matrix M now given by the product of j matrices.

B.2 Locally periodic media

If the medium consists of a finite number of repeating layers, it is said to be locally periodic [15]. In this case, the expression of the transfer matrix simplifies and its entries can be expressed in terms of Chebyshev polynomials of the second kind U_n.

Consider a locally periodic structure composed of a layer of length s alternated to a different one of length ε. This corresponds, for example, to a homogeneous string with periodic localized constant dishomogeneities, or a wave in a periodic localized potential well. The wave has the form

$$u(x,t) = \begin{cases} a_{j+1} e^{i(k(x-j\bar{x})-\omega t)} + b_{j+1} e^{-i(k(x-j\bar{x})+\omega t)}, & j\bar{x} < x < (j+1)\bar{x} - \varepsilon \\ u_\varepsilon(x,t), & (j+1)\bar{x} - \varepsilon < x < (j+1)\bar{x} \end{cases}$$

where $\bar{x} := s + \varepsilon$ and $j \in \mathbb{Z}$. Since the system is periodic, $M_j = M_1 \, \forall j$, and therefore

$$\begin{pmatrix} a_{j+1} \\ b_{j+1} \end{pmatrix} = M_1^j \begin{pmatrix} a_1 \\ b_1 \end{pmatrix}.$$

From the Cayley-Hamilton theorem and the recursion for the Chebyshev polynomial (A.1), the following identity can be proven (see [6]):

$$M_1^j = U_{j-1}(z) M_1 - U_{j-2}(z) \mathbb{I}, \qquad j \geq 2 \tag{B.1}$$

with $z := \frac{1}{2}\mathrm{Tr}(M_1)$ and $\mathbb{I}$ the 2×2 identity matrix.

Part III

Future perspectives

Chapter 6

Partially damped mechanical systems

The analysis that we conducted for the study of our model in Part II naturally raises the question of what the dynamics of the (full) nonlinear system is. We observe that the linearised system is a good approximation for asymptotically long times, since the amplitudes of oscillation of the pendula decrease over time, as evidenced by the strictly negative real parts of the eigenvalues of our linearised system. However, the nonlinear system is in principle remarkably more complicated (for example, the vertical and the horizontal systems are coupled). For the linearised system we were able to conclude that the asymptotic dynamics is greatly influenced by the fact that the viscoelasticity of the string leads to frequency-dependent decay rates of the damped normal modes. The phase space is hence decomposable into invariant subspaces on which the 'amount' of dissipation is different. As a consequence, any damped small oscillation tends exponentially fast toward progressively lower-dimensional and less-damped subspaces.

In this concluding part, we enter the nonlinear framework and make an attempt to describe the influence of dissipation on the nonlinear dynamics of mechanical systems and, again, on the emergence of synchronization. We restrict the study now to finite-dimensional systems. The analysis is very germinal and no conclusive results have been found; however, we advance some recommendations for future studies.

6.1 Motivating examples

To begin, we introduce two very simple models which favour physical intuition and suggest possible research strategies. The first one is a minimal degree-of-freedom example, where two rigid pendula touch each other and are directly coupled through the contact friction. The second is a more advanced example, where two identical pendula are placed on a common moving rigid support, which is responsible for the coupling. Both examples share the following key features with the more complex system described in Part II:

· dissipation is introduced by the coupling;

· other concurrent dissipative contributions may be neglected.

6.1.1 Example 1

The first system we consider consists of two identical heavy L-shaped rigid bars. They are constrained so that one leg of each bar lays horizontally and with the extremities in contact, while the other leg is free to rotate in a perpendicular plane (see Figure 6.1). We assume that the forces acting on the system are the gravity and dissipative forces given by the friction between the two bars and the viscosity of the air.

The configuration manifold is diffeomorphic to $\mathbb{T}^2$, and we parameterise it by the angles (θ_1, θ_2) measured from the downward vertical. In time-rescaled units, the Lagrangian of the conservative system is

$$L(\theta_1, \theta_2, \dot\theta_1, \dot\theta_2) = \frac{1}{2}(\dot\theta_1^2 + \dot\theta_2^2) + (\cos\theta_1 + \cos\theta_2).$$

We include the following dissipative forces: the friction at the interface of the bars, which we model as a linear term proportional to the relative velocity of the two bars, with damping coefficient $\gamma > 0$, and the viscosity of the air, with damping coefficient $\nu > 0$. The equations of motion are therefore

$$\begin{cases} \ddot\theta_1 + \sin\theta_1 + \gamma(\dot\theta_1 - \dot\theta_2) + \nu\dot\theta_1 = 0 \\ \ddot\theta_2 + \sin\theta_2 + \gamma(\dot\theta_2 - \dot\theta_1) + \nu\dot\theta_2 = 0. \end{cases} \tag{6.1}$$

It is intuitive that for $\nu \ll \gamma$ the two bars asymptotically synchronise in phase. Hence, we are motivated to look for attracting submanifolds in the phase space on which the dissipation is weak.

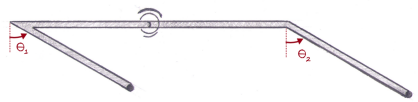

Figure 6.1: Sketch of the model of Example 1.

6.1.2 Example 2

The second system we consider is sketched in Figure 6.2 and consists of two identical pendula on a common rigid support, which is constrained to move horizontally in one dimension and is connected to a spring. We assume that the forces acting on the system are the gravity and dissipative forces given by the viscous friction acting on the base support and the viscosity of the air.

The configuration manifold of the system is diffeomorphic to $\mathbb{R} \times \mathbb{T}^2$. Let z and $\phi = (\phi_1, \phi_2)$ be the generalised coordinates, representing the horizontal displacement of the support and the angular displacements of the pendula about their pivot points,

respectively. Let m and M denote the mass of each pendulum and the support, respectively, l the length of the pendula and k the elastic constant of the spring.

The conservative system is described by a Lagrangian $L = L(z, \phi_1, \phi_2, \dot{z}, \dot{\phi}_1, \dot{\phi}_2)$,

$$L = \frac{1}{2}(M+2m)\dot{z}^2 + \sum_{i=1}^{2}\left[\frac{m}{2}l^2\dot{\phi}_i^2 + ml\dot{z}\dot{\phi}_i\cos\phi_i + mgl\cos\phi_i\right] - \frac{k}{2}z^2.$$

Rescaling the variables $z \to lz$, $t \to \sqrt{\frac{l}{g}}\,t$ and defining the parameters $\mu := \frac{M+2m}{m}$ and $\alpha := \frac{kl}{mg}$, the Lagrangian becomes

$$L = \frac{1}{2}\mu\dot{z}^2 + \sum_{i=1}^{2}\left[\frac{1}{2}\dot{\phi}_i^2 + \dot{z}\dot{\phi}_i\cos\phi_i + \cos\phi_i\right] - \frac{1}{2}\alpha z^2.$$

We include the following dissipative forces: the viscous friction acting on the base support, with damping coefficient $\gamma > 0$, and the viscosity of the air, with damping coefficient $\nu > 0$.

The Lagrange equations with the inclusion of the dissipative forces are (see e.g. [46])

$$\begin{cases} \mu\ddot{z} + \sum_{i=1}^{2}\left(\ddot{\phi}_i\cos\phi_i - \dot{\phi}_i^2\sin\phi_i\right) + \alpha z + (\gamma+\nu)\dot{z} + \nu\sum_{i=1}^{2}(\dot{z} + \dot{\phi}_i\cos\phi_i) = 0 \\ \ddot{\phi}_i + \ddot{z}\cos\phi_i + \sin\phi_i + \nu(\dot{z}\cos\phi_i + \dot{\phi}_i) = 0, \quad i = 1,2. \end{cases} \tag{6.2}$$

Intuition now suggests that, for $\nu \ll \gamma$, the system will spontaneously tend, as $t \to +\infty$, to a state in which the bar stops and the two pendula oscillate, with decreasing amplitudes, in anti-phase.

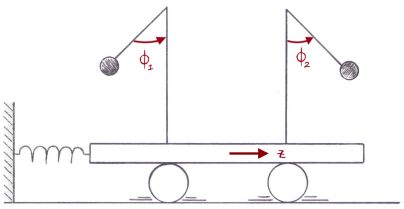

Figure 6.2: Sketch of the model of Example 2.

Note that this is a basic model for Huygens synchronization. Some versions of it are indeed present in various studies (see Part I for some references).

6.2 LaSalle invariance principle

The two very simple examples introduced in the previous section suggest that a possible approach to the nonlinear study is to first consider the case in which the dissipation is only partial. For the two models, this corresponds to assuming $\nu = 0$ and $\gamma > 0$. In

particular, the study [38], which deals with a system analogous to Example 2, indicates that the asymptotic dynamics in this case can be studied via LaSalle invariance principle. In a different context, [4] uses the same theorem to analyse the asymptotic spin-orbit synchronization for a celestial body.

Therefore, we are motivated to look for a systematic approach via the LaSalle invariance principle to investigate the nonlinear dynamics of "partially damped" mechanical systems.

In this section, we recall some of the fundamental concepts needed in the study of the asymptotic evolution of a generic dynamical system, while in the following section we focus on mechanical systems. Preliminarily, we fix the notation.

Let $\mathcal{M}$ be a smooth m-dimensional manifold, $X \in \mathfrak{X}(\mathcal{M})$ a smooth vector field on $\mathcal{M}$, and consider the autonomous differential equation in $\mathcal{M}$

$$\dot{z} = X(z), \qquad z \in \mathcal{M}. \tag{6.3}$$

We assume that X is complete, namely all its integral curves are defined for all times, so that there exists a smooth map $\Phi_t^X : \mathcal{M} \to \mathcal{M}$ – the flow of X at time t – such that $\Phi_0^X = \mathrm{id}_{\mathcal{M}}$ and $\dfrac{d\Phi_t^X}{dt}(z) = X(\Phi_t^X(z))\ \forall t \in \mathbb{R}$ and $z \in \mathcal{M}$. Namely, $\Phi_t^X(z)$ is the solution of (6.3) at time t through z. Then, $(\mathcal{M}, \mathbb{R}, \Phi^X)$ is a differentiable dynamical system with flow $\Phi^X := \{\Phi_t^X : t \in \mathbb{R}\}$.

6.2.1 Preliminaries: invariance and stability

We recall here the basics for sets in the phase space which are *invariant* under the flow of a vector field and their *stability* properties (see, e.g., [49]).

Definition 6.1. A subset N of $\mathcal{M}$ is *invariant* (resp. *positively invariant*) under the flow of X if $\Phi_t^X(N) \subseteq N\ \forall t \in \mathbb{R}$ (resp. $t \geq 0$). N is said to be *locally invariant* (resp. *positively locally invariant*) under the flow of X in an open set $U \subset \mathcal{M}$ if for any $z \in N \cap U$, $\Phi_t^X(z) \in N\ \forall t \in \mathbb{R}$ (resp. $t \geq 0$) for which $\Phi_t^X(z) \in U$.

In particular, if the invariant set N is a smooth submanifold of $\mathcal{M}$, then $(N, \mathbb{R}, \Phi^X|_{\mathbb{R}\times N})$ is a differentiable dynamical system, where $\Phi^X|_{\mathbb{R}\times N} : \mathbb{R} \times N \to N$ is the restriction of Φ^X to the submanifold.

Definition 6.2. Let $\mathcal{N} \subset \mathcal{M}$ be a smooth submanifold of $\mathcal{M}$. The vector field X on $\mathcal{M}$ is said to be *tangent* to $\mathcal{N}$ if $X(z) \in T_z\mathcal{N}\ \forall z \in \mathcal{N}$, while it is said to be *transverse* to $\mathcal{N}$ if $X(z) \notin T_z\mathcal{N}\ \forall z \in \mathcal{N}$

Proposition 6.1. *Let $\mathcal{N}$ be a smooth submanifold of $\mathcal{M}$, and $U \subset \mathcal{M}$ an open set.*

$\mathcal{N}$ is locally invariant in U if and only if $X(z) \in T_z\mathcal{N}\ \forall z \in \mathcal{N} \cap U$ and $(\overline{\mathcal{N}} \setminus \mathcal{N}) \cap U = \varnothing$, and in such a case, solutions starting in $\mathcal{N} \cap U$ might leave $\mathcal{N}$ only by crossing $\overline{U}$.

If $\mathcal{N}$ is closed and X is tangent to $\mathcal{N}$, then $\mathcal{N}$ is invariant under the flow of X.

Examples.

- The smallest invariant sets are equilibria, that is, points $z^* \in \mathcal{M}$ such that $X(z^*) = 0$.
- Any orbit $\mathcal{O}_z := \{\Phi_t^X(z) : t \in \mathbb{R}\}$ (resp. positive semi-orbit $\mathcal{O}_z^+ := \{\Phi_t^X(z) : t \geq 0\}$) is a one-dimensional invariant (resp. positively invariant) submanifold. Conversely, any connected invariant one-dimensional submanifold that does not contain equilibria is an orbit.
- Each level set of a smooth submersion $F : \mathcal{M} \to \mathbb{R}^k$ whose components are first integrals is a closed invariant smooth submanifold of $\mathcal{M}$ of codimension k.

The behaviour of orbits near an equilibrium point can be described in terms of their stability properties. Consequently, we recall here the notions of Lyapunov-stability for equilibria.

Definition 6.3. Let $z^* \in \mathcal{M}$ be an equilibrium of X.

z^* is said to be *stable* if, for any neighbourhood U of z^*, there exists a neighbourhood U_0 of z^* such that $\Phi_t^X(U_0) \subseteq U$ for all $t \geq 0$.

z^* is said to be *attractive* if there exists a neighbourhood U of z^* such that $\lim_{t\to+\infty} \Phi_t^X(z) = z^*$ for all $z \in U$.

z^* is said to be *asymptotically stable* if it is stable and attractive.

By extension, the definitions of stability and asymptotic stability for invariant sets read as follows.

Definition 6.4. Let N be a closed invariant set of $\mathcal{M}$.

N is *stable* if, for any neighbourhood U of N in $\mathcal{M}$, there exists a neighbourhood U_0 of N such that $\Phi_t^X(U_0) \subseteq U$ for all $t \geq 0$.

N is an *attracting set* if there is a positively invariant neighbourhood U of N such that $\bigcap_{t>0} \Phi_t^X(U) = N$. The set U is called a *trapping region* of N. The *basin of attraction* of N is the open set given by $\bigcup_{t\leq 0} \Phi_t^X(U)$ for any trapping region U of N, and it does not depend on the choice of U.

6.2.2 Preliminaries: asymptotic behaviour

Next, we recall the notion of *ω-limit set* and the classical *LaSalle invariance principle* (see [25–27]), which enables to get information regarding the ω-limit sets of positively bounded solutions, by employing a *Lyapunov function*.

Preliminarily we give a few definitions.

Definition 6.5. Let $z \in \mathcal{M}$. A point $p \in \mathcal{M}$ is called *ω-limit point* of z if there exists a sequence $\{t_n : t_n \in \mathbb{R}\}_{n\in\mathbb{N}}$ such that $t_n \to +\infty$ as $n \to \infty$ and $\lim_{n\to\infty} \Phi_{t_n}^X(z) = p$. The collection $\omega(z)$ of all ω-limit points of z is called *ω-limit set* of z.

Proposition 6.2. *If $N \subset \mathcal{M}$ is a positively invariant compact (or positively precompact) subset, then, for any $z \in N$, $\omega(z)$ is contained in N, is nonempty, compact, connected and invariant under the flow of X.*

Denote by $\mathcal{L}_X$ the Lie derivative along the vector field X, namely $\mathcal{L}_X : \mathcal{C}^1(\mathcal{M}) \to \mathcal{C}^1(\mathcal{M})$, $\mathcal{L}_X f := \dfrac{d}{dt}(f \circ \Phi_t^X)\Big|_{t=0}$. Sometimes we will also denote such time derivative of f along the flow of X by $\dot{f}$.

Definition 6.6. Let $\mathcal{W} : \mathcal{M} \to \mathbb{R}$ be a $\mathcal{C}^1$ function on $\mathcal{M}$, and $\Omega \subset \mathcal{M}$. $\mathcal{W}$ is said to be a *Lyapunov function* for X on Ω if $\mathcal{L}_X \mathcal{W}(z) \leq 0 \ \forall z \in \Omega$.

Now, we state – and, for completeness, prove – LaSalle's theorem.

Theorem 6.1 (LaSalle Invariance Principle)**.** *Let $\Omega \subset \mathcal{M}$ be a positively invariant open set such that $\overline{\Omega}$ is compact, and let $\mathcal{W}$ be a Lyapunov function for X on Ω. Let M be the largest invariant subset in $\mathcal{E} = \{z \in \overline{\Omega} : \mathcal{L}_X \mathcal{W}(z) = 0\}$. Then, for any $z_0 \in \Omega$, there exists $w \in \mathbb{R}$ such that $\omega(z_0) \subseteq M \cap \mathcal{W}^{-1}(w)$.*

Proof. Let $z_0 \in \Omega$. Being $\mathcal{W}$ a Lyapunov function on a Ω positively invariant, the function $t \mapsto \mathcal{W}(\Phi_t^X(z_0))$ is decreasing for every $t \geq 0$ and therefore it has a limit $\lim_{t\to+\infty} \mathcal{W}(\Phi_t^X(z_0)) =: w$, which belongs to $\overline{\Omega}$. Since $\overline{\Omega}$ is compact, $\omega(z_0)$ is nonempty and contained in $\overline{\Omega}$. Hence, taking $p \in \omega(z_0)$, by the continuity of $\mathcal{W}$,

$$\mathcal{W}(p) = \mathcal{W}(\lim_{n\to\infty} \Phi_{t_n}^X(z_0)) = \lim_{n\to\infty} \mathcal{W}(\Phi_{t_n}^X(z)) = w.$$

Thus, for this w, $\mathcal{W}(p) = w$ for each $p \in \omega(z_0)$, namely $\omega(z_0) \subseteq \mathcal{W}^{-1}(w)$. On the other hand, the continuity of the flow gives

$$\mathcal{W}(\Phi_t^X(p)) = \mathcal{W}\big(\Phi_t^X(\lim_{n\to\infty} \Phi_{t_n}^X(z_0))\big) = \mathcal{W}\big(\lim_{n\to\infty} \Phi_{t+t_n}^X(z)\big) = \mathcal{W}(p)$$

and therefore $t \mapsto \mathcal{W} \circ \Phi_t^X(p)$ is constant and, by the definition of $\mathcal{E}$, $\omega(z_0) \subseteq \mathcal{E}$. Since $\omega(z_0)$ is an invariant set, it is contained in M. □

Therefore, LaSalle invariance principle is a precious tool for the study of the asymptotic behaviour of a dynamical system since it provides a method to localise the ω-limit sets. Moreover, this result gives information on the size of the region of attractivity, which strongly depends on the nonlinearities of the vector field and can hence be determined only recurring to global objects, such as a Lyapunov function, and not from linear approximations. In particular,

Corollary 6.1. *In the hypotheses of Theorem 6.1, if $M \subset \Omega$, then M is an attracting set and Ω is a trapping region.*

In addition, it is worth remarking that the Lyapunov function itself can often be used to construct the trapping region. Indeed, if the open set $\Omega_l \subset \mathcal{M}$, defined by the condition $\mathcal{W} < l$, for some $l > 0$, is positively precompact (i.e. bounded for all $t \geq 0$ and with no limit points on the boundary), then Theorem 6.1 ensures that the ω-limit set of any point in Ω_l belongs to $\mathcal{E} = \{z \in \Omega_l : \mathcal{L}_X \mathcal{W}(z) = 0\}$.

Finally, we recall that, as a particular case for equilibria, from Theorem 6.1 the following refinement of Lyapunov's stability theorem follows.

Corollary 6.2 (LaSalle-Krasovskii principle)**.** *In the hypotheses of Theorem 6.1, let z^* be an equilibrium for X in Ω which is a strict minimum point of $\mathcal{W}$. If $\{z^*\}$ is the only positive semi-orbit orbit in $\mathcal{E}$, then z^* is asymptotically stable.*

6.2.3 Particular case

We now investigate the case in which the set $\mathcal{E}$ – locus of the zeroes of the Lie derivative of the Lyapunov function – has a manifold structure.

Proposition 6.3. *In the hypotheses of Theorem 6.1, if $\mathcal{E}$ is a smooth submanifold of $\mathcal{M}$, then, for any $z_0 \in \Omega$, $\omega(z_0)$ belongs to the largest invariant subset of*

$$\mathcal{T}_{\mathcal{E}}^{(1)} := \{z \in \mathcal{E} \,:\, X(z) \in T_z\mathcal{E}\}. \tag{6.4}$$

Proof. Let $z_0 \in \Omega$ and take $p \in \omega(z_0)$. By LaSalle's theorem 6.1, $p \in \mathcal{E}$. Since, by Proposition 6.2, $\omega(z_0)$ is invariant, then, for any $t \in \mathbb{R}$, $\Phi_t^X(p) \in \omega(z_0) \subset \mathcal{E}$. Therefore, $X(p) \in T_p\mathcal{E}$, which proves the statement. □

Define inductively $\mathcal{T}_{\mathcal{E}}^{(0)} := \mathcal{E}$,

$$\mathcal{T}_{\mathcal{E}}^{(j)} := \{z \in \mathcal{T}_{\mathcal{E}}^{(j-1)} \,:\, X(z) \in T_z\mathcal{T}_{\mathcal{E}}^{(j-1)}\}, \quad j \geq 1.$$

Proposition 6.4. *If $\mathcal{T}_{\mathcal{E}}^{(1)}, \ldots, \mathcal{T}_{\mathcal{E}}^{(j-1)}$, for $j \geq 2$, are smooth submanifold of $\mathcal{E}$, then, for any $z_0 \in \Omega$, $\omega(z_0)$ belongs to the largest invariant subset of $\mathcal{T}_{\mathcal{E}}^{(j)}$.*

Proof. By induction. □

6.3 Mechanical systems with partial viscous friction

We now focus on mechanical systems, motivated by Examples 1 and 2 introduced at the beginning of the chapter. Specifically, we study finite-dimensional mechanical systems, holonomically constrained, subject to conservative forces and velocity-proportional dissipative forces.

6.3.1 Setting

In this section, we fix the notation, mainly in accordance with [13], and set our working hypotheses.

Let $\mathcal{Q}$ be a smooth d-dimensional manifold and $T\mathcal{Q}$ its tangent bundle. We consider a mechanical system, subject to ideal holonomic constraints, with configuration manifold $\mathcal{Q}$, and described by a Lagrangian function $L : T\mathcal{Q} \to \mathbb{R}$ of the form $L(q, \dot{q}) = T(q, \dot{q}) - V(q)$ with T a kinetic energy quadratic in the velocity and $V : \mathcal{Q} \to \mathbb{R}$ a smooth potential energy independent from the velocity. Let g be the Riemannian metric on $\mathcal{Q}$ given by the kinetic energy, namely $T(q, \dot{q}) = \frac{1}{2} g_q(\dot{q}, \dot{q})$. In addition, we assume that on the system act dissipative forces which are linear in the velocity, $f : T\mathcal{Q} \to T^*\mathcal{Q}$, $f(q, \dot{q}) = -\Gamma(q)\dot{q}$ with Γ a symmetric and positive semi-definite tensor. Forces of this type are commonly known also as "forces of viscous friction" (e.g., [3]).

The equations of motion, in lifted local coordinates $(q^1, \dots, q^d, \dot{q}^1, \dots, \dot{q}^d)$ on $T\mathcal{Q}$, are the Lagrange equations with the inclusion of the damping force*:

$$\left(\frac{d}{dt}\frac{\partial L}{\partial \dot{q}^i}\right)(q, \dot{q}, \ddot{q}) - \frac{\partial L}{\partial q^i}(q, \dot{q}) = f_i(q, \dot{q}) \qquad i = 1, \dots, d, \tag{6.5}$$

which are a system of d second-order ordinary differential equations. Written as the equivalent first-order system, equations (6.5) are

$$\begin{cases} \dot{q} = v \\ \dot{v} = \xi(q, v) - \operatorname{grad}_g V(q) - F(q, v) \end{cases} \tag{6.6}$$

where the i-th component of each term is $\xi^i(q, v) := -\frac{1}{2} g^{il}(q)\Big(\frac{\partial g_{jl}(q)}{\partial q^k} + \frac{\partial g_{kl}(q)}{\partial q^j} - \frac{\partial g_{jk}(q)}{\partial q^l}\Big) v^j v^k$, $(\operatorname{grad}_g V(q))^i = g^{ij}(q)\frac{\partial V(q)}{\partial q^j}$ and $F^i(q, v) := g^{il}(q)\Gamma_{lj}(q)v^j$, having adopted the convention of summation over repeated indexes. Equations (6.6) define a smooth vector field $X \in \mathfrak{X}(T\mathcal{Q})$,

$$X(q, v) := (v, \xi(q, v) - \operatorname{grad}_g V(q) - F(q, v))^T.$$

We shall assume that X is complete, and we denote by $\Phi_t^X : T\mathcal{Q} \to T\mathcal{Q}$ the flow of X at time $t \in \mathbb{R}$. Then, $(T\mathcal{Q}, \mathbb{R}, \Phi^X)$ is a differentiable dynamical system with flow $\Phi^X := \{\Phi_t^X : t \in \mathbb{R}\}$.
Finally, we require the following two conditions for the potential energy V and the "damping tensor" Γ:

c)i. V has a strict (local) minimum at q^*. Without loss of generality, assume $V(q^*) = 0$;

c)ii. $\Gamma(q)$ has constant rank $d - k$ for all $q \in \mathcal{Q}$, for some $0 \le k < d$.

In this setting, we first derive the following basic properties for system (6.5).

Lemma 6.1. *The energy function $E : T\mathcal{Q} \to \mathbb{R}$,*

$$E(q, \dot{q}) := T(q, \dot{q}) + V(q), \tag{6.7}$$

is a Lyapunov function for X on $T\mathcal{Q}$.

Proof. Since $E(q, \dot{q}) = \sum_{i=1}^d \dot{q}^i \frac{\partial L}{\partial \dot{q}^i}(q, \dot{q}) - L(q, \dot{q})$, straightforwardly from equation (6.5) it follows that

$$\mathcal{L}_X E(q, \dot{q}) = -\Gamma_{ij}(q)\dot{q}^i\dot{q}^j.$$

Since $\Gamma(q)$ is positive semi-definite for every $q \in \mathcal{Q}$, $\mathcal{L}_X E(q, \dot{q}) \le 0 \ \forall (q, \dot{q}) \in T\mathcal{Q}$. □

Lemma 6.2. *1. $(q^*, 0)$ is a stable equilibrium for system (6.6).*

2. If $\Gamma(q^*)$ has rank d, $(q^*, 0)$ is asymptotically stable.

*We use the same symbol to denote both an object in $T\mathcal{Q}$ and its local representative in a parametrisation of $T\mathcal{Q}$.

Proof. 1. From hypothesis *c)i.*, since q^* is a critical point for V, $X(q^*, 0) = (0, 0)$, and therefore q^* is an equilibrium configuration. To prove its stability, use E as Lyapunov function: $(q^*, 0)$ is a strict minimum for E, since V has a strict minimum in q^* and T is a positive definite quadratic function in $\dot{q}$ for any q; the conclusion follows from Lyapunov stability criterion.

2. If $\Gamma(q^*)$ has rank d, by hypothesis *c)ii.*, $k = 0$ for any $q \in \mathcal{Q}$ and $\mathcal{L}_X E = 0$ if and only if $\dot{q} = 0$. Being q^* a strict local extremum of V, there exists a neighbourhood of $(q^*, 0)$ in which q^* is a strict absolute extremum. The conclusion follows from Corollary 6.2.

□

For the rest of the section, we will assume that the damping tensor has not full rank, namely that, in *c)ii.*, $0 < k < d$. In this scenario, we want to describe the dynamics sufficiently close to the stable equilibrium $(q^*, 0)$.

6.3.2 Some results

For any $q \in \mathcal{Q}$, $\ker \Gamma(q) := \{\dot{q} \in T_q\mathcal{Q} : \Gamma(q)\dot{q} = 0\}$ is a vector subspace of $T_q\mathcal{Q}$ of codimension equal to the rank of $\Gamma(q)$. Thus, $\ker \Gamma$ defines a distribution D on $\mathcal{Q}$, which, by hypothesis *c)ii.*, is regular, with rank k and fibers $D_q := \ker \Gamma(q)$ for any $q \in \mathcal{Q}$. Then, $\mathcal{D} \subset T\mathcal{Q}$ defined as

$$\mathcal{D} := \{(q, \dot{q}) \in T\mathcal{Q} : \dot{q} \in \ker \Gamma(q)\}$$

is a smooth $(d + k)$-dimensional manifold.

Now, since we are interested in the dynamics near the stable equilibrium, we define a convenient neighbourhood of $(q^*, 0)$ to which we shall restrict the study of the flow of X. Note that since $V(q^*) = 0$, we have $E(q^*, 0) = 0$. For any $E_0 > 0$, define the (nonempty) open set $\Omega_{E_0} \subset T\mathcal{Q}$ as the connected component of the region $\{(q, \dot{q}) \in T\mathcal{Q} : E(q, \dot{q}) < E_0\}$ which contains $(q^*, 0)$. We fix E_0 sufficiently small (and, under the circumstances, this is always possible) so that

c)iii. $\overline{\Omega}_{E_0}$ is precompact;

We have the following result (see Figure 6.3).

Proposition 6.5. *For every $(q_0, \dot{q}_0) \in \Omega_{E_0}$, $\omega(q_0, \dot{q}_0)$ belongs to the largest invariant subset of $\mathfrak{T}^{(1)}_{\mathcal{D}} \cap \Omega_{E_0}$, where*

$$\mathfrak{T}^{(1)}_{\mathcal{D}} := \{(q, \dot{q}) \in \mathcal{D} : X(q, \dot{q}) \in T_{(q,\dot{q})}\mathcal{D}\}.$$

Proof. First, we notice that Ω_{E_0} is positively invariant under the flow of X, since it is a (component of a) sublevel set of a Lyapunov function. Moreover, condition *c)iii.* implies that for every $(q, \dot{q}) \in \Omega_{E_0}$, $t \to \Phi^X_t(q, \dot{q})$ is bounded for every $t \geq 0$.

Next, we observe that $\mathcal{D} \cap \Omega_{E_0} = \mathcal{L}_X E|^{-1}_{\Omega_{E_0}}(0)$. Indeed, since Γ is symmetric and positive semi-definite, $\mathcal{L}_X E(q, \dot{q}) = -\Gamma_{ij}(q)\dot{q}^i\dot{q}^j$ vanishes if and only if $\dot{q} \in \ker \Gamma(q)$, for any $(q, \dot{q}) \in T\mathcal{Q}$, and in particular for $(q, \dot{q}) \in \Omega_{E_0}$.

The conclusion follows from Proposition 6.3, by taking $\Omega = \Omega_{E_0}$, $\mathcal{W} = E$, $\mathcal{E} = \mathcal{D} \cap \Omega_{E_0}$. □

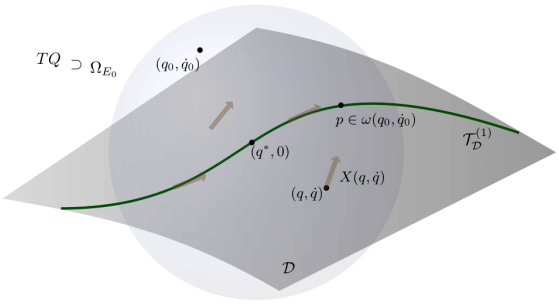

Figure 6.3: Schematic picture for the setting described in Proposition 6.5, for a three-dimensional phase space TQ.

Let $\Psi_0 : T\mathcal{Q} \to \mathbb{R}^{d-k}$, $\Psi_0(q, \dot{q}) := \Gamma(q)\dot{q}$, so that $\mathcal{D} = \Psi_0^{-1}(0)$. Then

$$\mathcal{T}^{(1)}_{\mathcal{D}} = \{(q, \dot{q}) \in T\mathcal{Q} : (\Psi_0' X)|_{\Psi_0^{-1}(0)}(q, \dot{q}) = 0\}.$$

In particular,

Corollary 6.3. *If $\Gamma(q) \equiv \Gamma$ $\forall q \in \mathcal{Q}$, then, in the hypotheses of Proposition 6.5,*

$$\mathcal{T}^{(1)}_{\mathcal{D}} := \{(q, \dot{q}) \in \mathcal{D} : \Gamma\,(\xi(q, v) - \mathrm{grad}_g\, V(q)) = 0\}.$$

Proof. If $\Gamma(q) \equiv \Gamma$ $\forall q \in \mathcal{Q}$, then $\Psi_0'(q, \dot{q}) = \begin{pmatrix} 0 & \Gamma \end{pmatrix}$. Recalling that $X|_{\mathcal{D}}(q, v) = (v, \xi(q, v) - \mathrm{grad}_g\, V(q))^T$, the condition $X(q, \dot{q}) \in T_{(q,\dot{q})}\mathcal{D}$, which is equivalent to $(\Psi_0' X)|_{\mathcal{D}} = 0$, gives the statement. □

Next, we remark that whenever the damping tensor is constant, $\ker \Gamma$ defines an integrable distribution on $\mathcal{Q}$. Therefore, we are motivated to refine the result of Proposition 6.5 for when D is an integrable distribution on $\mathcal{Q}$. Let $\mathcal{F}_{\bar{q}}$ be the integral manifold of D though $\bar{q}$, with $\bar{q} \in \mathcal{Q}$, namely such that $T_q\mathcal{F}_{\bar{q}} = D_q$ for every $q \in \mathcal{F}_{\bar{q}}$. Then, $\mathcal{D} \subset T\mathcal{Q}$ is a foliated manifold with leaves the $2k$-dimensional submanifolds

$$\mathcal{D}_{\bar{q}} := \{(q, \dot{q}) \in T\mathcal{Q} : q \in \mathcal{F}_{\bar{q}},\ \dot{q} \in D_q\} = T\mathcal{F}_{\bar{q}}, \quad \bar{q} \in \mathcal{Q}.$$

Proposition 6.6. *Assume D integrable. In the hypotheses of Proposition 6.5, for every $(q_0, \dot{q}_0) \in \Omega_{E_0}$, there exists a leaf $\mathcal{F}_{\bar{q}}$ of D (with any $\bar{q} \in \mathcal{Q}$) such that $\omega(q_0, \dot{q}_0)$ belongs to the largest invariant subset of $\mathcal{T}^{(1)}_{\mathcal{D}_{\bar{q}}} \cap \Omega_{E_0}$, where*

$$\mathcal{T}^{(1)}_{\mathcal{D}_{\bar{q}}} := \{(q, \dot{q}) \in \mathcal{D}_{\bar{q}} : X(q, \dot{q}) \in T_{(q,\dot{q})}\mathcal{D}_{\bar{q}}\}.$$

Proof. Since D is an integrable distribution, every solution $t \to q(t) \in \mathcal{Q}$ of the second order differential equations (6.5) necessarily belongs to a leaf $\mathcal{F}_{\bar{q}}$ whenever $(q(t), \dot{q}(t))$ is contained in $\mathcal{D}$. In particular, by Proposition 6.2, each ω-limit set is connected and therefore it belongs to the tangent of a leaf. □

Here too, there is an analogue of Proposition 6.4: for any $j \geq 2$, we can recursively define

$$\mathcal{T}_{\mathcal{D}}^{(j)} := \{(q, \dot{q}) \in \mathcal{T}_{\mathcal{D}}^{(j-1)} \, : \, X(q, \dot{q}) \in T_{(q,\dot{q})}\mathcal{T}_{\mathcal{D}}^{(j-1)}\},$$

as long as $\mathcal{T}_{\mathcal{D}}^{(1)}, \dots, \mathcal{T}_{\mathcal{D}}^{(j-1)}$ are submanifolds of $T\mathcal{Q}$, and look for the largest invariant subset within $\mathcal{T}_{\mathcal{D}}^{(j)}$. Moreover, if it happens that, for some $j \geq 1$, $\mathcal{T}_{\mathcal{D}}^{(j)}$ is both a submanifold of $T\mathcal{Q}$ and the largest invariant subset of $\mathcal{D}$, then $(\mathcal{T}_{\mathcal{D}}^{(j)}, \mathbb{R}, \Phi^X|_{\mathbb{R}\times\mathcal{T}_{\mathcal{D}}^{(j)}})$ is a conservative subsystem, since $\mathcal{T}_{\mathcal{D}}^{(j)} \subset \mathcal{D}$. Also, if, in addition, $\mathcal{T}_{\mathcal{D}}^{(j)}$ is the tangent bundle of a submanifold of $\mathcal{Q}$, then the dynamics on $\mathcal{T}_{\mathcal{D}}^{(j)}$ is described by a Lagrangian $L|_{\mathcal{T}_{\mathcal{D}}^{(j)}}$.

6.3.3 Examples

To conclude, we test the results found on the two models introduced at the beginning of this chapter, assuming $\gamma > 0$ and $\nu = 0$. In particular, this analysis will show how asymptotic synchronization enters this context but also some of the shortcomings of the method.

Example 1

We consider the system introduced in Section 6.1.1, consisting of two coupled rigid pendula, and we neglect the viscosity of the air, namely we set $\nu = 0$. Let $\mathcal{Q} = \mathbb{T}^2$, the vector field $X \in \mathfrak{X}(T\mathcal{Q})$ is

$$X(\theta_1, \theta_2, \dot{\theta}_1, \dot{\theta}_2) = \Big(\dot{\theta}_1, \dot{\theta}_2, -\sin\theta_1 - \gamma(\dot{\theta}_1 - \dot{\theta}_2), -\sin\theta_2 - \gamma(\dot{\theta}_2 - \dot{\theta}_1)\Big)^T, \qquad \gamma > 0.$$

Proposition 6.7. *The ω-limit set of any initial condition belongs to the set*

$$\{(\theta_1, \theta_1, \dot{\theta}_1, \dot{\theta}_1)\} \cup \{(0, \pi, 0, 0)\} \cup \{(\pi, 0, 0, 0)\}.$$

In particular, for any initial condition having negative energy, the two pendula synchronise in phase.

Proof. To begin with, we observe the following facts.

- $(\theta_1^*, \theta_2^*) = (0, 0)$ satisfies *c)i.* (up to an irrelevant constant translation of the potential energy).
- The damping tensor is represented by the constant matrix $\Gamma = \begin{pmatrix} \gamma & -\gamma \\ -\gamma & \gamma \end{pmatrix}$ and satisfies *c)ii.*, with $k = 1$. In particular, $\ker\Gamma(\theta_1, \theta_2) = \{\dot{\theta}_1 = \dot{\theta}_2\}$.

- $\mathcal{D} = \{(\theta_1, \theta_2, \dot\theta_1, \dot\theta_1)\}$ is a three-dimensional submanifold of $T\mathcal{Q}$. In particular, $\mathcal{D} = \Psi_0^{-1}(0)$ with $\Psi_0 : T\mathcal{Q} \to \mathbb{R}$,

$$\Psi_0(\theta_1, \theta_2, \dot\theta_1, \dot\theta_2) := \dot\theta_1 - \dot\theta_2.$$

- The energy of the system is $E(\theta_1, \theta_2, \dot\theta_1, \dot\theta_2) = \frac{1}{2}(\dot\theta_1^2 + \dot\theta_2^2) - (\cos\theta_1 + \cos\theta_2)$. In particular, $E(\theta_1^*, \theta_2^*, 0, 0) = -2$. For any $E_0 > -2$ finite, Ω_{E_0} satisfies *c)iii.*.

Next, we apply the result proved in Proposition 6.5 to locate the ω-limit sets of solutions in Ω_{E_0}. Moreover, since the damping tensor is constant, we compare such a procedure with the one which exploits the integrability property, applying the result of Proposition 6.6.

Method 1.

step 1. We compute $\mathcal{T}_{\mathcal{D}}^{(1)}$. We have $X|_{\mathcal{D}}(\theta_1, \theta_2, \dot\theta_1, \dot\theta_1) = (\dot\theta_1, \dot\theta_1, -\sin\theta_1, -\sin\theta_2)^T$, hence

$$\begin{aligned}\mathcal{T}_{\mathcal{D}}^{(1)} &= \{(\theta_1, \theta_2, \dot\theta_1, \dot\theta_1) : (\Psi_0' X)(\theta_1, \theta_2, \dot\theta_1, \dot\theta_1) = 0\} \\ &= \{(\theta_1, \theta_2, \dot\theta_1, \dot\theta_1) : \sin\theta_1 = \sin\theta_2\} \\ &= \{(\theta_1, \theta_1, \dot\theta_1, \dot\theta_1)\} \cup \{(\theta_1, \pi - \theta_1, \dot\theta_1, \dot\theta_1)\} =: \mathcal{T}_{\mathcal{D}}^{(1)-} \cup \mathcal{T}_{\mathcal{D}}^{(1)+}.\end{aligned}$$

Therefore, $\mathcal{T}_{\mathcal{D}}^{(1)}$ is a two-dimensional submanifold of $T\mathcal{Q}$, and so are $\mathcal{T}_{\mathcal{D}}^{(1)-}$ and $\mathcal{T}_{\mathcal{D}}^{(1)+}$. To find the largest invariant set within, we apply Proposition 6.5 once more.

step 2. We compute $\mathcal{T}_{\mathcal{D}}^{(2)}$. We have $X|_{\mathcal{T}_{\mathcal{D}}^{(1)}}(\theta_1, \theta_2, \dot\theta_1, \dot\theta_1) = (\dot\theta_1, \dot\theta_1, -\sin\theta_1, -\sin\theta_1)^T$. Moreover, $\mathcal{T}_{\mathcal{D}}^{(1)-} = \hat\Psi_{1-}^{-1}(0)$ with $\hat\Psi_{1-} : T\mathcal{Q} \to \mathbb{R}^2$, $\hat\Psi_{1-} = (\Psi_0, \Psi_{1-})^T$, where

$$\Psi_{1-}(\theta_1, \theta_2, \dot\theta_1, \dot\theta_2) := \theta_1 - \theta_2.$$

Similarly, $\mathcal{T}_{\mathcal{D}}^{(1)+} = \hat\Psi_{1+}^{-1}(0)$ with $\hat\Psi_{1+} : T\mathcal{Q} \to \mathbb{R}^2$, $\hat\Psi_{1+} = (\Psi_0, \Psi_{1+})^T$, where

$$\Psi_{1+}(\theta_1, \theta_2, \dot\theta_1, \dot\theta_2) := \theta_1 + \theta_2 - \pi.$$

Hence, $\mathcal{T}_{\mathcal{D}}^{(2)} = \mathcal{T}_{\mathcal{D}}^{(2)-} \cup \mathcal{T}_{\mathcal{D}}^{(2)+}$ with

$$\mathcal{T}_{\mathcal{D}}^{(2)-} = \{(\theta_1, \theta_1, \dot\theta_1, \dot\theta_1) : (\hat\Psi_{1-}' X)(\theta_1, \theta_1, \dot\theta_1, \dot\theta_1) = 0\} \equiv \mathcal{T}_{\mathcal{D}}^{(1)-}$$

and

$$\begin{aligned}\mathcal{T}_{\mathcal{D}}^{(2)+} &= \{(\theta_1, \pi - \theta_1, \dot\theta_1, \dot\theta_1) : (\hat\Psi_{1+}' X)(\theta_1, \pi - \theta_1, \dot\theta_1, \dot\theta_1) = 0\} \\ &= \{(\theta_1, \pi - \theta_1, 0, 0)\}.\end{aligned}$$

Hence, $\mathcal{T}_{\mathcal{D}}^{(1)-}$ is an invariant two-dimensional submanifold of $T\mathcal{Q}$ in $\mathcal{D}$. A further step is required to determine the largest invariant subset of $\mathcal{T}_{\mathcal{D}}^{(2)+}$, which is a one-dimensional submanifold.

step 3. We compute $\mathfrak{T}_{\mathcal{D}}^{(3)+}$. Since $X|_{\mathfrak{T}_{\mathcal{D}}^{(2)+}}(\theta_1, \pi - \theta_1, 0, 0) = (0, 0, -\sin\theta_1, -\sin\theta_1)^T$, the only orbits in $\mathfrak{T}_{\mathcal{D}}^{(2)+}$ are the equilibria, namely

$$\mathfrak{T}_{\mathcal{D}}^{(3)+} = \{(0, \pi, 0, 0)\} \cup \{(\pi, 0, 0, 0)\}.$$

Hence, the largest invariant set in $\mathcal{D}$ is $\mathfrak{T}_{\mathcal{D}}^{(3)} := \mathfrak{T}_{\mathcal{D}}^{(1)-} \cup \mathfrak{T}_{\mathcal{D}}^{(3)+}$.

Finally, we observe that $\mathfrak{T}_{\mathcal{D}}^{(3)}$ is not a manifold. However, if we bound the initial energy by $E_0 = 0$, then the ω-limit of every positive semi-orbit in Ω_{E_0} belongs to $\mathfrak{T}_{\mathcal{D}}^{(1)-}$, which is a two-dimensional submanifold of $T\mathcal{Q}$. In fact, $\mathfrak{T}_{\mathcal{D}}^{(1)-}$ is the tangent bundle of a one-dimensional manifold $S \subset \mathcal{Q}$, $S := \{(\theta_1, \theta_1)\}$. We can parametrise S with $\phi \in \mathbb{T}^1$. Then, the dynamics on $TS \cap \Omega_{E_0}$ is $\ddot{\phi} + \sin\phi = 0$, namely a pendulum.

Method 2.

We now exploit the integrability of the distribution defined by $\ker\Gamma(\theta_1, \theta_2) = \{\dot{\theta}_1 = \dot{\theta}_2\}$. For any $\bar{\theta} \in \mathbb{T}^1$, the integral leaf through $\bar{\theta}$ in $\mathcal{Q}$ is the one-dimensional manifold $\mathcal{F}_{\bar{\theta}} = \{(\theta_1, \theta_2) \in \mathcal{Q} : \theta_1 - \theta_2 = \bar{\theta}\}$[†]. Hence,

$$\mathcal{D}_{\bar{\theta}} = T\mathcal{F}_{\bar{\theta}} = \{(\theta_1, \theta_1 - \bar{\theta}, \dot{\theta}_1, \dot{\theta}_1)\}.$$

By Proposition 6.6, we have to determine, for each $\bar{\theta} \in \mathbb{T}^1$, the largest invariant subset contained in $\mathcal{F}_{\bar{\theta}}$. Since $X|_{\mathcal{D}_{\bar{\theta}}}(\theta_1, \theta_1 - \bar{\theta}, \dot{\theta}_1, \dot{\theta}_1) = (\dot{\theta}_1, \dot{\theta}_1, -\sin\theta_1, -\sin(\theta_1 - \bar{\theta}))^T$, we have, using Corollary 6.3,

$$\mathfrak{T}_{\mathcal{D}_{\bar{\theta}}}^{(1)} = \{(\theta_1, \theta_1 - \bar{\theta}, \dot{\theta}_1, \dot{\theta}_1) : \sin\theta_1 = \sin(\theta_1 - \bar{\theta})\}.$$

Therefore, the largest invariant set in $\mathcal{D}$ consists of the equilibria and the two-dimensional submanifold $\mathfrak{T}_{\mathcal{D}_0}^{(1)} = T\mathcal{F}_0$, which is the only invariant subbundle of $T\mathcal{Q}$. □

For this example, we are hence able to explicitly determine the largest invariant set containing the ω-limits of any solution. In particular, we are able to predict the emergence of asymptotic in-phase synchronization of the pendula, at least for low energies.

This is however a rather lucky case, and for more complicated systems the recursive chain might stop earlier, due to a loss of smoothness, preventing the ultimate determination of the largest invariant set following this methodology. The next example presents indeed more difficulties.

Example 2

We consider now the second model, introduced in Section 6.1.1. This system consists of two pendula coupled through a rigid support, and we neglect the viscosity of the air, that

[†]We implicitly mean the sums of angles to be defined mod2π.

is, we set $\nu = 0$. Let $\mathcal{Q} = \mathbb{R} \times \mathbb{T}^2$ and (z, ϕ), $\phi := (\phi_1, \phi_2)$, local coordinates; the vector field $X \in \mathfrak{X}(T\mathcal{Q})$ is $X(z, \phi, \dot{z}, \dot{\phi}) = (\dot{z}, \dot{\phi}, X_v(z, \phi, \dot{z}, \dot{\phi}))^T$ with

$$X_v := \frac{1}{c}\begin{pmatrix} -\gamma\dot{z} - \alpha z + \sum_{i=1}^2(\dot{\phi}_i^2 \sin\phi_i + \sin\phi_i \cos\phi_i) \\ -\cos\phi_1(-\gamma\dot{z} - \alpha z + \sum_{i=1}^2 \dot{\phi}_i^2 \sin\phi_i) - (\mu - \cos^2\phi_2)\sin\phi_1 - \cos\phi_1\cos\phi_2\sin\phi_2 \\ -\cos\phi_2(-\gamma\dot{z} - \alpha z + \sum_{i=1}^2 \dot{\phi}_i^2 \sin\phi_i) - (\mu - \cos^2\phi_1)\sin\phi_2 - \cos\phi_1\cos\phi_2\sin\phi_1 \end{pmatrix}$$

with $c := \mu - \sum_{i=1}^2(\cos\phi_i)^2$, and $\alpha > 0$, $\mu > 2$, $\gamma > 0$.

We apply Proposition 6.5 and try to determine the largest invariant set in the phase space in which dissipation does not act.

As before, we first observe the following facts.

- $(z^*, \phi^*) = (0, 0)$ satisfies *c)i.* (up to an irrelevant constant translation of the potential energy).
- The damping tensor is represented by the constant matrix $\Gamma = \begin{pmatrix} \gamma & 0 & 0 \\ 0 & 0 & 0 \\ 0 & 0 & 0 \end{pmatrix}$ and satisfies *c)ii.*, with $k = 2$. In particular, $\ker\Gamma(z, \phi) = \{\dot{z} = 0\}$.
- $\mathcal{D} = \{(z, \phi, 0, \dot{\phi})\}$ is a five-dimensional submanifold of $T\mathcal{Q}$. In particular, $\mathcal{D} = \Psi_0^{-1}(0)$ with $\Psi_0 : T\mathcal{Q} \to \mathbb{R}$,
$$\Psi_0(z, \phi, \dot{z}, \dot{\phi}) := \dot{z}.$$
- The energy of the system is $E(z, \phi, \dot{z}, \dot{\phi}) = \frac{1}{2}\mu\dot{z}^2 + \sum_{i=1}^2\left(\frac{1}{2}\dot{\phi}_i^2 + \dot{z}\dot{\phi}_i\cos\phi_i - \cos\phi_i\right) + \frac{1}{2}\alpha z^2$. In particular, $E(z^*, \phi^*, 0, 0) = -2$. For any $E_0 > -2$ finite, Ω_{E_0} satisfies *c)iii.*.

Next, we apply the result proved in Proposition 6.5 to locate the ω-limit sets of solutions in Ω_{E_0}.

step 1. We compute $\mathcal{T}_{\mathcal{D}}^{(1)}$. Since Γ is constant, it is convenient to apply Corollary 6.3, by which

$$\begin{aligned} \mathcal{T}_{\mathcal{D}}^{(1)} &= \{(z, \phi, 0, \dot{\phi}) : \Gamma\, X_v(z, \phi, 0, \dot{\phi}) = 0\} \\ &= \Big\{(z, \phi, 0, \dot{\phi}) : -\alpha z + \sum_{i=1}^2(\dot{\phi}_i^2 \sin\phi_i + \sin\phi_i\cos\phi_i) = 0\Big\}. \end{aligned}$$

In particular, $\mathcal{T}_{\mathcal{D}}^{(1)} = \hat{\Psi}_1^{-1}(0)$ with $\hat{\Psi}_1 : T\mathcal{Q} \to \mathbb{R}^2$, $\hat{\Psi}_1 = (\Psi_0, \Psi_1)^T$, where

$$\Psi_1(z, \phi, \dot{z}, \dot{\phi}) := -\alpha z + \sum_{i=1}^2(\dot{\phi}_i^2 \sin\phi_i + \sin\phi_i\cos\phi_i).$$

Therefore, $\mathcal{T}_{\mathcal{D}}^{(1)}$ is a four-dimensional submanifold of $T\mathcal{Q}$, since $\hat{\Psi}_1$ is submersive. To find the largest invariant set within, we apply Proposition 6.5 once more.

step 2. We compute $\mathcal{T}_{\mathcal{D}}^{(2)}$. We have $X|_{\mathcal{T}_{\mathcal{D}}^{(1)}}(z,\phi,0,\dot{\phi}) = \Big(0,\dot{\phi}_1,\dot{\phi}_2,0,-\sin\phi_1,-\sin\phi_2\Big)^T$. Hence,

$$\begin{aligned}\mathcal{T}_{\mathcal{D}}^{(2)} &= \Big\{\big(\tfrac{1}{\alpha}\textstyle\sum_{i=1}^{2}(\dot{\phi}_i^2\sin\phi_i+\sin\phi_i\cos\phi_i),\phi,0,\dot{\phi}\big)\,:\,(\hat{\Psi}_1'X)|_{\mathcal{T}_{\mathcal{D}}^{(1)}}(z,\phi,0,\dot{\phi})=0\Big\}\\ &= \Big\{\big(\tfrac{1}{\alpha}\textstyle\sum_{i=1}^{2}(\dot{\phi}_i^2\sin\phi_i+\sin\phi_i\cos\phi_i),\phi,0,\dot{\phi}\big)\,:\,\sum_{i=1}^{2}\dot{\phi}_i(\dot{\phi}_i^2c_i+c_i^2-3s_i^2)=0\Big\}\end{aligned}$$

where $c_i := \cos\phi_i$ and $s_i := \sin\phi_i$, $i = 1, 2$. Proposition 6.5 ensures that the ω-limit set of every positive semi-orbit in Ω_{E_0} belongs to the largest invariant subset in $\mathcal{T}_{\mathcal{D}}^{(2)}$.

We could carry on with the computation, however, it appears – at this step already – that the calculation is quite involved and we still might be unable to extrapolate information on the asymptotic dynamics, unlike the previous example.

Thus, on a critical note, this procedure allows one to obtain some information on the location of the ω-limit sets of bounded solutions in some (simple) cases, however, the sufficient condition provided by Proposition 6.5 appears to be too strong. Even so, this discussion might stimulate further investigation in this direction and provide some material useful for the definition of a more optimal strategy.

Bibliography

[1] V. I. Arnold, *Mathematical Methods of Classical Mechanics*, vol. 60, Graduate Texts in Mathematics, Springer New York, 1989.

[2] V. I. Arnold, *Lectures on Partial Differential Equations*, Universitext, Springer-Verlag Berlin Heidelberg, 2004.

[3] V. I. Arnold, V. V. Kozlov, and A. I. Neishtadt, *Mathematical Aspects of Classical and Celestial Mechanics*, vol. 3, Encyclopaedia of Mathematical Sciences, Springer Berlin Heidelberg, 2006.

[4] D. Bambusi and E. Haus, "Asymptotic stability of synchronous orbits for a gravitating viscoelastic sphere", in: *Celestial Mechanics and Dynamical Astronomy* **114** (2012), pp. 255–277.

[5] H. T. Banks et al., "On the Existence of Normal Modes of Damped Discrete-Continuous Systems", in: *Journal of Applied Mechanics* **65** (1998), pp. 1–26.

[6] J. M. Bendickson, J. P. Dowling, and M. Scalora, "Analytic expressions for the electromagnetic mode density in finite, one-dimensional, photonic band-gap structures", in: *Physical Review E* **53**.4 (1996), pp. 4107–4121.

[7] M. Bennett et al., "Huygens's clocks", in: *Proceedings of the Royal Society of London. Series A: Mathematical, Physical and Engineering Sciences* **458**.2019 (2002), pp. 563–579.

[8] I. I. Blekhman et al., "Self-synchronization and controlled synchronization: General definition and example design", in: *Mathematics and Computers in Simulation* **58**.4-6 (2002), pp. 367–384.

[9] S. Boccaletti et al., *Synchronization: From Coupled Systems to Complex Networks*, Cambridge University Press, 2018.

[10] M. Born, E. Wolf, and A. B. Bhatia, *Principles of Optics: Electromagnetic Theory of Propagation, Interference and Diffraction of Light*, Cambridge University Press, 1999.

[11] S. Cox and E. Zuazua, "The rate at which energy decays in a damped string", in: *Communications in Partial Differential Equations* **19**.1-2 (1994), pp. 213–243.

[12] R. Dilão, "On the problem of synchronization of identical dynamical systems: The Huygens's clocks", in: *Variational Methods in Aerospace Engineering, Springer Optimization and Its Applications*, vol. 33, Springer International Publishing, 2009, pp. 163–181.

[13] F. Fassò, *Dispense per il corso di Istituzioni di Fisica Matematica per il corso di laurea in Fisica - a.a. 2020/2021*, CLEUP, 2021.

[14] G. H. Goldsztein, A. N. Nadeau, and S. H. Strogatz, "Synchronization of clocks and metronomes: A perturbation analysis based on multiple timescales", in: *Chaos* **31**.023109 (2021), pp. 1–16.

[15] D. J. Griffiths and C Steinke, "Waves in locally periodic media", in: *American Journal of Physics* **69** (2001), pp. 137–154.

[16] J. K. Hale, "Diffusive coupling, dissipation, and synchronization", in: *Journal of Dynamics and Differential Equations* **9** (1997), pp. 1–52.

[17] C. Huygens, *Correspondance 1664-1665*, ed. by M. Nijhoff, 1893.

[18] C. Huygens, *Horologium Oscillatorium*, 1673.

[19] H. M. Irvine and G. B. Sinclair, "The suspended elastic cable under the action of concentrated vertical loads", in: *International Journal of Solids and Structures* **12**.4 (1976), pp. 309–317.

[20] V. Jovanovic and S. Koshkin, "Synchronization of Huygens clocks and the Poincaré method", in: *Journal of Sound and Vibration* **331**.12 (2012), pp. 2887–2900.

[21] M. Kapitaniak et al., "Synchronization of clocks", in: *Physics Reports* **517**.1-2 (2012), pp. 1–69.

[22] D. J. Korteweg, *Les horloges sympathiques de Huygens*, Archives Neerlandaises, sér. II, tome XI, pp. 273-295, The Hague: Martinus Nijhoff, 1906.

[23] P. Lancaster and A Shkalikov, "Damped vibrations of beam and related spectral problems", in: *Canadian Applied Mathematics Quarterly* **2**.1 (1994), pp. 45–90.

[24] S. Lang, *Differential and Riemannian Manifolds*, Graduate Texts in Mathematics, Springer, 1995.

[25] J. P. LaSalle, "Some Extensions of Liapunov's Second Method*", in: *IEEE Transactions on Circuits and Systems I-regular Papers* **7** (1960), pp. 520–527.

[26] J. P. LaSalle, *The Stability of Dynamical Systems*, CBMS-NSF Regional Conference Series in Applied Mathematics, SIAM, 1976.

[27] J. P. LaSalle and S. Lefschetz, *Stability by Liapunov's direct method : with applications*, vol. 4, Mathematics in Science and Engineering, Academic Press, 1961.

[28] L. Marcheggiani, R. Chacón, and S. Lenci, "On the synchronization of chains of nonlinear pendula connected by linear springs", in: *European Physical Journal: Special Topics* **223**.4 (2014), pp. 729–756.

[29] J. Marsden and T. Ratiu, *Introduction to Mechanics and Symmetry: A Basic Exposition of Classical Mechanical Systems*, 2nd ed., Texts in Applied Mathematics, Springer New York, 1999.

[30] J. C. Mason and D. C. Handscomb, *Chebyshev polynomials*, CRC Press, 2002.

[31] H. Nijmeijer and A. Rodriguez-Angeles, *Synchronization of Mechanical Systems*, vol. 46, World Scientific Series on Nonlinear Science Series A, World Scientific, 2003.

[32] H. M. Oliveira and L. V. Melo, "Huygens synchronization of two clocks", in: *Scientific Reports* **5** (2015), pp. 1–11.

[33] G. Óttarsson and C. Pierre, "Vibration and wave localization in a nearly periodic beaded string", in: *The Journal of the Acoustical Society of America* **101**.6 (1997), pp. 3430–3442.

[34] J. Pantaleone, "Synchronization of metronomes", in: *American Journal of Physics* **70**.992 (2002), pp. 992–1000.

[35] J. Peña Ramirez, "Huygens' synchronization of dynamical systems : beyond pendulum clocks", PhD thesis, Technische Universiteit Eindhoven, 2013.

[36] J. Peña Ramirez et al., "The sympathy of two pendulum clocks: Beyond Huygens' observations", in: *Scientific Reports* **6**.1 (2016), pp. 1–16.

[37] A. Pikovsky, M. Rosenblum, and J. Kurths, *Synchronization: A Universal Concept in Nonlinear Sciences*, Cambridge Nonlinear Science Series, Cambridge University Press, 2001.

[38] A. Y. Pogromsky, V. N. Belykh, and H. Nijmeijer, "A study of controlled synchronization of Huijgens' pendula", in: *Lecture Notes in Control and Information Sciences* **336** (2006), pp. 205–216.

[39] J. P. Ramirez and H. Nijmeijer, "The secret of the synchronized pendulums", in: *Physics World* **33**.1 (2020), pp. 36–40.

[40] J. Rayleigh, *The Theory of Sound*, Dover Publications, 1877.

[41] D. L. Russell, "On Mathematical Models for the Elastic Beam with Frequency-Proportional Damping", in: *Control and Estimation in Distributed Parameter Systems*, SIAM, 1992, pp. 125–169.

[42] G. Salesi, M. Greselin, and R. Leporini, "Thermalization of a coupled oscillator chain", in: *AIMETA 2017 - Proceedings of the 23rd Conference of the Italian Association of Theoretical and Applied Mechanics* **5** (2017), pp. 985–991.

[43] S. Salsa, *Partial Differential Equations in Action: From Modelling to Theory*, UNITEXT, Springer International Publishing, 2016.

[44] M. Senator, "Synchronization of two coupled escapement-driven pendulum clocks", in: *Journal of Sound and Vibration* **291**.3-5 (2006), pp. 566–603.

[45] T. Stankovski et al., "Coupling functions: Universal insights into dynamical interaction mechanisms", in: *Reviews of Modern Physics* **89** (2017), pp. 045001–1–045001–50.

[46] F. Talamucci, "Synchronization of two coupled pendula in absence of escapement", in: *Applied Mathematics and Mechanics (English Edition)* (2016), pp. 1721–1738.

[47] A. N. Tikhonov and A. A. Samarskii, *Equations of Mathematical Physics*, Dover Publications, 1963.

[48] J. H. Van Drie and P. W. Murphy, "Chebyshev polynomials in the loaded-string problem", in: *American Journal of Physics* **43**.4 (1975), pp. 361–362.

[49] S. Wiggins, *Introduction to Applied Nonlinear Dynamical Systems and Chaos*, 2nd ed., Texts in Applied Mathematics, Springer, New York, 2003.